Effects of Crowding and Cosolutes on Biomolecular Function at Extreme Environmental Conditions

Judith Peters, Rosario Oliva, Antonino Caliò, Philippe Oger, Roland Winter

Effects of Crowding and Cosolutes on Biomolecular Function at Extreme Environmental Conditions

Judith Peters[1,2,3,*], Rosario Oliva[4], Antonino Calio[5], Philippe Oger[6], and Roland Winter[7,*]

Abstract

The extent of the effect of cellular crowding and cosolutes on the functioning of proteins and cells is manifold and includes the stabilization of the biomolecular systems, the excluded volume effect, and the modulation of molecular dynamics. Simultaneously, it is becoming increasingly clear how important it is to take the environment into account if we are to shed light on biological function under various external conditions. Many biosystems thrive under extreme conditions, including the deep sea and subsea floor crust, and can take advantage of some of the effects of crowding. These relationships have been studied in recent years using various biophysical techniques, including neutron and X-ray scattering, calorimetry, FTIR, UV/Vis and fluorescence spectroscopies. Combining knowledge of the structure and conformational dynamics of biomolecules under extreme conditions, such as temperature, high hydrostatic pressure, and high salinity, we highlight the importance of considering all results in the context of the environment. Here we discuss crowding and cosolute effects on proteins, nucleic acids, membranes, and live cells, and explain how it is possible to experimentally separate crowding-induced effects from other influences. Such findings will contribute to a better understanding of the homeoviscous adaptation of organisms and the limits of life in general.

CONTENTS

1. Introduction

Crowding is manifested at the molecular level in biological systems like whole cells or spores. It designates an environment that is densely packed in water by a multitude of different biomolecules. It can be modelled in other states like in wet powders, gels, pellets or dense liquids. When macromolecules are present in a large number in a restricted environment, i.e. the volume fraction of macromolecular species lies in between 10 and 40 % of the total solution's volume, this defines the term of crowding. However, a single species is not necessarily present at high concentration. One calls molecular self-crowding the situation where high concentrations of proteins of the same kind are present in a solution. Otherwise, several types of biomacromolecules are mixed or different cosolutes added to the solution. Such situations are typically encountered in living matter, i.e., in the biological cell.

Living cells comprise a large number of biomacromolecules, among them nucleic acids, proteins, lipids, carbohydrates, and others.[1] The total concentration of biomolecules varies in different systems and is estimated to be 300 – 400 g/L in *Escherichia coli*, 100 – 400 g/L in cell's nuclei, 50 – 400 g/L in the eukaryotic cytoplasm, 100 – 200 g/L in nuclear organelles, and 270 – 560 g/L in the mitochondrial basic structure.[2-9] These concentrations are well above those used for classical laboratory experiments in biochemistry and biophysics, which are typically below 10 g/L. One should note that experimental measurements of enzymatic reactions or biochemical properties are in general carried out in low concentrated solutions (e.g., ligand binding constants or enzymatic turnover numbers). The results can differ significantly, by many orders of magnitude, from the more realistic values seen in living cells (*in vivo*). *In vitro* studies using molecular crowding agents are helping to bridge the gaps in our molecular-level understanding of reactions of biomolecules and their function in cellular environments. However, the information one can get out of such experiments may still not represent the physiological reality, i.e., out-of-equilibrium situations of a highly dynamic heterogeneous system, which varies rapidly in spatial organization and time.

Experimentally, one could consider to measure whole live cells, however this is sometimes prohibited by the experimental technique due to the size of the cell or the information content required might be obnubilated. In such cases, cellular crowding might be mimicked by several possible

approaches: (i) the concentration of the biomolecules can be increased drastically, (ii) the hydration can be reduced to produce a highly concentrated wet powder, or (iii) crowding agents can be employed (Figure 1). Examples of direct measurements of live cells as well as of all these approaches to mimic crowding will be given in this article. One has to bear in mind that these procedures miss still some aspects of cellular crowding, namely the dynamic heterogeneity of the environment in a cell and the spatial limitation, imposed, for example, by neighboring lipid interfaces.

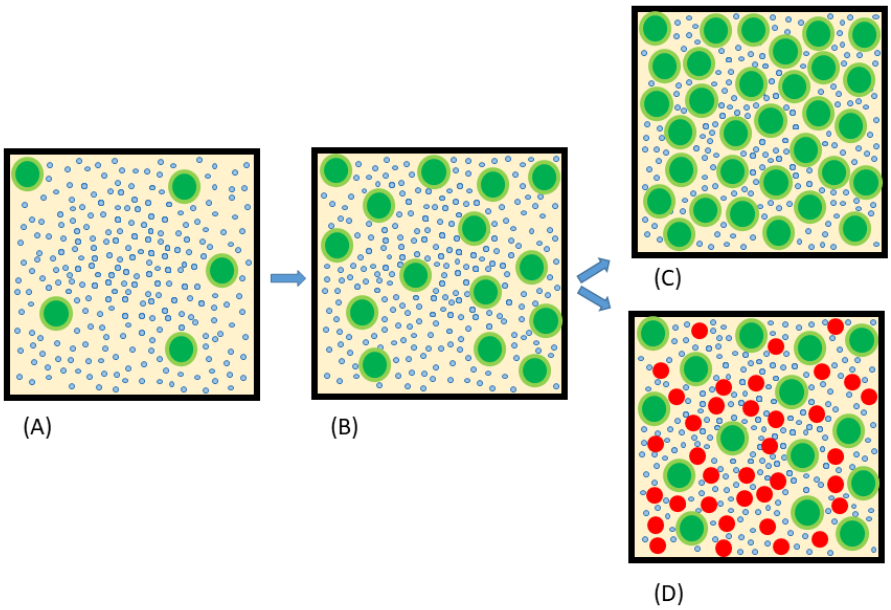

Figure 1. Different approaches to mimic cellular crowding of a diluted sample (A) of biomolecules (green) by increasing their concentration (B), by using a hydrated powder (C), or by adding appropriate crowding agents (red dots) (D).

Whereas an increase of concentration in a solution leads normally to more interactions in the form of collisions, to a higher probability of interactions, to a faster mixing and homogenization of a solution, macromolecular crowding goes far beyond these effects. The phenomenon, which is crucial to understand the importance of crowding is the excluded volume effect. Molecules diluted in a solution cannot penetrate each other due to steric repulsion so that a cosolute can only move in between them if the molecules are far enough. In case of a higher concentration and/or a larger cosolute, it can only pass through the interstitial space between two molecules if the distance between them is larger than the diameter of the cosolute. This excluded volume effect reduces the entropy of the system ($\Delta S < 0$) due to the restriction of motions and consequently leads to an increase of the free energy $\Delta G = \Delta H - T\,\Delta S$ (ΔH is the enthalpy variation of the system).

Crowding inevitably reduces the volume of the cellular environment. As denatured proteins are unfolding, leading to a larger required space as, for example, evidenced by small-angle scattering measurements, crowding is expected to increase the stability of native proteins over unfolded ones.[10] This simple picture was, however, challenged by some recent experimental results, where it was shown that specific environments lead to no change of the unfolding ("melting") temperature, T_m, of proteins or even to a small decrease of T_m, indicating that soft intermolecular (enthalpic) interactions can play a significant role as well.[11, 12] Thus, besides the entropy-driven excluded volume effect, enthalpic interactions between crowders and biomolecules (also denoted "quinary" interactions) can be

encountered. Hence, all thermodynamic properties of the system, including the chemical potential of the constituents, are affected by the confinement and modulate their activity and reactivity.

The impact of excluded volume applies also to the water molecules, which may no longer access the molecule's surface and sufficiently hydrate, for instance, a protein. On the other hand, cosolutes or crowding agents can interact directly with the protein backbone or be preferentially excluded from the protein surface and instead interact strongly with the surrounding water. In both cases, they will alter the interaction between the biomolecule and water network, i.e., change the hydration properties, which, in turn, can significantly influence the dynamic properties of the system. Further, crowding can have consequences for the diffusional mobility of biomolecules (affecting, for example, diffusion-controlled reactions), for the conformational dynamics of nucleic acids and proteins and their stability, for the equilibria and kinetics of protein-protein and protein-DNA mixtures, and for the enzymatic activity and the regulation of cell volume. In this way, the activity and reactivity of the components of the biological cell can be efficiently controlled and modulated in space and time.

Synthetic polymeric osmolytes, such as Ficoll, dextran or polyethylene glycol (PEG), can be associated in high concentrations to dilute solutions of proteins and other biomolecules to investigate crowding *in vitro*. Dextran is a polymer of variable length with linkages between glucose monomers. Ficoll is a copolymer of sucrose and epichlorohydrin, (poly-(saccharose-co-epichlorhydrin)), which is also neutral, dissolves in water, and is also available at different lengths. PEG is a linear polyether compound which is soluble in water and also in a lipidic environment (Figure 2). The choice to use one of them is mainly motivated by the fact to have crowding agents which do not specifically interact with the proteins (which has to be checked beforehand), are highly water soluble, and allow tuning the extent of macromolecular crowding in a controlled way.

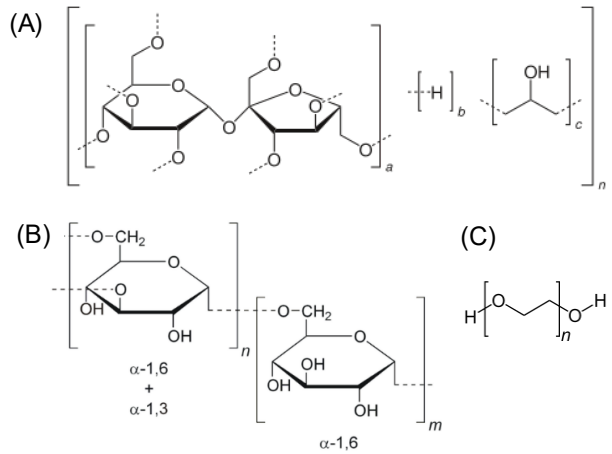

Figure 2. Examples of some crowding agents used in the studies described here: (A) dextran, (B) Ficoll, and (C) PEG.

For a given solute *i*, the partial molar volume, V_i, is the derivative of its chemical potential, μ_i, with respect to pressure at constant temperature:

$$V_i = \left(\frac{\partial \mu_i}{\partial p}\right)_T = \left(\frac{\partial V_{\text{soln}}}{\partial n_i}\right)_{p,T,n_{j\neq i}} = \lim_{c_i \to 0} \left(\frac{\partial V_{\text{soln}}}{\partial n_i}\right)_{p,T}, \quad (1)$$

p being the pressure, T the temperature, V_{soln} the solution's volume, n_i is the number of moles of the solute, and c_i its concentration. In other words, it corresponds to the volume occupied by one mole of solute at infinite dissolution where the concentration of other species, j, is constant. Hence, the partial molar volume of a biomolecule, for instance a protein, and its solvating surroundings may be decomposed into a sum of contributions, i.e., $V_{\mathrm{protein}} = V_{\mathrm{atom}} + V_{\mathrm{void}} + V_{\mathrm{hydration}}$, where V_{atom} accounts for the van der Waals volume of the molecule, which is essentially incompressible, V_{void} represents the cavities inside the protein and in the interstitial spaces, which can be perturbed by pressure application, and $V_{hydration}$ takes into account the interaction between the solvent and the protein and represents the volume change upon hydration of the biomolecule (compared to bulk water).[13-15] It can be assumed that crowding agents essentially have an influence on $V_{hydration}$, only. The crowding agent might change the hydration layer structure and density via exclusion from the protein interface, or interact with the protein surface via weak intermolecular interactions. The effect will also depend on the chemical make-up of the crowder and its concentration, i.e., if it is present at low concentration or above its overlap concentration, c^*.

2. Extreme Environmental Conditions and their Relation to Crowding

It is common to classify microorganisms into three domains of life: bacteria, archaea (sometimes called prokarya together), which are single-celled, and eukarya containing a cell nucleus.[16] Their components include, next to water and the cytoplasm, among others, ribosomes, proteins, nucleic acids, membranes and cell walls, and in addition in eukarya the nucleus and various organelles such as the endoplasmic reticulum, Golgi apparatus, chloroplasts and mitochondria, which are surrounded by a membrane. Characteristic for all three is the high amount of intracellular crowding, which contributes to the stability of the cells. Extremophiles often, but not exclusively, belong to the domain of archaea, which have characteristic features permitting adaptation processes[17] or structural and dynamical particularities allowing them to adopt to harsh external conditions.[18] In the context of this review on crowding and its impact on biomolecular function, some of them will be discussed in more detail. The components of cells vary in their sensitivity to extreme external conditions, so it is important to recall the typical composition of a cell (Figure 3).

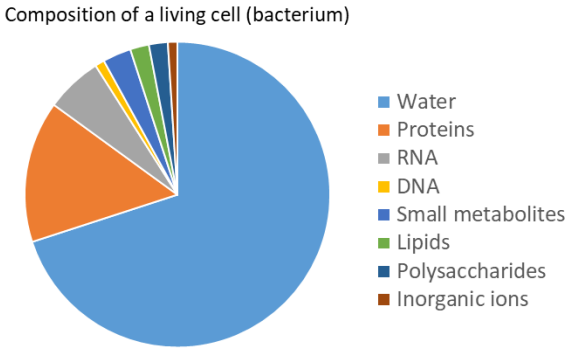

Figure 3. The chemical composition of a typical bacterial cell (data from [1]).

The study of biological systems under extreme environmental conditions can bring to light very interesting features, as such extremes can reveal the limits of stability and function, but also structural, compositional and dynamic rearrangements can be explored when organisms are exposed to such

conditions. Further, the response to stresses discloses the adaptive capacity of the biological systems. As many different environmental conditions can impact the system, individually or conjointly, it is of paramount importance to study, model and describe them in all these situations. For example, proteins unfold and denature at high temperatures, which is a well-known effect. The conformation and dynamic properties of proteins at very low temperatures, including cold denaturation, in concert with high pressure exposure, as they exist in the depth of the oceans on Earth or proposed for the profound salt lakes of the Martian subsurface, are far less understood.[17, 19, 20] Such knowledge is also required to understand, for example, the freezing and pressurizing of food stuff in high-pressure food processing, methods used to preserve nutritional value. The deep sea hosts also hydrothermal vents, which are surrounded by compressed and hot water that bursts out into the cold water. Regardless of such hostile environment, hydrothermal vents have a rich biodiversity. Organisms living in the deep sea can be considered perfect examples of biological resilience. Hence, knowledge of the biochemical mechanisms and adaptations evolved by organisms to thrive in the deep ocean can serve as paradigm for biotechnological advances.

To the human observer, the normal conditions of an environment correspond to the usual living conditions of humans on the surface of the Earth. They match rather small windows around the temperature of 20 °C (often referred to as room temperature, RT), atmospheric pressure around 1 bar (1 bar = 10^5 Pa = 0.1 MPa), a pH close to 7.4, and a salinity around 0.9% to 3%.[19] However, it is important to keep in mind that the majority of organisms on Earth live under other conditions, generally referred to as extreme. Microbial life can indeed adapt to survival in arctic or antarctic oceans[20] below 0 °C, to medium high temperatures, or to a hot and even very hot environment. Today, the known record for high-temperature life is held by *Methanopyrus kandleri* with a growth temperature of 122 °C.[21] Such organisms are termed psychrophilic, mesophilic, thermophilic, and hyperthermophilic, respectively, and typical representative cells of these classes are *Psychrophilus arcticus*, *Eschericia coli*, *Thermus thermophilus,* and *Aquifex aeolicus*. Due to the lack of sunlight penetrating deep water, the deep sea below 100 m reaches on average only 3 °C, but many organisms can be found there.

More than 88% of the Earth's surface are covered by oceans and hydrostatic pressure grows with an approximate rate of about 100 bar/km in the water column. The deepest point in the oceans is the Challenger Deep in the Mariana trench close to Japan with a depth of about 11 km and a hydrostatic pressure of about 1100 bar at the deepest point. In the continental crust, pressure increases even further.[22] The limit of the deep biosphere was fixed rather arbitrarily at 200 bar. The average oceanic depth is 3800 m, therefore most of the organisms (estimated to about 70%) thrive at high hydrostatic pressure (HHP) conditions of about 400 bar. One distinguishes piezosensitive and piezotolerant organisms according to their capacity to live and grow only around ambient pressure or slightly above. Piezophilic and obligate piezophilic organisms need HHP to grow, although piezophiles like *Thermococcus barophilus* can still tolerate ambient pressure temporarily. *Pyrococcus yayanosii* grows best above 600 bar,[23] and is the only obligate piezophilic hyperthermophilic archaeon known so far.

Temperature and pressure have often been shown to have opposite effects on biological systems, as an increase of temperature causes more motion on the molecular level, while increasing the pressure provokes a change to the state with the smallest volume according to Le Châtelier's principle,[24] resulting in compression and often a decrease in motion. In lipid membranes, temperature induces phase transitions from an ordered gel to the liquid-crystalline (fluid-like) phase or even a non-

lamellar fluid structure (Figure 4), whereas HHP generally has the opposite effect. Hence, cell membranes require the capacity to vary their lipid composition to maintain an appropriate membrane fluidity and functionality, termed homeoviscous adaptation.[25]

As mentioned above, crowding can affect all thermodynamic parameters of a system. This will, for example, affect the stability of proteins, i.e., the Gibbs free energy of unfolding, ΔG. According to Hawley's 1971 paper,[26] assuming a two-state process of unfolding, ΔG is approximatively given by

$$\Delta G \approx \Delta G_0 + \frac{\Delta\kappa'}{2}(p-p_0)^2 + \Delta\alpha'(p-p_0)(T-T_0) - \Delta C_p\left[T\left(\ln\left(\frac{T}{T_0}\right)-1\right)+T_0\right] + \Delta V_0(p-p_0) - \Delta S_0(T-T_0)\,, \quad (2)$$

where T_0 and p_0 designate the temperature and pressure of an arbitrary reference state (e.g., ambient temperature and pressure conditions), and Δ stands for the difference between the unfolded (denatured) and native state. The Hawley equation contains six thermodynamic parameters: the compressibility factor $\kappa' = \left.\frac{\partial V}{\partial p}\right|_T$, the thermal expansivity factor $\alpha' = \left.\frac{\partial V}{\partial T}\right|_p$, and the changes in heat capacity C_p, volume V_0 and entropy S_0 at the reference point. The equation points to the fact that both temperature and pressure determine the stability of a protein under a given condition. For $\Delta G = 0$, the *T, p*-stability diagram is obtained, which exhibits an elliptic-like shape for proteins, demonstrating that pressure can shift the thermostability towards lower or higher temperatures, and, conversely, temperature can modify the piezostability of the protein.[27] For few examples, the parameter space given in Eq. (2) has been determined experimentally, only. However, Hawley's equation does not contain any information on the effect of the protein concentration, crowding, cosolvents, pH, or salinity on the stability of the system, although all of these factors are non-negligible. For instance, protein concentration and crowding will directly affect the accessible volume as HHP does. The study of protein's stability and function under such solution conditions is thus of paramount importance for understanding the physiology of extremophiles.

Most water on Earth contains large quantities of dissolved salts, e.g. oceans, soda lakes, or saline groundwater.[28] Thus, saline and hypersaline environments are frequent and salt stress one of the major stresses on cells and cellular components. Saline environments range from sea water concentrations, which is about 35 g NaCl per liter to saturation. Despite these deleterious effects, life can colonize all saline environments, even those at saturation. Inhabitants of salt environments are called halotolerant or halophiles. The most extreme cells, such as *Halobacterium salinarum*, grow best at 4.5 M NaCl and require at least 3 M salt for growth. These species are called obligate halophiles. Living at such salt concentration is a challenge though. Salt causes protein structural collapse because of increased hydrophobic interactions. Indeed, because they are charged, salts impact electrostatic interactions in or between biological macromolecules, lowering salt bridges' strength. Finally, it reduces water activity below the threshold needed to sustain essential biological functions at high concentrations as salt ions compete strongly for water.

2.1. Temperature Effects

Temperature, T, is linearly related to thermal energy, E_{th}, and it is a potential source of energy for many chemical reactions in living organisms. The availability of thermal energy, generally inducing more atomic motion, in turn facilitates the breaking of chemical bounds, inducing, for example, unfolding of proteins at high temperatures. All components of a cell can be differently affected by a heat shock, but well beyond the temperature of cell death they are definitely irreversibly damaged. Figure 4 shows schematically typical effects of temperature on biological systems.

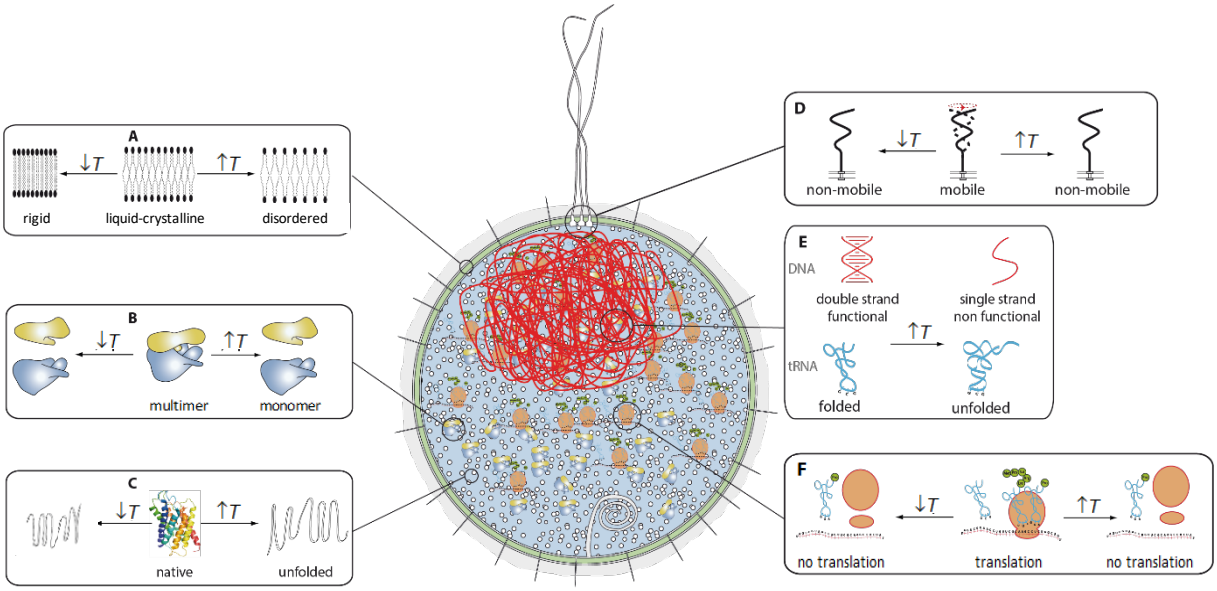

Figure 4. Schematic representation of possible impacts of temperature on biological systems.

Due to their amphiphilic character, lipids usually self-assemble into bilayers, which form closed spherical objects. This phase is known as lamellar phase. The fluid or liquid-crystalline phase is the physiologically relevant one, where the lipid tails have a certain flexibility and the whole membrane the required fluidity and low permeability. Under varying conditions of temperature and pressure, the membrane can undergo phase transitions, to the gel phase with more ordered lipid tails at low temperature or high pressure, and to fluid phases with very disordered lipid tails, sometimes also to non-lamellar (inverse cubic or hexagonal) phases, at high temperature. Both are not suitable for proper physiological function under normal conditions.

The complex biological membranes can easily lose their integrity due to heat shock. Bacterial membranes consist of an outer and inner leaflet. Initial damage can be seen to the outer leaflet already at lower temperatures, leading to structural changes, such as the loss of lipopolysaccharide, which alters the permeability, leads to detachment of periplasmic proteins, and the intrusion of deleterious compounds.[29, 30] It was observed that the outer leaflet of *Cronobacter sakazakii* was altered after application of a heat stress of 47 °C for 15 minutes.[31] The inner leaflet is even more sensitive to heat than the outer one. Heat damage disrupts the biochemical and transport functions of the inner membrane part.[29] Temperature increase induces a change in membrane potential, corresponding to depolarization, which depends on temperature and exposure time. The lipid composition impacts the fluidity, stability and activity of the lipid bilayer. A higher level of saturated lipids guarantees better

maintenance of the integrity at high temperatures, whereas unsaturated chains are more flexible and allow better adaptation to lower temperatures or higher pressures (see below).

Structural and functional proteins are the preferential targets for thermal inactivation because they are vital for cellular functioning. Protein denaturation occurs when cells are thermally stressed, and a clear correlation can be established between the thermodynamic criteria corresponding to protein unfolding and the observed mortality rates of various organisms. Temperature acts on various chemical bonds, hydrophobic interactions and disulfide bridges are particularly heat sensitive. Upon heat stress, the bonds are broken and the proteins lose their conformations and thus their functionality. At very high temperatures, proteins aggregate, leading to an irreversible loss of viability and thus to cell death at a temperature specific for a given cell type.[29, 32] In the highly crowded cell, a multitude of undesirable intermolecular interactions can occur in the cytoplasm at high temperatures, which also affect the conformational stability of proteins, protein-protein interactions through changes of their association and dissociation rates, and hence their activity.[3, 32]

Cells have various protection mechanisms that can prevent their proteome from unfolding within certain limits. High temperatures, usually above 80 °C,[33] causes irreversible denaturation of proteins from organisms that are not adapted to such conditions. Cells are able to synthesize "heat shock" proteins (HSPs), which are molecular chaperones, to protect them against high temperature. HSPs not only preclude denaturation of proteins, but may assist to refold denatured proteins, or remove irreversibly spoilt molecules.[34] Another way for protecting cells from difficult environmental conditions is producing or upregulating particular osmolytes.[35] Osmolytes are small cosolutes assembled by the cell to reinforce the structure of proteins to counteract the impact of harsh conditions.[36] As nanocrowders, osmolytes also increase crowding in cells and restrict the structural arrangement and conformational dynamics of proteins.[37] For more details about cosolvent effects, see Sections 3 and 7.

Nucleic acids are generally more stable against heat denaturation[38] and are thus thought to be not the primary reason of cell inactivation. Very high temperature is required to degrade chemical bonds between the nucleobases in DNA. Ribosomal RNA degradation occurs before the loss of cellular viability, but has been shown to be reversible.[38]

2.2. High Hydrostatic Pressure Effects

The Nobel Prize laureate P. W. Bridgman discovered in 1914 that protein unfolding and denaturation can be induced by high pressure,[39] and many other studies have shown that HHP can lead to the breakdown of intermolecular interactions. At the same time, the native folded structure of the protein is lost, an effect that goes hand in hand with a decrease in the total volume of the protein and the water system favored by unfolding. Temperature change impacts both the thermal energy and the volume, V, of the folded and unfolded states of the protein, which are also affected by pressure, hence

$$\Delta V = \Delta V_0 + \Delta\alpha'(T - T_0) - \Delta\kappa' (p - p_0) \quad (3)$$

with the thermal expansivity factor $\alpha' = \partial V/\partial T$) and the compressibility factor $\kappa' = \partial V/\partial p$ of the two different states contributing to the volume change of unfolding, ΔV. Henceforth, temperature and pressure are equally important to fully understand the conformational behavior of biosystems. Liquid

water with its low compressibility is an additional essential factor in understanding the impact of pressure. One to two layers of water molecules bind usually more strongly on the surface of a biomolecule,[40] the so-called hydration water, with properties slightly different from those of bulk water. Notably, the hydration water adopts a different network structure and exhibits a different sensitivity to temperature and pressure changes.[41] Pressures below 10 kbar generally affect essentially van der Waals and hydrogen bonding as well as hydrophobic interactions, which results in changes of the conformational dynamics and interactions, only. In contrast, high pressure values beyond 10-20 kbar are needed to impact non-covalent interactions,[15] which corresponds to a pressure range beyond the freezing point of water.

The importance to use HHP as an additional variable when probing thermodynamics and kinetics has been brought to mind and increased largely such biophysical studies in the last decades.[27, 42-45] Not only pressure application is of general interest to probe physical-chemical properties, it is also important in a biological context, e.g., for understanding the physiology of organisms adapted to a high-pressure environment, which survive at pressures up to about 1 kbar or more in the deep ocean and sub-seafloor.[17, 46-49] In addition, HHP emerged as an interesting variable for biotechnological applications.[43, 50] High pressure allows refolding of protein aggregates (also cellular inclusion bodies), and pressure applied to foodstuff (termed 'pascalization') has analogous effects to temperature sterilization inactivating microorganisms, viruses and enzymes. In contrast, the flavor and nutrient content of food are widely preserved.[50] Diseases like insulin, islet amyloid polypeptide, β2 microglobulin, Aβ, and α-synuclein have their origin in proteins which are not correctly folded and lose their function, leading to the formation of aggregates (denoted amyloids) in various tissues. Amyloids are aggregations of monomeric proteins in their native, unfolded or intermediate form with ordered secondary structure elements which adopt the canonical cross-β structure, forming β-sheets with β-strands oriented perpendicular to the fibril axis. Although many forms of amyloid fibrils are known to be toxic, their role in these diseases is still debated. It has been assumed that precursors of amyloid fibrils are much more toxic than the amyloids themselves. Hence, pressure and cosolvent perturbations have been used to study the stability, energetics, packing, and intermolecular interactions of amyloid fibrils.[45, 51] The pressure sensitivity of protein oligomers depends on their level of structural order and compaction. While unstructured aggregates generally respond more sensitively to pressure and tend to refold typically at sub-kbar pressures, in fully developed fibrils the degree of dissociation due to pressure depends on the exact type of polypeptide backbone and side-chain packing. Therefore, the use of HHP permits to discriminate between different levels of amyloid formation and to acquire valuable structural and thermodynamic data at different stages of the transformation. Finally, pressure application allows identifying intermediate structures and thus mechanisms leading to different toxic amyloid fibril forms, but can also provide precious targets for inhibitor development.[45, 51]

An overview on basic concepts and high-pressure instrumentation is given in ref.[43]. Here, we discuss the impact of both pressure and crowding agents on the conformation of biomolecules, largely focusing on proteins and their effect on ligand binding and enzymatic reactions. A schematic representation of the effect of high hydrostatic pressure on biological systems can be found in ref. [52]

2.3. Salinity

Organisms living in high salinity environments were amongst the first cultivated extremophiles in the late 19th century. Indeed, life can thrive from zero salinity up to saturation (> 6 M NaCl).[53] Under these conditions, cells experience a strong stress due to the presence of charged ions in solutions, including mostly sodium, magnesium and potassium cations. As mentioned above, protein folding and activity is highly dependent on the hydration layer. Protein solubility is mainly determined by the properties of the solvent-protein interface. Weak attractive forces promote aggregation, whereas repulsive interactions favour dissolution. The presence of salt alters the equilibrium established between the soluble and the aggregated forms. Stabilizing salts include Na^+ or K^+, sulphate and phosphate. Under salt-rich conditions, proteins from mesophilic organisms tend to aggregate, while proteins from halophiles remain soluble.[54-57] The presence of salt in excess has strongly deleterious effects on proteins, mostly due to the fact that the charged ions compete with water and perturb the dielectric environment of proteins, which tends to destabilize them. A direct consequence is protein denaturation and/or aggregation. Cells adapt to salt stress by accumulating organic cosolutes, called osmolytes.[58] They generate an osmotic flow of water that is directed into the interior of the cell[59] by the way compensating the osmotic pressure arising from the high salt concentration outside the cell. At the same time, an ion-pumping mechanism can be activated by the cells to maintain the intracellular ionic concentration in the physiological range,[35] protecting the biomacromolecules from the adverse effects of salt ions. This is known as *salt-out* strategy, which can function at salt concentrations up to 1.5 M.[58] In these organisms, there is no or little requirement for protein adaptation. However, the presence of large amounts of the organic osmolytes leads to further crowding within the cell.[59]

Species living at salt concentrations higher than 1.5 M, essentially archaea, developed a much simpler approach to deal with osmotic stress: they accumulate intracellular salt to match the ionic strength of the environment, thus equilibrating the ionic forces exerted on both sides of the cell membrane.[60] This is called the *salt-in* strategy. In these extreme halophiles, the ions usually accumulated are K^+ and Na^+, regardless of the nature of the extracellular cation (usually Na^+).[61] Intracellular KCl concentrations can achieve conditions near saturation and up to 5 M as in *Halobacterium salinarum*. The physical principle behind is the same as the one responsible for the accumulation of compatible solutes. As a consequence, the intracellular space, and all the biomacromolecules, are experiencing molar concentrations of salt. This strategy implies that proteins are capable to fold and function under high salt conditions, which requires substantial protein structural adaptations.[57, 62] Hence, cellular and molecular adaptation to high salinity is highly dependent on crowding, either by small organic cosolutes in species living up to 1.5 M salinity or by inorganic osmolytes in those living at higher concentrations. For more details about cosolvent effects, see Section 3.

3. Pressure and Cosolute/Crowding Effects on Proteins

The pressures relevant for the study of biological systems typically range from 1 bar to 10 kbar, i.e., a pressure range in which water does not freeze at ambient temperature. Such pressures alter intermolecular distances between molecules, affect the conformational dynamics and loosely packed supramolecular structures of biomolecular systems, but generally do not break covalent bonds

(disulfide bonds are an exception). The quantitative description of the effect of pressure on any chemical equilibrium and reaction rate (e.g., protein folding, protein/nucleic acid-ligand interactions, enzymatic reactions) is given by Eq. 4:[27, 42, 43]

$$\left(\frac{\partial \ln K}{\partial p}\right)_T = -\frac{\Delta V}{RT}, \qquad \left(\frac{\partial \ln k}{\partial p}\right)_T = -\frac{\Delta V^{\neq}}{RT} \tag{4}$$

where K is the pressure-dependent equilibrium constant, k is the pressure-dependent rate constant of the reaction, ΔV the reaction volume, and $\Delta V^{\#}$ the activation volume of the reaction. The mechanistic description based on ΔV and $\Delta V^{\#}$ provides information on the existence of different conformational states (denoted conformational substates, CS) and the structure of the transition state of a reaction or a conformational transition. Any reaction associated with a negative $\Delta V^{\neq}$, i.e., when the transition state of the reaction has a smaller volume than the partial volumes of the reactants, is accelerated upon pressurization, and *vice versa*. For example, for enzymatic reactions, $\Delta V^{\neq}$ describes the volume difference between the transition state ($ES^{\neq}$) and the ground state of the enzyme-substrate complex (ES) (but includes also the reactant states (E, S) at low substrate concentrations). Because of the different compressibilities of the reactants, the ES complex and the transition state, the $\Delta V^{\neq}$-values can be positive or negative, which may change with increasing pressure amplitude, however. The volume change, ΔV, of a biochemical process, e.g., upon ligand binding or unfolding of a protein, can be determined by measuring the pressure dependence of K, and the activation volume can be obtained by measuring the effect of pressure on the rate constant, k, as indicated in Eq. 4. Since the volume changes encompass contributions from steric (packing) and solvational (hydration changes) factors, the magnitude and sign of the volume change can provide mechanistic information about the reaction in question.

A large number of studies have reported the effect of macromolecular crowding on protein folding, ligand binding, and biochemical reactions. To elucidate the stabilizing or destabilizing effect of crowding on folding, steric (excluded volume, entropy driven) and nonspecific chemical ("soft" (weak) or quinary) interactions between the biomolecule and the cosolute have been invoked (Figure 5).[36, 63] The enthalpic contribution depends on both temperature and the chemical compositions of the biomolecule, the crowder, and the solvent. Electrostatic repulsion of equal charges, for example, can enhance the stabilizing effect of excluded volume, while attractive interactions (e.g., H-bonding, electrostatic, cation-π, and hydrophobic interactions) can counteract the influence of the steric repulsion.

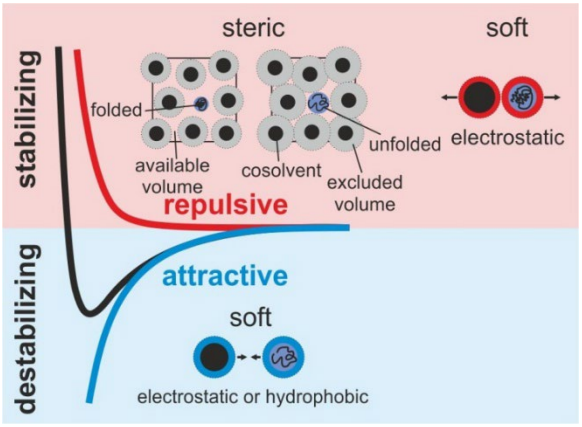

Figure 5. Schematics of the various contributions that determine the effect of macromolecular crowding on the folding reaction of biomolecules (e.g., proteins). In general, the interaction between a biomolecule (solute) and the surrounding crowding agent (cosolute) consists of short-ranged hard-core repulsion (entropically driven) and non-specific weak (enthalpically driven) interactions. The volume exclusion results from the mutual impenetrability of the biomacromolecules and inherently stabilizes compact states, such as the folded state of proteins. Depending on their chemical composition, the weak interactions between the solute and cosolute can be attractive or repulsive. Repulsive electrostatic (e.g., Coulombic) interactions enhance the entropic depletion force and thus stabilize the compact structure, while attractive electrostatic and hydrophobic interactions have a destabilizing effect. Reproduced from ref. [36]. Copyright 2017 Wiley-VCH Verlag GmbH & Co. KGaA, Weinheim.

At pressures beyond several kbar (typically between 2 and 8 kbar), most monomeric proteins unfold reversibly.[15, 27, 42, 43, 64-68] However, multimeric proteins and multiprotein complexes generally dissociate into their subunits at much lower pressures (typically below 2 kbar). The dissociation of oligomeric protein complexes at rather low pressures can be explained by the imperfect packing of amino acid residues at the interface of their subunits.[27, 36, 42, 43, 66, 69] Next to release and subsequent hydration of void spaces upon unfolding, negative volume changes result also from the disruption of salt bridges and polar bonds and subsequent hydration (denoted electrostrictive effect).[27, 42, 43] Of note, HHP is also effective in the unfolding and subsequent (upon pressure release) refolding of proteins from insoluble aggregates such as inclusion bodies.[70]

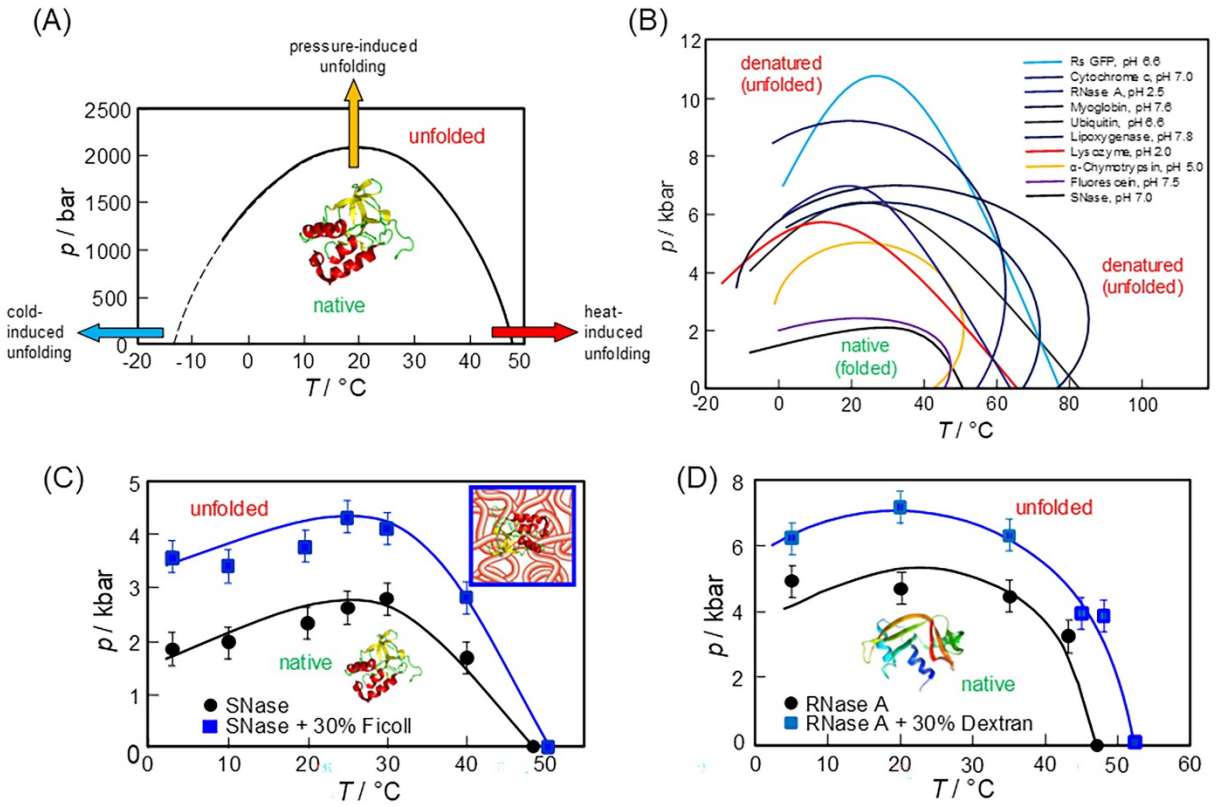

Figure 6. (A) Temperature-pressure stability phase diagram of the monomeric protein staphylococcal nuclease (SNase) in buffer solution. Reproduced from ref.[27] Copyright 2007 De Gruyter (B) (*p*-*T*)-stability diagram of selected monomeric proteins.[27, 42, 44] Adapted from ref.[44] Copyright 2023 American Chemical Society (C) Effect of macromolecular crowding (30 wt% Ficoll) on the (*p*-*T*)-stability diagram of SNase. Reproduced from ref.[71] Copyright 2014 PCCP Owner Societies (D) Effect of 30 wt% of the macromolecular crowding agent Ficoll on the (*p*-*T*)-stability diagram of RNase A.[27, 44, 71, 72] Reproduced from ref.[72] Copyright 2012 Wiley-VCH Verlag GmbH & Co. KGaA, Weinheim.

Figure 6A demonstrates that proteins can also unfold in the cold, which generally takes place between -30 and -10 °C. Whereas heat-induced denaturation is mainly driven by the large configurational entropy gain upon unfolding, cold denaturation is a milder form of unfolding (similar to HHP-induced unfolding), which leads to partial unfolding of the protein only, leaving many residual secondary structure elements intact. At low temperatures, a sufficiently negative hydration enthalpy due to favourable interactions between water molecules and the protein leads to destabilisation of the native protein structure. Dry proteins have been observed to be highly resistant to pressure. A similar mechanism was suggested to explain the high resistance of spores against harsh environmental conditions, which is largely due to the low level of hydration inside these particles.[73]

Changes in the unfolding/denaturation temperature and pressure have been determined for several proteins, including SNase, in the presence of cosolvents or osmolytes (Figure 6B). A significant increase in unfolding temperature (T_m) and pressure (p_m) was determined in case of sucrose, sorbitol, glycerol, and the deep-sea osmolyte trimethylamine-*N*-oxide (TMAO), with typical values of ΔT_m = 2-4 °C/M cosolvent and Δp_m = 2 kbar/M cosolvent, respectively). In these cases, the cosolvents are preferentially excluded from the surface of the protein, this is to say, the proteins are preferentially

hydrated. As the excluded volume is proportional to the solvent-accessible surface area (SASA) of the protein, exclusion of the cosolvent stabilizes protein conformations with smaller SASA, such as the compact folded native state of proteins (and other biomacromolecules).

Small-angle X-ray scattering (SAXS), differential scanning calorimetry (DSC), and Fourier-transform infrared (FT-IR) spectroscopy were used to also investigate the effect of neutral macromolecular crowder agents, including dextran, Ficoll, and PEG (Figure 2), on the temperature- and pressure-dependent stability diagram of proteins. It was found that temperature- and pressure-induced equilibrium unfolding of SNase in 30 wt% Ficoll solutions, mimicking strong intracellular crowding conditions, is significantly shifted to higher temperatures and pressures (Figure 6C).[71] At ambient temperature, the unfolding pressure increased by Δp_m = 1.8 kbar, and the unfolding temperature at ambient pressure was found to shift by ΔT_m = 4 °C. This stabilizing effect is largely due to the steric excluded volume effect caused by the crowder molecules, which favors the more compact native state of the protein. A similar stabilizing effect has been observed for the protein RNase A (Figure 6D),[72] which is even stronger in solid mesopores.[74] Results based on transient fluorescence and absorption spectroscopies by Das and coworkers showed that the effect of cosolvents and crowding agents on the dynamical properties the hydration water contribute to stabilization of the protein's native fold as well.[75] For dextran and Ficoll, slower water dynamics (solvation) was observed for human serum albumin (HSA), indicating that the bound water forms stronger H-bonds with the protein in the presence of these two crowders than in the crowder-free solution. This is to say, the associated water molecules have less flexibility. These results are in good agreement with THz experiments probing water network dynamical properties.[76, 77] Such a decrease in entropy of the associated water makes the protein less likely to unfold, rendering the entropic component (i.e., lower degrees of freedom) of protein unfolding stabilizing. This situation is hence similar to the traditional excluded volume picture, where the crowder-induced positional restriction leads to a decrease of the protein's entropy. Differences between the various crowding agents are supposedly due to their different polarities.[75] PEG-35, being more hydrophobic than the carbohydrate-based crowders, exhibits a faster solvation time of HSA, indicating the presence of less rigid and more flexible associated water molecules, i.e., a more disordered hydration network, which in turn must have a destabilizing entropic effect on the protein stability. Generally, cosolvents and crowding agents have been shown to strongly affect not only the dynamics of the hydration water, but also the conformational and internal dynamics of proteins, and thus also their response to high pressure.[78, 79]

Winter and coworkers investigated the influence of high pressure on the sub-ns dynamics of the internal H-atoms of lysozyme in aqueous solution by elastic incoherent neutron scattering (EINS) up to pressures of several kbar.[79] They observed a significant reduction of the mean-squared displacement (MSD) of the H-atoms of the protein already at rather low pressures of several hundred bar in bulk buffer solution. Under strong self-crowding conditions, i.e., at a protein concentration of 160 mg/mL, a typical protein concentration also found in the biological cell, a strong restriction of the dynamics was observed, which reduced the MSD of the H-atoms by ~60% and rendered their pressure-dependence almost negligible. Significantly reduced internal sub-ns dynamics was also observed in the presence of high TMAO concentrations.

Next to affecting the stability of proteins against unfolding, high pressure also often inhibits polymerization of proteins. Mitosis of eukaryotic cells is inhibited already at a pressure of about 300

bar, which is attributed to the disorganization of microtubules, which makes up the main component of the spindle apparatus of the cell. Gao et al.[80] investigated the pressure stability of microtubules at different structural and dynamics levels employing high-pressure SAXS and FT-IR spectroscopy. They showed that microtubules are indeed hardly stable under abyssal conditions where pressures up to at least 1 kbar are encountered. The high pressure sensitivity is thought to be largely due to packing defects and the internal voids in the microtubules. The authors also showed that a crowded cellular environment created by PEG 20k as mimic and accessory proteins can increase their pressure stability markedly and accelerate the very pressure-sensitive *de novo* formation of microtubules.[80-82] Further, the presence of 10 wt% Ficoll 70, exhibiting mainly hard-core repulsion, was found to lead to a decrease in the lag time and the half-life of tubulin polymerization as well as an increase in the growth rate of microtubules by one order of magnitude. Due to the excluded volume effect, more compact structures of tubulin are favored, such as oligomeric and polymeric assemblies. Additional properties of the crowded biological cell, such as a multitude of weak nonspecific interactions and an increased viscosity, had a minor effect on the polymerization kinetics of tubulin. Also the polymerization of actin has been shown to be very pressure sensitive in *vivo*.[83, 84] HHP of 1 kbar decreased the *de novo* nucleation rate of actin polymerization even by approximately two orders of magnitude, corresponding to a large positive activation volume of $\Delta V^{\neq}$ = 104 mL mol^{-1}, which suggests that the initial assembly of G-actin oligomers creates significant void space at the contact sites, rendering nuclei formation the most pressure-sensitive process of the polymerization process. Crowding agents such as Ficoll dramatically increase the stability of the protein and allow actin to be sufficiently stable under the temperature and pressure conditions that exist in the extreme conditions on Earth. Yet, the use of different protein-based crowding agents (e.g., lysozyme and BSA) has shown that, in case of unlike-charged protein pairs, the enthalpic contribution of the crowding effect can significantly retard or even inhibit the polymerization process of actin.

Crossing the elliptic-like (*p*-*T*)-phase boundary (Figure 6A) of proteins by applying fast pressure-jumps also allows exploration of the folding kinetics of proteins.[71, 85-87] Employing high-pressure SAXS on SNase at ambient temperature showed that a rapid decrease of pressure from 4000 bar (which corresponds to unfolding/denaturing conditions) to 800 bar (which corresponds to native conditions) decreased the radius of gyration, R_g, from 29 to 18 Å, following a relaxation profile that can be described by a single exponential decay with time constant, τ, of 4.5 s. Conversely, a positive pressure-jump from the native folded state to the unfolded state resulted in a very slow relaxation with a much longer exponential time constant of τ = 14 min. From the analysis of the kinetic SAXS and complementary fluorescence spectroscopic data, the activation volumes for folding and unfolding could be determined. The activation volume for folding was found to be large and positive ($\Delta V_f^{\neq}$ = 57 mL mol^{-1}) and that for unfolding small and negative ($\Delta V_u^{\neq}$ = -23 mL mol^{-1}). For comparison, the overall volume change of unfolding, ΔV, of SNase is -80 mL mol^{-1}. Hence, the volume of the protein in the transition state is thus significantly larger than in the unfolded state, but slightly smaller than in the folded state. The positive $\Delta V_f^{\neq}$ value indicates that the transition state is accompanied by chain collapse with significant dehydration. The addition of 30 wt% Ficoll does not strongly influence the unfolded state structure of the protein, the protein folding/unfolding kinetics changes significantly in the presence of the crowding agent, however.[71] Contrary to the common assumption that macromolecular crowding increases the rate of protein folding, the data showed that the folding rate of SNase actually decreased markedly in the presence of Ficoll PM 70. These results suggest that besides the excluded volume effect, other factors need to be taken into account. Among these factors, crowder-induced

microviscosity changes appear to be most important and may even exceed the contribution of excluded volume. Such an interpretation is consistent with the notion that the protein folding process requires many nonlocal and large-scale movements.

3.1 Protein-Protein Interactions and Liquid-Liquid Phase Separation

Knowledge of the phase behavior and underlying intermolecular interactions of concentrated protein solutions up to several hundred grams per liter are of high relevance, e.g., for understanding the properties of the crowded cellular milieu, for food processing of proteins, the delivery of concentrated antibody solutions, or for understanding diseases associated with the fluid-to-solid phase transition and aggregation of fibril-forming amyloidogenic proteins (e.g., α-synuclein in Parkinson's disease).[51, 70, 88, 89] Both, intermolecular interactions between proteins and their phase behavior are affected by crowding agents and HHP, both principally favoring reduction of intermolecular spacing (below the limit of pressure-induced unfolding). High-pressure SAXS experiments have been used in conjunction with liquid-state-physics theoretical approaches to determine the protein-protein interaction potential, $V(r)$, at high pressure both in the absence and presence of crowding agents and various osmolytes.[90-93] Protein-protein interactions in 10 wt% lysozyme solutions at pH 7, where the protein is positively charged, have been shown to be affected by pressure in a nonlinear way and modulated by these cosolutes. The depth of the attractive part, J, of $V(r)$ has been shown to decrease slightly from $\sim$4.3 k_BT at 1 bar to $\sim$3.5 k_BT at 1.5 kbar, but increases again to 4.6 k_BT at 4 kbar in neat buffer at room temperature. As a result, the mean intermolecular distances initially decrease upon compression up to 2 kbar (by $\sim$2%; from 8.4 nm to 8.2 nm) and then increase again by about the same amount up to 4 kbar. The origin of this effect is probably due to changes of the water structure and increased repulsion (including hydration repulsion) at very high pressures. Measurements in the presence of various osmolytes revealed that the compatible deep-sea osmolyte TMAO distinctly increases the attractive part of lysozyme's pair-interaction potential, J, whereas other osmolytes (glycine, urea, betaine, proline, etc.) rendered $V(r)$ more repulsive.

The effect of neutral crowding agents, such as PEGs, on $V(r)$ was found to depend sensitively on the polymer concentration and the size ratio between the polymer and protein. The strongest effect was observed with small-size PEG molecules, where a decrease of the mean intermolecular spacing of protein molecules with increasing crowder concentration was observed.[94] The mean intermolecular distance changes from 6.1 nm to 4.4 nm for 10 wt% lysozyme in 50 mM Bis-Tris buffer in the presence of 30% (w/v) of PEG 200, but no significant effect was observed for PEG 20 kDa. For comparison, the thickness of a water layer is about 0.25 nm. The effect weakens at intermolecular distances when the second hydration shell of the protein is reached. Strong repulsive forces, such as weak protein-PEG interactions and hydration-shell repulsion appear to be operative at short distances. Such interactions are expected to stabilize the protein against depletion-induced aggregation, even at pressures as high as those in the deepest ocean trench ($\sim$1 kbar). The increase in polymer concentration beyond a polymer-size specific threshold, i.e. beyond the overlap concentration c^*, where the structure of the polymer solution changes from single dispersed polymer chains to an entangled network, leads to maintenance of the distance comparable to that in the polymer-free system.[93]

Many proteins, including lysozyme, undergo (often metastable) liquid-liquid phase separation (LLPS) at low temperatures and high protein concentrations, i.e., they exhibit an upper critical solution

temperature (UPCS, Figure 7A). Hence, LLPS is another method to create a strongly crowded environment. Such biomolecular droplet phases (also denoted liquid condensates) form non-membraneous compartments in biological cells, carrying out a number of biological functions, including signal transduction, translation, cell division, and stress response.[95] Recent studies on the effect of high pressures on proteinaceous LLPS systems revealed a remarkably high pressure-sensitivity of such protein condensates.[96-101] Liquid droplets formed by the eye lens-protein γ-crystallin or the PSD-95/SynGAP protein system that mimics postsynaptic densities in neurons showed dissolution of the droplet phase already at tens to hundreds of bar. Figure 7B shows the effect of the spherocylindrical crowding agent Ficoll (70 kDa, hydrodynamic radius of ~4.7 nm) on the LLPS region of γD-crystallin at two different concentrations. γD-crystallin is an eye-lens protein exhibiting a metastable LLPS region at low temperatures. As depicted in Figure 7B, Ficoll 70 leads to a drastic increase of the cloud point temperature, T_{cloud}, here shown for two different protein concentrations.

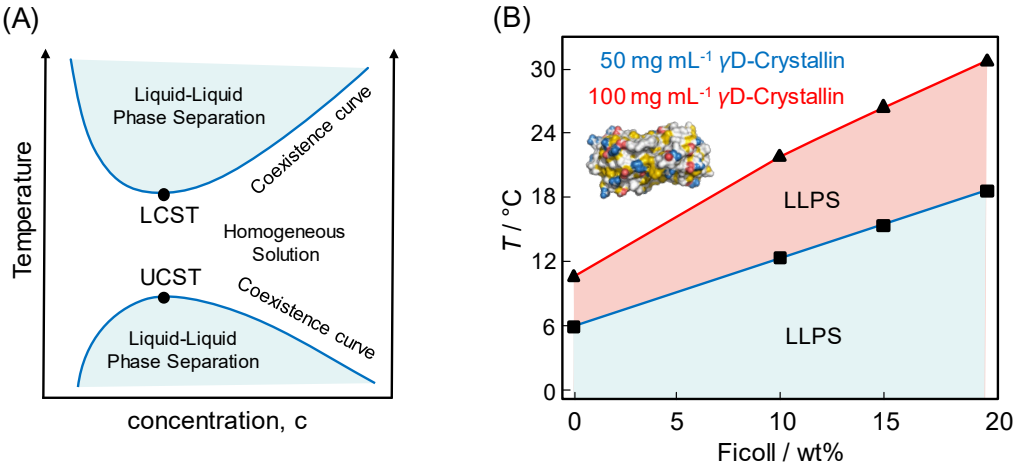

Figure 7. (A) Schematic representation of the temperature-protein concentration phase diagram of a highly concentrated protein solution with an upper (UCST, e.g. γD-crystallin) and lower (LCST, e.g. elastin) critical solution temperature. Reprinted from ref.[98] Copyright 2019 American Chemical Society (B) $T_{cloud}(c_{Ficoll})$ phase diagram for two different γD-crystallin concentrations at ambient pressure.[97, 98]

As another example, we show the effect of pressure and crowding on the LLPS of the RNA binding protein FUS (Fused in Sarcoma), an intrinsically disordered protein that is found inside ribonucleoprotein granules and other membraneless organelles. In neat buffer, a 3 μM concentrated FUS solution forms droplets below its upper critical solution temperature of $T_c \approx 30$ °C. Addition of 100 mg/mL Ficoll shifts the cloud point temperature to ~42 °C. i.e., by as much as 12 °C. The pressure-dependence of the LLPS of the protein is also markedly altered upon addition of the crowding agent. The protein droplets dissolve at ~500 bar in pure buffer, but at a pressure as high as ~1200 bar in the presence of 100 mg/mL Ficoll 70. The crowding agent increases the effective protein concentration through the excluded volume effect, leading to an increased effective attraction between the FUS molecules and making the LLPS state more stable.[98] Li et al.[101] also found that the droplet phase of FUS disappears with increasing pressure, but reappears again at pressures beyond ~2 kbar. The high pressure-sensitivity of the droplet phase can, again, be attributed to a large number of water-inaccessible void spaces formed transiently by dynamic contacts between neighboring FUS molecules. The behavior of the reentrant high-pressure phase of FUS has been attributed to favorable π-π-, cation-

π-, and (water-mediated) hydrophobic interactions within the more densely packed protein droplets.[101]

The reentrant high-pressure LLPS formation was also observed in other protein condensates, e.g., concentrated lysozyme solutions at low temperatures.[94, 102] SAXS measurements were carried out to determine the phase boundaries (binodals) for LLPS in 285 mg/mL lysozyme in Bis-Tris buffer solutions with an ionic strength of 0.5 M NaCl at hydrostatic pressures up to 3.5 kbar in the absence and presence of the crowding agent Ficoll. Figure 8 depicts the temperature-concentration phase diagrams of the system as a function of protein volume fraction, ϕ, and, for $\phi = 0.2$ as a function of pressure in neat buffer solution and in the presence of just 1.25% (w/v) Ficoll PM 70 as determined by high-pressure light transmission (turbidity) measurements. Clearly, the low-pressure (LLPS)- and high-pressure (HP)-LLPS boundaries in the (*p*-*T*)-phase diagram are shifted to higher temperatures in the presence of Ficoll PM 70, as was also observed upon increasing the protein concentration (i.e., under self-crowding conditions). Further, phase separation is promoted upon addition of the macromolecular crowder Ficoll PM 70, leading to a stabilization of the droplet phase by about 1 kbar. Thus, the crowding agent Ficoll seems to simply act by excluding the available volume to the protein, effectively increasing the protein concentration. The reentrant LLPS found for concentrated protein solutions in pure buffer at kbar pressures reflects the increasing attraction of the protein molecules at high pressure and/or changes in solvent-mediated interactions. Of note, the more apolar macromolecular crowding agent PEG revealed an opposite effect, i.e., leads to more repulsive effective protein-protein interactions and destabilizes the droplet phase, probably due to soft enthalpic PEG-protein interactions.[93] Certainly, changes in the dielectric permittivity of the solutions by adding the different cosolutes leads to changes of the Coulomb term in $V(r)$ as well.

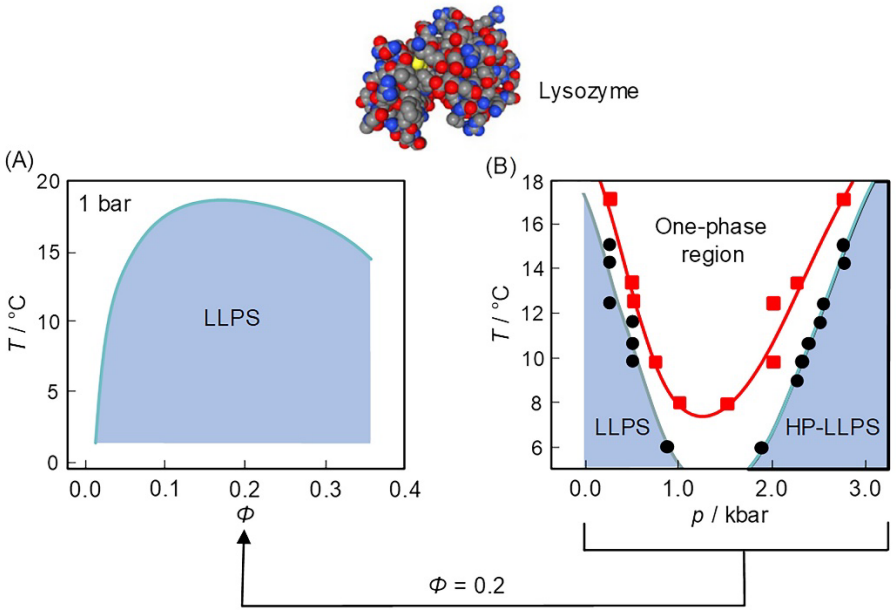

Figure 8. (A) Temperature-concentration phase diagram of an aqueous lysozyme solution (pH 7.8, 0.5 M NaCl); ϕ is the volume fraction of the protein. The critical protein concentration is 23 ± 1 wt% (w/v), which corresponds to a volume fraction of $\phi \approx 0.18$. (B) (*p*-*T*)-phase diagram of the LLPS region for a lysozyme concentration of $\phi = 0.18$. Low (LLPS) and high pressure (HP-LLPS) areas of the LLPS of the neat lysozyme solution are marked in blue. The red line marks the LLPS region of the protein upon

addition of 1.25% (w/v) Ficoll PM 70.[94, 102] Adapted from ref.[98] Copyright 2019 Wiley-VCH Verlag GmbH & Co. KGaA, Weinheim.

Of note, crowded environment effects as imposed by PEG and dextran may also promote droplet densification, droplet fusion, and partitioning in the condensed droplet phase.[103] Further, the crowding agents may significantly vary the surface tension of the phase droplets, invoking changes in their morphology. Using biphasic coacervate droplets by coacervation of poly(L-lysine) and oligonucleotides in crowded media provided by PEG and dextran, Bai et al.[103] showed, owing to their different partitioning behavior, evolvement of spherical droplets into clusters and networks in PEG solution, while in dextran solution, the coacervates retain the morphology but vary in phase ratio. More complex structures are formed in the mixed PEG/dextran crowding medium.[103]

Recently, X-ray photon correlation spectroscopy (XPCS) in concert with high-pressure SAXS was used to study also the kinetics and dynamic fingerprints of pressure-induced LLPS formation in a concentrated water-lysozyme solution at near critical protein concentration (238 mg/mL, 0.5 M NaCl) as a function of quench-depth into the two-phase region.[104] XPCS is a powerful technique to investigate dynamic processes at nanometer length scales and ms-to-s time scales in soft condensed matter systems. In XPXS, the dynamics of the sample is revealed by the intensity fluctuations of the recorded speckle patterns of the scattered synchrotron X-ray beam. Depending on the time scale, ranging from ms to tens of seconds, and the quench depth into the spinodal two-phase region, different processes could be identified: a rapid diffusion-driven growth and fusion of droplets, followed by a slower coarsening process with the onset of physical gel formation and appearance of viscoelasticity at deep quenches into the spinodal region. A similar behavior was observed upon entering the HP-LLPS region of lysozyme (Figure 8), except that formation of larger structures at the beginning of the coarsening process and a slower growth of correlation lengths in the later phase of the phase transition was recorded.[105] No glass-like behavior and complete dynamic arrest could be observed as in corresponding deep temperature-quench experiments.[104, 105] In fact, highly concentrated globular proteins such as lysozyme are able of forming soft nanostructured protein gels upon reduction of the repulsive part of $V(r)$, as achieved here by adding charge-screening 0.5 M NaCl. Addition of 5 (w/v)% of the crowding agents PEG2k and PEG4k, i.e., at a concentration below their overlap concentration, c^* (c^*(PEG2k) = 13 (w/v)%, c^*(PEG4k) = 8 (w/v)%), resulted in a slower growth dynamics and a decrease of the correlation length of fluctuations, which is probably due to soft crowder-protein interactions.[105] Compared to temperature-quenching, the quench depth into the two-phase region of a *p*-jump of 1 kbar corresponds only to an about 1 k_BT change in interaction energy, hence full dynamic arrest by passing the glass line is not yet reached and the overall dynamics is slower compared to temperature-quenches.

4. Pressure and Cosolute/Crowding Effects on Nucleic Acids

Unlike proteins, pressure has been shown to have a very small effect on the structure and stability of canonical double-stranded polymeric DNA (B-DNA).[106, 107] However, it has been lately shown that kbar pressures can significantly destabilize non-canonical nucleic acid structures, such as small hairpins, i-motifs, and G-quadruplexes, which is mainly due to hydration changes upon unfolding, the electrostrictive effect upon release of internal cations, and/or packing defects within their folded

structures.[108-112] The single-molecule Förster resonance energy transfer (smFRET) methodology was used to directly determine the population distribution of such structures both at ambient and high pressure conditions. Upon pressurization, a conformational transition takes place from a closed native state to an open state, accompanied by a volume decrease of typically -10 to -30 cm^3/mol, which leads to an about 1.5- to 4-fold increase of unfolded state conformations upon a pressure increase of 1 kbar. Also in this case, stabilizing osmolytes such as TMAO as well as crowding agents like Ficoll are able to shift the conformational equilibrium toward the more compact native (closed) state of DNA hairpins (DNA-HP), such as the polyA loop DNA-HP studied by Patra et al.[112] In pure buffer, pressurization shifts the conformational equilibrium of the DNA-HP towards the fully unfolded state. The volume change upon unfolding of ΔV_u = -17.7 cm^3/mol indicates a smaller partial molar volume of the unfolded state compared to the folded state (Figure 9), which can be attributed to the electrostrictive effect, i.e., a change in hydration volume upon unfolding as the unfolded state has a larger SASA than the folded state. Packing defects of the bases in the folded structure of the DNA-HP, i.e. void spaces that are filled with water upon unfolding, contributes probably also to ΔV_u. In the presence of Ficoll, ΔV_u reduces to -6.6 cm^3/mol, i.e., leads to a smaller volume change upon unfolding, rendering the DNA-HP rather pressure stable. Dwell time analysis of the smFRET data revealed a folding rate of the DNA-HP of 48.9 s^{-1}, which is drastically faster than the value of 9.2 s^{-1} observed for neat buffer. The unfolding rate of 4.1 s^{-1} observed in the presence of 20 wt% Ficoll does not differ significantly from the pure buffer value of 3.3 s^{-1}, however (Figure 9), i.e., the crowding agent stabilizes the folded state kinetically by significantly increasing the folding rate. Patra et al.[112] also found that compatible cosolvents and crowding populate different conformational substates to some extent that do not occur in neat buffer solution, suggesting existence of a rugged free energy landscape for the DNA-HP. These data again demonstrate the important role of cellular crowding and compatible osmolytes in rescuing biological functions under extreme environmental conditions, such as at high pressure. The thermodynamic and kinetic parameters at high-pressure conditions are controlled by the influence of the cosolutes on the volumetric properties of the biomolecule in its different states.

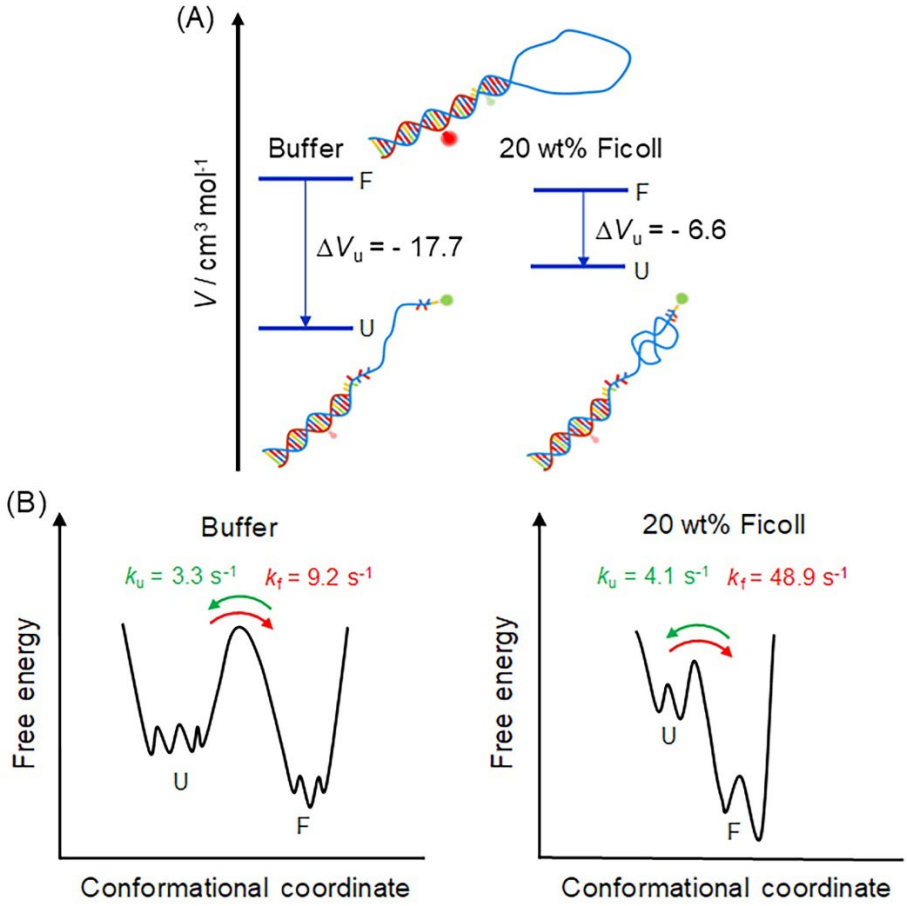

Figure 9. (A) Volumetric profile of a polyA loop DNA-HP at T = 25 °C for the unfolding transition in pure buffer and in the presence of the crowding agent Ficoll 70. $\Delta V_u = V_u - V_f$ denotes the partial molar volume change upon unfolding. In the presence of 20 wt% Ficoll 70, the unfolded state (ensemble) is more collapsed, resulting in an overall larger volume compared to V_u in pure buffer. (B) Free energy landscape of the DNA-HP in pure buffer and in 20 wt% Ficoll 70. U and F denote unfolded and folded conformations, respectively. The green and red curved arrows indicate unfolding and folding, respectively. Adapted from ref.[112]. Copyright 2018 The Authors, Oxford University Press under Creative Commons CCBY license.

5. Pressure and Crowding Effects on Membrane Systems

Biological membranes form the boundary for individual biological cells and several of their intracellular organelles. Their basic structural element consists of a phospholipid bilayer matrix that is self-assembled by the hydrophobic effect. In addition to their barrier function, they serve as interfaces for a number of membrane-associated biochemical reactions, including metabolism, transport, and signal transduction. Membrane proteins, which make up a large part of biological membranes and 25-30% of all proteins, include not only integral proteins with transmembrane domains, but also proteins peripherally bound to the lipid interface via hydrophobic patches, amphipathic helices, or lipid anchors. Biological membranes are among the most pressure-sensitive biomolecular systems. The physicochemical properties of the membrane, such as its bending modulus, lipid packing, fluidity, and the lateral organization of lipids and membrane-associated proteins that affect lipid-protein interactions and hence membrane protein function are significantly affected by high pressure. Lamellar phospholipid bilayers generally exhibit one or more phase transitions, such as a gel-to-fluid

(liquid-crystalline) chain-melting transition. A fluid-like phase is required for optimal physiological function. In the fluid phase, the two acyl-chains of the lipid molecules are conformationally disordered ("melted"), whereas in their gel phases, the chains are ordered and densely packed (Figure 10). Pressure shifts the lipid phase towards more ordered phases such as the gel or solid-ordered crystalline phase. For particular phospholipids, also non-lamellar phases, such as inverse hexagonal and bicontinuous cubic structures can be observed at high temperatures.[113, 114] The application of pressure leads to the ordering of lipid chains and eventually to the transition to a densely packed gel phase, which retards lipid dynamics and compromises the function of membrane proteins. A slope of about 20 °C/kbar was determined for the gel/fluid phase boundary of saturated phospholipids (e.g., DMPC, DPPC) using fluorescence, NMR and FT-IR spectroscopiy and small-angle X-ray and neutron scattering techniques, which report on the membrane fluidity, the lipids' conformational state and the bilayer structure.[27, 42, 43, 113, 115, 116] Different from saturated lipid bilayer chains, phospholipids with *cis*-double bonds (e.g., DOPC) lead to very low chain-melting temperatures and less steep *T*(*p*)-phase transition slopes. Unsaturated phospholipids impose kinks in the linear conformations of the lipid acyl-chains, creating significant free volume fluctuations in the bilayer so that the ordering effect of HHP is reduced (Figure 10). Hence, to maintain a physiologically appropriate fluid state also at high pressures, more of such cis-unsaturated lipids are incorporated into cellular membranes of deep sea organisms that must survive at ~3-4 °C and pressures up to about 1 kbar or even more in sub-seafloor environments. Increasing the amount of unsaturated phospholipids represents only one form of homeoviscous adaptation. Similar adaptation mechanisms have also been observed in archaeal membranes through changes in their specific lipid chain structures, which include methyl branches and bolalipids (membrane-spanning ether-lipids). However, nature is also able to modulate the fluidity and stability of its membranes in other ways, such as by the incorporation of lipids with headgroups promoting inverted lipid phases (e.g., phosphatidylethanolamines), plasmalogens, sterols, alkanes or polyisoprenoids.

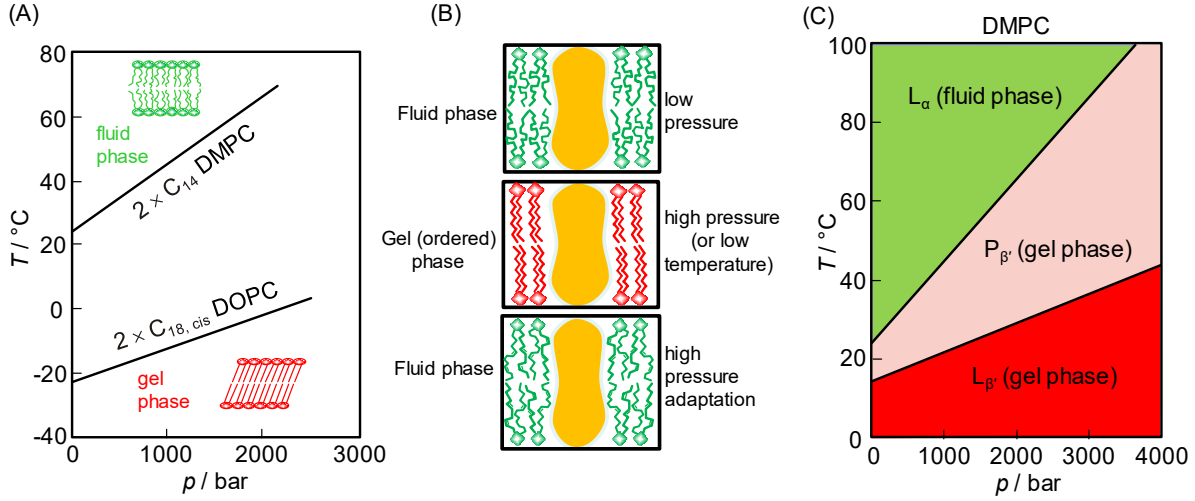

Figure 10. (A) (*T*-*p*)-phase diagram of a representative saturated (1,2-dimyristoyl-*sn*-glycero-3-phosphocholine, DMPC) and an unsaturated (1,2-dioleoyl-*sn*-glycero-3-phosphocholine, DOPC) phospholipid bilayer membrane. (B) Schematics showing the packing of a lipid bilayer with embedded integral membrane protein (yellow) at ambient (atmospheric) pressure, at high pressure (or low temperature) where the lipid acyl-chains adopt an ordered structure, and at high pressure in the presence of unsaturated lipids, demonstrating adaptation through incorporation of more unsaturated phospholipids like DOPC, providing sufficiently high fluidity even at high pressure. (C) (*T*-*p*)-phase

diagram of DMPC in excess water showing two different gel phases ($P_{\beta'}$ and $L_{\beta'}$), which are both densely packed but differ in the tilt angle of the densely packed lipid molecules.[27, 42, 113, 115] Reproduced from ref. [27] Copyright 2007 De Gruyter.

The (*T*-*p*)-phase diagram of biologically more relevant binary, ternary, and quaternary lipid mixtures (including heterogeneous membranes consisting of liquid-disordered and liquid-ordered cholesterol-rich domains) as well as of natural lipid extracts (such as giant plasma membrane vesicles) have also been determined.[27, 42, 44, 117, 118] Generally, an essentially overall ordered membrane structure has been observed at pressures of about 1-2 kbar (depending on the respective temperature) even in complex multicomponent heterogeneous membrane systems that exhibit coexistence of liquid-disordered (fluid) and liquid-ordered phases at ambient conditions. This is the pressure range at which loss of membrane protein function has been observed in natural membrane environments for a number of cases.[27, 42] This observation may be related to the fact that the lipid bilayer matrix reaches a physiologically unacceptable, overall ordered and dynamically largely arrested state at these pressures, leading to loss of lateral lipid organization, membrane protein function, and possibly lysis.

The high density of membrane proteins within the heterogeneous lipid bilayer and at the lipid bilayer interface suggests that macromolecular crowding is also an important factor affecting not only the protein-lipid and protein-protein interactions, but also the lateral organization of the membrane, and its associated reactions. Crowding may operate in two different ways, through entropy-based steric exclusion and weak (quinary) intermolecular interactions. Steric exclusion is expected to induce compaction of conformations and may even lead to clustering of protein molecules within the lipid bilayer and at the lipid interface.[119, 120] Intermolecular interactions may counterbalance these steric effects, however. For example, lipid diffusion was found to decrease almost linearly with increasing protein-to-lipid ratio with a maximum reduction by a factor of 20 due to caging of lipids in the void space between proteins. Also strong crowding in the aqueous cytosolic phase may cause protein accumulation at the surface and modulate protein-lipid and protein-protein interactions, induce oligomerization or remodel the lateral structure (e.g., phase separated nanodomains), and may even induce fission of vesicles. Bulky molecules, such as polysaccharides and the cytoskeleton at the lipid interface, may also cause membrane deformation (e.g., tubulation) and fission. Therefore, the localization of proteins at the membrane depends not only on the intrinsic lipid-protein and protein-protein interactions, but also on the crowding conditions close to the membrane interface and the composition of the cellular milieu.

Phospholipase A1 was found to have a twofold higher affinity for lipid vesicles when only 2% of the inert polysaccharide Ficoll 400 was added to the solution.[120] Mechanosensitive channels found in eukaryotes and bacteria switch between an open and closed conformations to allow the flux of ions (and water) in response to changes in membrane tension. Because crowder molecules can interact with the large extramembrane domain of the ion channels, macromolecular crowding near the membrane interface affects the activity of small conductance (MscS) channels. Another example of a crowded membrane interface are the postsynaptic densities (PSD) at synapses consisting of a high density of soluble scaffold proteins, in which the ubiquitous receptors of neurotransmitters ensure the transmission of the nerve signal across the membrane to trigger the response cascade. Under the highly crowded conditions within the PSD, scaffold proteins like PSD-95, SynGAP and others undergo liquid-liquid phase separation (see above) and form densely packed droplets near the synaptic membrane surface. They colocalize with membrane domains enriched with receptors, suggesting that macromolecular crowding may help keep receptors within the functional domain.

Al-Ayoubi et al.[121] studied the combined effect of high pressure and PEG on multilamellar vesicles (MLVs) of DMPC. HHP favors the state of the smallest volume, whereas osmotic pressure leads to displacement of water from the MLV array because the water activity is reduced by the addition of the osmotically active cosolute PEG. Osmotic pressure leads to a decrease of the headgroup hydration and a contraction of the acyl-chains' cross sectional area. In addition to the chain area contraction, pressurization leads also to a longitudinal extension of the lipid bilayer, which is a consequence of the pressure-induced chain ordering and results in an increased interlamellar lattice constant, as recorded by small-angle scattering experiments. Laurdan fluorescence spectroscopy data revealed a diminished penetration of water molecules into the bilayer at the level of the glycerol backbone. Unlike sugars such as trehalose, the polymeric PEG molecules are excluded from the intermembrane space of MLVs. Due to the attractive depletion forces, the membrane order increases and the intermembrane spacing deceases concomitantly. Such alterations of the order of membrane stacks are of particular importance, because such multilamellar structures exist, for example, as stacked cytoplasmic assemblies in the Golgi bodies, in myelin sheaths of nerve cells, and the thylakoid membrane of chloroplasts. It remains still to be shown, however, how membrane-associated processes and morphological changes are affected both by HHP and in the presence of crowders, both modifying mechanical properties of the lipid bilayer and hence membrane-associated processes, and needs further *in vitro*, *in silico*, and *in vivo* studies.

To conclude this part, while the temperature dependence of cellular constituents is probably the best-studied external parameter, the influence of HHP on biosystems is still poorly understood, largely due to technological difficulties in building equipment that allows the experimental study of biomolecules under HHP and to difficulties to yield cultivars of sufficient amount and purity from deep sea environments. As low and high temperature and HHP extremes are often encountered in combination in habitats of extremophiles (e.g., at the seafloor and near hot vents) the effects of both parameters in concert with cosolute effects needs further studies.

6. Crowding in Living Cells

6.1. Biological Cells and Lysed Cells

Living cells are naturally crowded objects and crowding likely contributes to the stability and functioning of their components. Experiments performed on whole cells, which are highly complex systems including thousands of atoms forming well-defined structures, comprise the difficulty that often only averaged information can be obtained as it is very complicated to disentangle the effect of external parameters on different components or individual particles. Accordingly, the contribution of the sole effect of, for instance, temperature or pressure cannot directly be separated from the presence of crowding. In addition, many cells are adapted to a specific environment by structural and dynamical characteristics, so that they differ naturally from cells that are not adapted to the same conditions. This adds to the difficulty to investigate the impact of crowding separately.

Different strategies can be adopted to circumvent, at least partially, these problems. On the one hand, studies were undertaken under self-crowding conditions, for example, when the concentration by one and the same type of proteins was highly increased. [122] This has the advantage of using only biological systems, but is anyway different from natural conditions. First, crowding and confinement in cells are always limited by the presence of neighboring membranes, which are important for compartmentalization. Second, a self-crowded sample is highly homogeneous and does neither

represent the diversity in sizes of molecules inside the cytoplasmic medium, nor the distribution of surface charges. If all the macromolecules under investigation have the same electrical charges (e.g., lysozyme has a net positive surface charge at neutral pH [123]), they will repel each other so that the sample cannot be compressed anymore above a certain concentration (Figure 11).

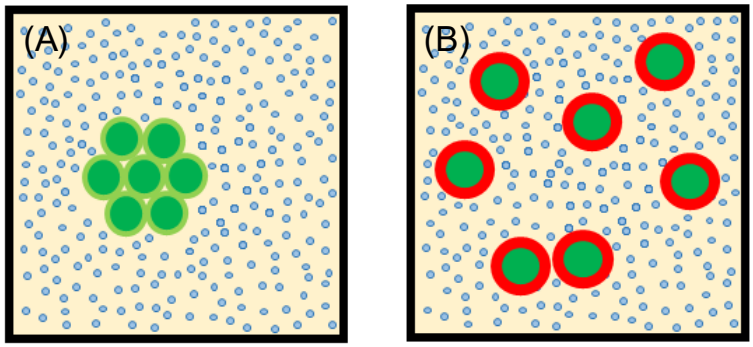

Figure 11. (A) For non-charged particles (green circles), excluding volume effects are the prevalent force. (B) For particles having a net surface charge (red halo around green circles), repulsive forces can dominate over the excluding volume forces (adapted from [124]).

On the other hand, cosolutes and osmolytes were used to mimic the intracellular environment. Such molecules are indeed found in natural cells. They have generally the advantage of stabilizing proteins like the natural cytoplasm and mimicking protein interactions within the cell, but at the expense of the complexity and heterogeneity of the intracellular media (see Section 7). Other attempts have been made using synthetic polymers in the form of organic (e.g., PEG, Ficoll or Dextran) or inorganic (salts, e.g., K^+) osmolytes. Apart from the fact that they are often not natural components of cells, their interaction with the water network or the biomolecules sometimes proves problematic as they can change the water activity and hydration properties of the biomacromolecules.

Another idea to simulate a natural cellular environment is to use lysed cells, for example of *Escherichia coli*, from which the membranes have been removed, and to concentrate them to mimic the cytosolic medium.[125] Here, high complexity and polydispersity of the environment are maintained. M. Grimaldo et al.[125] used this technique in combination with small-angle scattering (SAS) and quasi-elastic neutron scattering (QENS) to highlight the signal from a tracer protein (polyclonal bovine immunoglobulin, Ig) against the crowders by employing lysates from perdeuterated *E. coli* cells. This allowed them to mimic the intracellular environment under controlled crowding conditions by varying the volume fractions, φ, of the Ig's and lysate. The short-time (sub-nanosecond) diffusion of the system, where hydrodynamic interactions dominate over protein collisions, was observed by QENS. After subtraction of the signal from the lysate, the authors extracted an apparent diffusion coefficient, $D(\varphi)$,[126] which includes translational and rotational motions. They found that $D(\varphi)$ decreases significantly with increasing φ, and, surprisingly, remains almost the same regardless of the exact nature of the crowded environment (Figure 12).

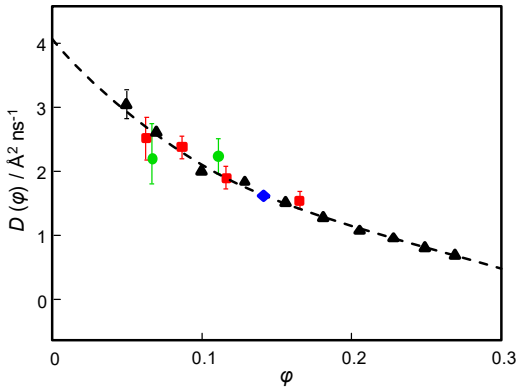

Figure 12. Apparent diffusion coefficient, $D(\varphi)$, in dependence of the total volume fraction, φ, of immunoglobulin, recorded at room temperature. The dark symbols are from samples without lysate, the other colors represent various samples in the presence of lysate, with the signal from the pure lysate being subtracted. The polynomial fitting of the diffusion of Ig in pure D_2O is presented as a dashed line (for more details see [125]).

To shed more light on these findings, they performed simulations based on Stokesian dynamics,[127] in which the polydisperse environment was approximated by spheres of various sizes. According to their results, the deviation of the diffusion coefficient from the crowding-free case depends mainly on the ratio between the hydrodynamic radius of the protein Ig, R_{Ig}, and an averaged radius of the spheres of the crowding model, $R_{eff} = \langle R_i^3 \rangle^{1/3}$, in the sense that larger particles are slowed down more strongly than smaller particles in the cytosol on the nanoseconds timescale. For the ratios considered in their study, $R_{Ig}/R_{eff} \approx 0.9 - 1.3$, the diffusion coefficients were found to be rather insensitive to the surrounding lysate. Transferred to the interior of a natural cell, where it is not possible to measure this parameter locally but only in an averaged way, one can probably conclude that slowing down of the overall dynamics does indeed occur, but does not depend markedly on the exact composition and nature of the crowded cellular milieu.

Recently, our laboratory has undertaken the comparison of two hyperthermophilic archaeal species from the *Thermococcales* order, which are structurally very similar. *Thermococcus barophilus* is piezophilic and originates from the Snake Pit hydrothermal vent site of the mid Atlantic ridge at a depth of 3550 m.[23] *Thermococcus kodakarensis* is piezosensitive and was taken from a surface solfatara of Kodakara island, Japan.[128] Both share similar growth conditions in terms of temperature, as their optimum is at 85 °C, but the former lives at around 400 bar whereas the latter thrives at the Earth's surface. Genetically, these two prokaryotes are very similar, what makes them a perfect target to compare their adaptation to HHP. Quasi-elastic incoherent neutron scattering gives access to averaged molecular dynamics of cell pellets, which were immersed in D_2O to minimize the water signal. Deuterium has indeed a much smaller incoherent cross section than hydrogen.[129] The comparison of the two cells pointed to a peculiar adaptation mechanism to HHP,[130] and were the first to shed light on a pressure adaptation mechanism, which the genomic approach could not provide so far. However, it did not permit to identify the involvement of cellular crowding in such mechanism. To this end, we compared the same archaeal species using whole living cells and lysed cells from *T. kodakarensis* for comparison, at room temperature and at ambient and high pressure. In this way, we were able to take the crowding conditions into account in a controlled manner to study the dynamic features (Figure 13).

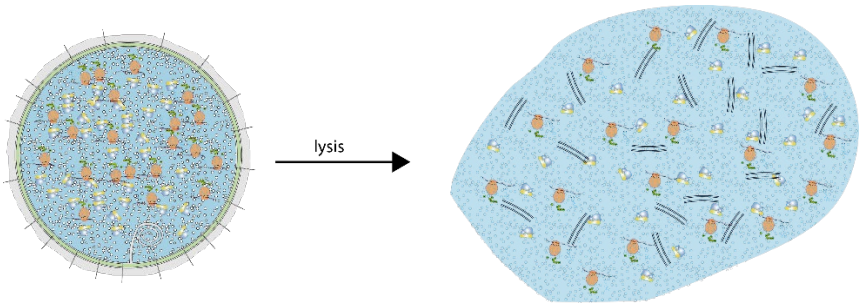

Figure 13. Crowded living cells against lysed cells, in which the cell contents are released into the total volume at disposal so that the concentration of cytoplasmic components becomes much lower (modified from [131]).

We compared mean-squared displacements (MSDs) of *T. barophilus* and of *T. kodakarensis* cells before and after lysis (Figure 14) as a function of pressure.[131] The MSDs, $\langle u^2 \rangle$, were obtained by elastic incoherent neutron scattering (EINS) and represent averaged motions of atomic nuclei around their equilibrium positions in a given state of hydration and at a given external condition. They can be extracted from the elastic dynamical structure factor $S_{el}(q, 0 \pm \Delta E)$, at zero energy transfer and half width half maximum (HWHM) of the instrumental energy resolution ΔE, within the Gaussian approximation [132] by the slope of the semi-logarithmic plot:

$$\langle u^2 \rangle \approx -3 \frac{\mathrm{d} \ln S_{\mathrm{el}}(q, 0 \pm \Delta E)}{\mathrm{d} q^2} . \qquad (5)$$

Here q is the momentum transfer from the neutron to the scattering atom in units of ħ. The neutron intensities summed over all accessible q-values, I_{sum}, are inversely proportional to the MSD, but are afflicted with smaller error bars due to the better statistics on which they are based.[133] Therefore, this quantity is sometimes used in the following. For comparison between samples, we are also sometimes using the force constant, which describes the overall mechanical stability or resilience of a given sample (here, the proteome) according to [134]

$$\langle k \rangle = 0.00138/(\mathrm{d}\langle u^2 \rangle/\mathrm{d}T), \qquad (6)$$

where $\langle k \rangle$ is obtained in Newton per meter when $\langle u^2 \rangle$ is expressed in Angstroem squared and T is the temperature in Kelvin.

T. barophilus and *T. kodakarensis* intact cells were found to undergo a marked drop in mobility with increasing pressure until they reach their optimal growth pressures, around 30 bar for *T. kodakarensis* and around 250 bar for *T. barophilus*.[135] Above these values, the MSDs stay essentially constant, indicating that the cells are able to withstand the pressure. The MSDs of the lysed cells are significantly higher than those of the whole *T. kodakarensis* cells and converge close to those of *T. barophilus*. Such finding reveals the strong impact of crowding on the local dynamics of the proteome in archaeal cells. However, analysis and interpretation of these results are not straightforward as shown in ref. [136]. The higher flexibility of the piezophilic cells and the higher stability of the piezosensitive cells probably govern the dynamical properties of the proteome, whereas the lysed cells allow a direct action of HHP on the proteome without the protection provided by the enclosed cytosol, leading to compression and reduction of motions.

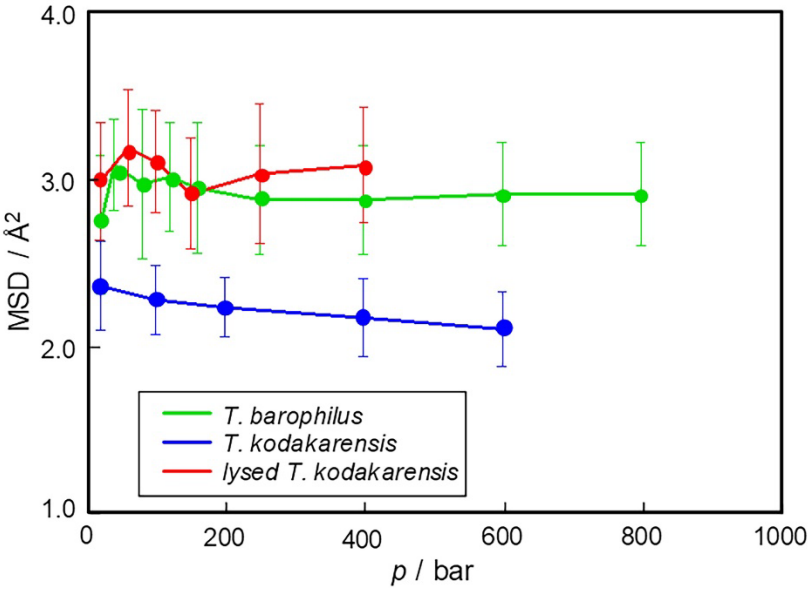

Figure 14. MSD of *T. barophilus* and of *T. kodakarensis* cells, for intact and lysed cells (modified from [131]).

We have complemented the elastic neutron scattering experiments by QENS experiments and discuss here the results at ambient pressure. QENS informs about the dynamical structure factor *S(q,ω)*, a function of the momentum *q* transferred between the neutron and the sample and the energy transfer *ω*, both multiples of *ħ*. One of the benefits of quasi-elastic neutron scattering is to inform simultaneously about the space-scale and time-scale, which are the complementary variables of the momentum and energy. The latter can be obtained by Fourier transform. The dynamical structure factor *S(q,ω)* obtained experimentally can be modeled through a series of dynamical components, including water, which allow to separate the different contributions arising from global protein motions and internal molecular diffusive dynamics,[137] and to systematically investigate the effect of crowding. As detailed in the book of M. Bée [138] and exhaustive review articles (see for instance [139]), various dynamical parameters can be extracted from these data by using suitable models when fitting the neutron data. It is known that bacterial cell pellets contain about 70 – 80% of water and in addition biomolecules. [140] Hence, a model previously developed to analyze QENS data on neurological tissue [141] or on the same prokaryotes [130] having a similar or identical molecular composition was applied:

$$S(q,\omega) \approx \begin{bmatrix} p_{\mathrm{el}} \times \delta(\omega) + p_{\mathrm{bulk}} \times S_1\left(q,\omega,D_{T_{\mathrm{bulk}}},\tau_{\mathrm{bulk}},D_{R_{\mathrm{bulk}}}\right) + \\ p_{\mathrm{hyd}} \times S_2\left(q,\omega,D_{T_{\mathrm{hyd}}},\tau_{\mathrm{hyd}},D_{R_{\mathrm{hyd}}}\right) + p_{\mathrm{prot}} \times S_3\left(q,\omega,\Gamma_{\mathrm{prot}}\right) + B(Q) \end{bmatrix} \otimes R(q,\omega), \quad (7)$$

where *B(q)* stands for the background and *R(q,ω)* for the resolution, by which the theoretical model function must be convoluted to account for instrumental broadening. The parameters which could be extracted were the fractions of atoms contributing to elastic scattering (p_{el}), bulk (p_{bulk}) and hydration water (p_{hyd}) and the proteome (p_{prot}), with $p_{\mathrm{el}} + p_{\mathrm{bulk}} + p_{\mathrm{hyd}} + p_{\mathrm{prot}} = 1$. The atoms contributing to elastic scattering undergo only local motions. The various dynamical contributions are summed up, each individual structure factor S_i being characterised by specific parameters: D_{T} and D_{R} stand for the translational and rotational diffusion coefficients, τ is the residence time, a parameter quantifying the average time a particle oscillates around its equilibrium position before performing diffusional

motions,[142] but it is also related to interactions between molecules.[143] Γ_{prot} stands for the HWHM of the proteomic component and is representative for its flexibility under a given external condition.

The findings are summarized in Table 1. As for the EINS results described above, we find accordance between the *T. barophilus* and the lysed *T. kodakarensis* cells. The fractions of elastic scattering signal, hydration water and the residence time are almost the same within the experimental accuracy. The percentage of hydration water is strongly decreased during lysis, since the confinement for the lysed cells is removed and water molecules can rearrange more freely. The residence time has large uncertainties and is therefore less informative. The only parameters that seem clearly related to the removal of crowding are the fraction of atoms contributing to the signal of the proteome, p_{prot}, and the translational diffusion coefficient of bulk water, $D_{T,bulk}$. Both are enhanced compared to the crowded cell, indicating relaxation of the constraints imposed by the cellular crowding. The p_{prot} value reflects a higher flexibility of the proteins being no longer confined by the cell walls. While the translational diffusion coefficient $D_{T,bulk}$ remained similar for the two intact cells, it became much more similar to that of free water for lysed cells,[144] reflecting the water's higher degree of freedom when binding to other molecules is not hindering it. The width of the function of the third structure factor, Γ_{prot}, which reflects the motions of the proteins, seems to be the sole parameter that is an intrinsic property of the type of biomolecule as it is very similar for the intact and lysed cells of *T. kodakarensis* and smaller compared to cells of *T. barophilus*. The diffusion coefficient is the only parameter which changes for all three samples, and it is lower for the lysed cells compared to the intact ones. Altogether, these findings suggest that crowding has indeed an important, albeit sometimes indirect impact on the cellular dynamics, which can be driven through the surrounding solvent.

Table 1. Fit results for *T. barophilus*, *T. kodakarensis* and lysed *T. barophilus* cells at 1 bar. The values in the first two columns are reproduced from,[130] those of the last column are reproduced from [131]. The fields in orange show accordance between *T. barophilus* and the lysed cells of *T. kodakarensis*, the fields marked in green show resemblance between the intact and lysed cells of *T. kodakarensis*, the fields in blue correspond to the only parameter which differs for both crowding and pressure. The numbers in red are characteristic for the cellular crowding effect.

	T. barophilus	*T. kodakarensis*	Lysed *T. kodakarensis*
p_{el}	0.01 ± 0.01	0.03 ± 0.01	0.015 ± 0.005
p_{hyd}	0.10 ± 0.01	0.17 ± 0.01	0.06 ± 0.03
p_{bulk}	0.67 ± 0.04	0.60 ± 0.03	0.63 ± 0.03
p_{prot}	0.23 ± 0.03	0.23 ± 0.03	**0.29 ± 0.03**
$D_{T,bulk}$ (10^{-5} cm^2 s^{-1})	1.98 ± 0.02	1.98 ± 0.02	**2.105 ± 0.05**
τ_{bulk} (ps)	1.05 ± 0.11	1.28 ± 0.13	0.9 ± 0.1
$D_{T,hyd}$ (10^{-7} cm^2 s^{-1})	5.17 ± 0.12	4.86 ± 0.10	4.3 ± 0.5
Γ_{prot} (meV)	0.431 ± 0.004	0.363 ± 0.005	0.350 ± 0.010

6.2. Relation to External Stress: Temperature

Although the structure of biological cells is apparently similar among eukaryotes, bacteria and archaea, each individual cell type and cell has its own cell death temperature, which can vary greatly depending onto the environment in which the cell lives. Proteins are the most sensitive to temperature changes and most abundant components of cells (Figure 3), while double stranded DNA are much less sensitive.

This is the reason for primarily studying the proteome and its response to thermal stress, albeit under crowding conditions to improve our understanding of cellular function.

Heating of proteins at high temperatures leads to denaturation, which is generally accompanied by an unfolding of its three-dimensional structure, resulting in irreversible aggregation or gelation.[145] However, since the late 1980s it has been known that it is not only the structure that determines protein functionality, but also its dynamics [146-148] and the environment. Molecular motions occur at different levels, including small-scale vibrations due to thermal agitation, described by the Debye-Waller-factor, [138] diffusional motions associated with relaxation processes, and translational diffusion of the whole molecule in solution. They are associated at different levels with the functioning of the protein and the whole cell.[149] All of these motions occur within pico- to nanoseconds and it is far from being trivial to separate them experimentally. The focus here is on QENS measurements, which allow identifying various dynamical contributions at these time scales.[138, 150, 151] What is known so far about dynamical motions around thermal denaturation is the strong correlation with the hydrogens of the water layer at the protein's surface. In addition, the activity of the protein is determined by the flexibility of the amino acids' side chains, which depends on the lifetime of hydrogen bonds. At high temperature, it becomes so short that the hydrogen bonds break and the protein unfolds. The unfolding is not necessarily irreversible, but depends, among others, on the maximum temperature which is reached and on the time spent there. Such facts can be described by an intermediate state in which other conformational substates are realized.

In case of lysozyme, misfolding is generally caused by the formation of hydrogen-bonded β-sheet structures, induced by a "helix-to-β-sheet" conformational change.[152] Well beyond the denaturation temperature, the protein definitely unfolds, occupying a larger volume than the native protein. Similar findings are reported by Murayama & Tomida [153] for the defatted monomer bovine serum albumin (BSA), which irreversibly forms intermolecular β-sheets at the expense of α-helical structures when heated above 70 °C. EINS measurements on proteins going beyond their denaturation temperature revealed evidence of a sudden rise in the atomic movements on an Angstroem-nanosecond scale.[154-156]

Using QENS, Grimaldo et al. performed a study on BSA at high concentration, reaching self-crowding conditions (Figure 15).[157, 158] Data analysis around the denaturation temperature enabled the separation of global, backbone, and side-chain motions. Global motions are characterized by the global apparent diffusion coefficient *D*, including contributions from rotational and translational motions of the whole protein. The backbone and side-chain movements are described by the diffusion coefficients D_1 and D_2, respectively. As depicted in Figure 15, self-crowding resulted in reduced dynamics, as expected, and to a slight shift of the slope's turning point to lower temperature. The slowest motion corresponds to global diffusion of the whole protein and can be expressed by a two-state model, where the native proteins are initially represented as a colloidal suspension that turns into a gel-like network after denaturation. The dynamics of the backbone atoms are the least affected by denaturation, with only a slight increase in slope beyond the denaturation temperature, probably due to the transition from the α-helical to a disordered coil structure. The side-chains are subject to an effect that is entirely due to self-crowding, as the transition becomes only visible at higher protein concentrations. Their dynamics is increasingly constrained by the crowding as the side-chains are more exposed to the surrounding solution as the protein unfolds. Taken together, the data suggest that crowding leads to

an overall reduction in motions of the native protein, as the high concentration leads to more interactions and more obstruction of the degrees of freedom, as well as an earlier onset of temperature-induced changes. Proteins thus show a clear response to heat shock and the temperature of denaturation is clearly marked in the molecular dynamics, and the motions at different hierarchical levels depend on the crowding state of the proteins.

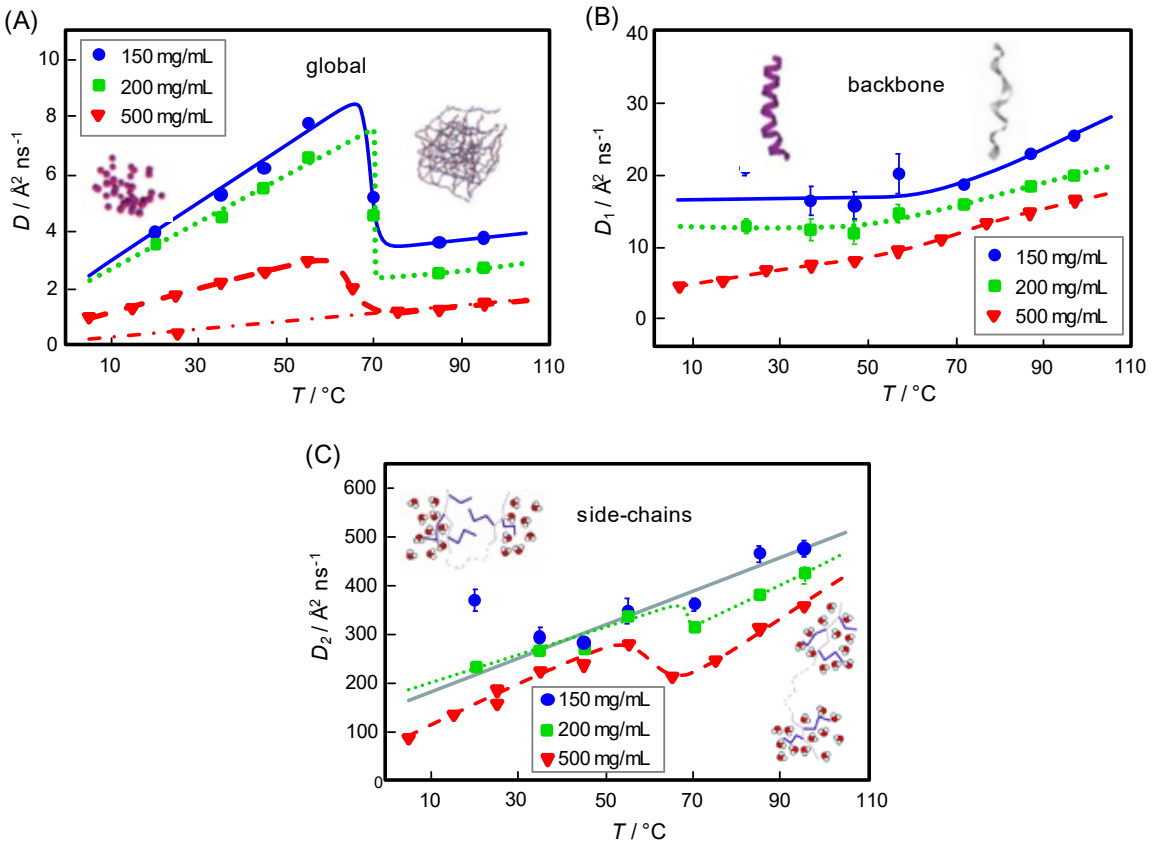

Figure 15. (A) Apparent self-diffusion coefficient, *D*, of the global motion of the protein in solution and the diffusion coefficients D_1 and D_2 of the backbone (B) and side-chains (C) of the protein as a function of temperature (reproduced from Grimaldo et al. 2015 [157]).

Based on statistical thermodynamics, Dill and co-workers hypothesized the physical limits of cells and proteomes.[159, 160] They introduced the notion of "denaturation catastrophe" of the proteome (likely inspired from an earlier work by Kozak and Benham [161]), which coincides with the cell-death (CD), i.e., a major fraction of the proteins denatures immediately when the denaturation temperature is reached. More recently, taking advantage of novel results, Leuenberger et al. [162] measured numerous proteins that make up cells to determine their denaturation profiles. They were able to establish a protein-protein interaction network of *E. coli* and correlated it with the thermostability of the components. In contrast to the previous work by Dill et al., they reported that at the CD temperature, T_{CD}, only a small number of proteins essential for cell functioning are denatured. It remains an open question how such temperature induced processes affect the diffusional transport of proteins within cells, which is a limiting factor for all biochemical processes.

To move forward and obtain more biologically relevant information, our laboratory studied the proteome of a model cell, the cell *E. coli*, which thrives at approximately the physiological temperature

of a human body (~36 °C) and has a local protein concentration between 200 and 400 g/L.[3] Using incoherent neutron scattering,[130, 163, 164] we carried out measurements on *E. coli* cells in D_2O, which have a T_{CD} of 50 °C, and compared the data with results from molecular dynamics (MD) coarse-grained and all-atom simulations.[165] The advantage of such simulations is the accessible time scale of a few nanoseconds and the amplitudes of motion of a few Å, which perfectly match the experimentally obtained information. By using a model inspired from the work by Grimaldo et al. [158], we determined experimentally from QENS the diffusion coefficients of the global apparent self-diffusion, D, which corresponds to a superposition of translations and rotations, and the local dynamics, D_L, of the proteome (Figure 16) upon heating and cooling. The local dynamics was well reproduced by a jump-diffusion model proposed by Singwi & Sjölander,[166] where a particle performs very small leaps characterized by a negligible jump time and the residence time τ, i.e., the time an atom remains in its equilibrium position (Figure 16).

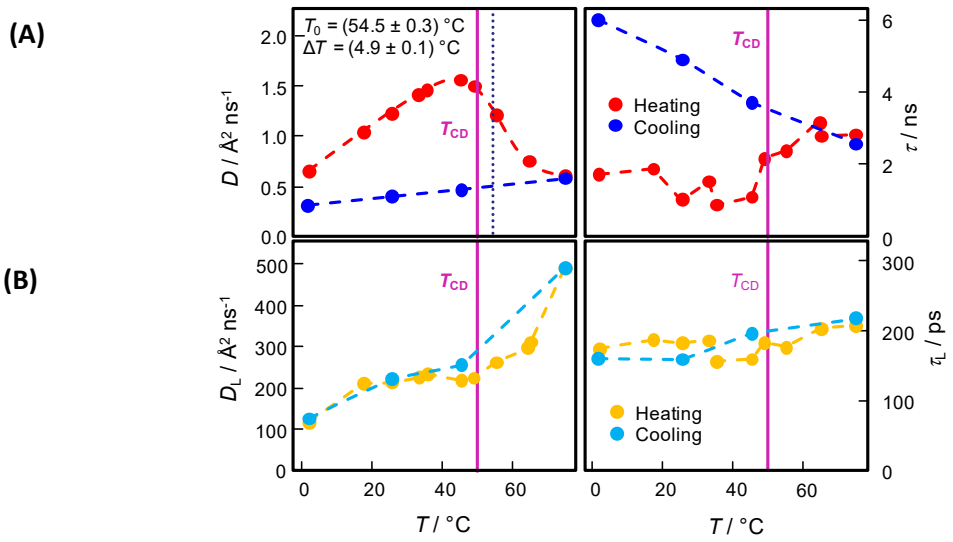

Figure 16. (A) Temperature dependence of the global apparent self-diffusion coefficient, D, of the proteins in the *E. coli* cellular plasma. The right side shows the residence time, τ, for the global motions as a function of temperature, which exhibits a significant increase beyond T_{CD} and continues to rise upon subsequent cooling. (B) Diffusion coefficient, D_L, for the local motions of the side-chains as function of temperature. The right-hand side shows the residence time τ_L for the internal dynamics, which remains almost constant (adapted from [165]).

As for the global motions, we observed a sudden drop of the diffusion coefficient around T_{CD}, resembling the decrease of the diffusion coefficient for BSA. One has to bear in mind that the multitude of proteins in *E. coli* cells leads to a certain distribution of CD temperatures, which explains the broad transition region upon denaturation. Increasing self-crowding of the proteins leads to broader transitions as well (Figure 15). On cooling, D decreases linearly, indicating irreversibility and slowing down due to gelation of the cytoplasm. This irreversibility is also visible in the residence time, τ, which increases first around T_{CD}, and even furthermore upon cooling. The residence time is indicative for intermolecular interactions and macromolecular confinement,[167] both of which are enhanced following unfolding. The diffusion coefficient and residence time for local motions determined are similar to the side-chain motions in the study of Grimaldo et al.[157] The diffusion coefficient D_L increases steeply beyond T_{CD} and the residence time τ_L was found to be very long (~180 ps), remaining almost constant for all investigated temperature values. Due to the smaller scale of motions, crowding had no

significant effect on the local motions, but enhanced the interactions with water and other molecules. Previously, Tehei et al.[168] observed similar long residence times for intracellular water in cells of Dead Sea organisms and attributed this to a specific water structure due to the high amount of K^+ ions in *Haloarcula marismortui*. Polydisperse crowding can certainly have a similar effect and increase τ_L.

The corresponding MD data provided deeper molecular insights into the impact of a heat shock and crowding on the cellular proteome. The protein content within the *E. coli* cell was adapted from a previous computational model.[32] The authors studied there the proteins of *E. coli* grown under minimal media conditions.[169] The coarse-grained model contained 45 different protein species as well as five types of RNA and RNA–protein complexes and permitted to obtain a resolution at the level of the residues to shed light on the local structure of the crowded cytoplasm. The lattice Boltzmann molecular dynamics (LBMD) approach[170, 171,172] was used for the coarse-grained simulations (Figure 17) in combination with the OPEP force field.[173] Very recently, a new version of the force field was published,[174] specifically optimized for crowded protein solutions. The all-atoms structures of the proteins were taken from the PDB and simulated according to [175] to gain insight into protein diffusion of selected sub-boxes. For that, five different sub-boxes containing 10 to 20 proteins each were chosen to represent the heterogeneity of the cytoplasm. We distinguished additional boxes with folded or unfolded proteins and subjected both to a heating protocol.

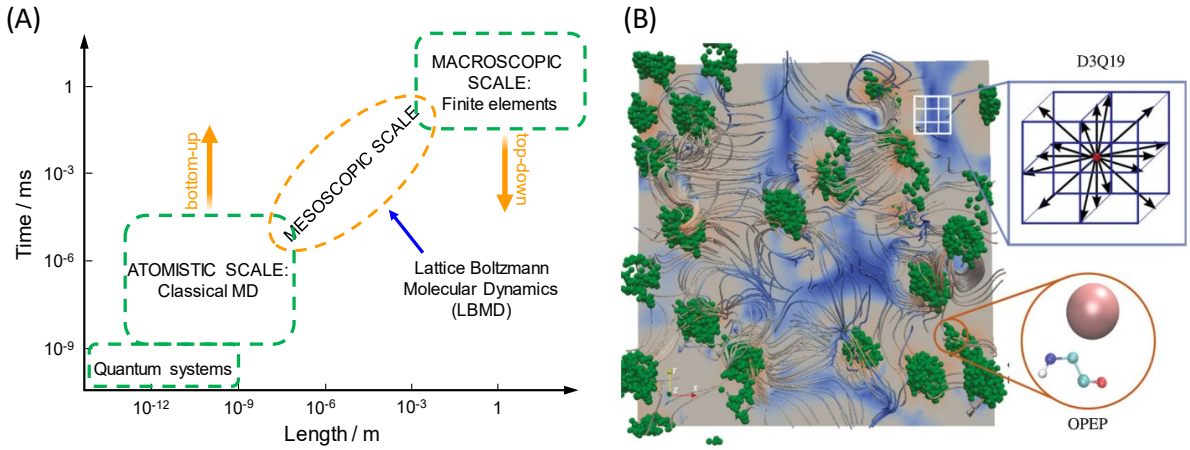

Figure 17. (A) Sketch of the time and length scales of coarse-grained and all-atom simulations. (B) Schematic representation of the multiscale approach. Proteins are included at the microscopic level, interact according to the coarse-grained optimized potential for efficient protein structure prediction (OPEP) coarse-grained force field [173] and move in a continuum (reproduced with permission from [176]).

The all-atom simulations revealed a substantial decrease of the global diffusion coefficient upon unfolding (Figure 18A) and a linear increase as a function of temperature. The main reason for the slowdown appears to be a significant increase in the average number of atom-atom contacts in the case of unfolded proteins (Figure 18B). Among them, the interactions between non-polar atoms were the strongest at a protein concentration of 288 g/L. At lower concentrations (≤ 200 g/L), the formation of transient protein clusters in crowded solution was observed and associated with the slowing down of diffusion.[177] Our data show that unfolded proteins are most contributing to this effect.

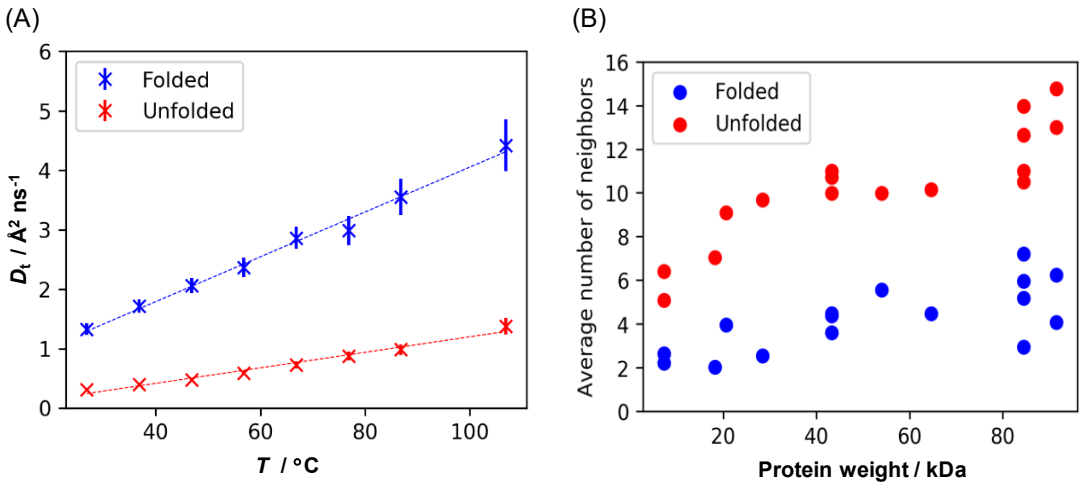

Figure 18. (A) Global apparent diffusion coefficient, D_t, as obtained from all-atom simulations indicating the strong decrease of diffusivity among unfolded proteins. (B) Average number of atom-atom contacts in the simulation box containing folded or unfolded proteins (reproduced from [165]).

To relate the effects observed by the MD simulations to the experimental results from neutron scattering, it is of importance to estimate the fraction of proteins unfolding immediately above the cell-death temperature, T_{CD}. To this end, we repeated the all-atom simulations with an increasing fraction of unfolded proteins in the sub-box and showed that even a small amount of unfolded protein can considerably reduce the global translational diffusion coefficient (Figure 19). To quantify the effect, we expressed the diffusion coefficient by a linear combination of the diffusion coefficients of the folded (f) and unfolded (u) proteins by

$$D_t = (1 - a_u)D_t^{(f)} + a_u D_t^{(u)}, \quad (8)$$

where a_u is the "apparent" unfolded fraction and permits to quantify the contribution from the folded and unfolded proteins. From a_u, the fraction of unfolded proteins, r_u, can be estimated. Figure 19 shows the temperature dependence of the fraction of unfolded proteins, $r_u^{QENS}(T)$, as obtained from the QENS data and the comparison with the statistical thermodynamics results by Dill et al.[159] It can be clearly seen that our results are at odds with the picture of the denaturation catastrophe of the proteome, but rather support the experimental results of Leuenberger et al. [162] predicting a small number of proteins (less than 25%) with key functions unfolding around T_{CD}. This finding may be indicative of a protective effect by crowding against protein denaturation when subjected to a heat shock.

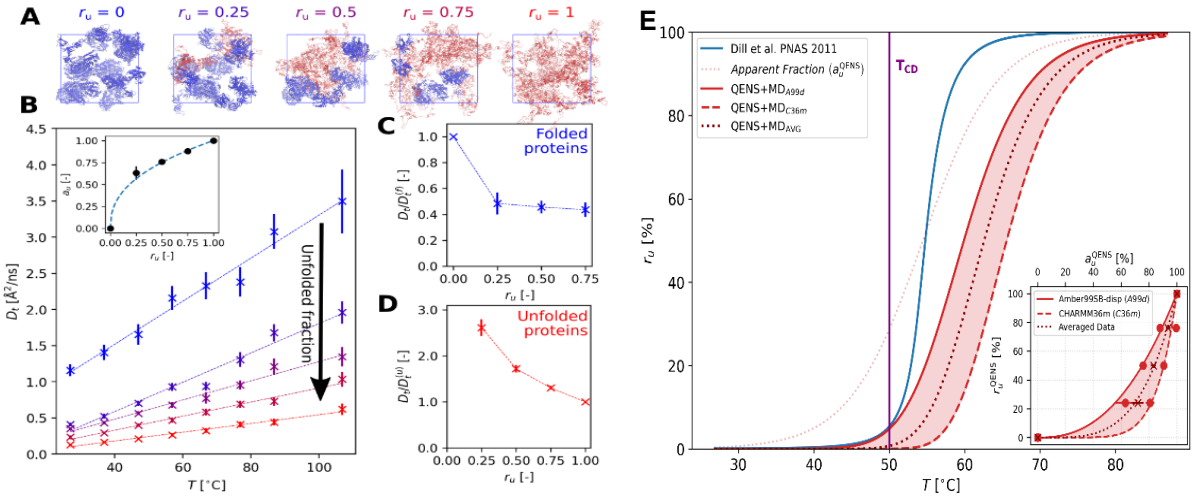

Figure 19. (A) Sub-boxes (288 g/L) with different fractions r_u of unfolded proteins. (B) Translational diffusion coefficients, D_t, in the same sub-boxes as represented in (A), where blue is used to show folded proteins and red for unfolded proteins. (C, D) The two graphs show the reduction in the translational diffusion coefficient of folded and unfolded proteins inside the partially unfolded sub-box as function of r_u. The inset in figure (B) shows a_u as a function of r_u. (E) The increase of the percentage of r_u of unfolded proteins in *E. coli* as a function of temperature. T_{CD}, marked by a vertical purple line, is the cell death temperature (50 °C) and was determined from the *E. coli* growth rate. The solid and dashed red lines show the experimental $r_u^{QENS}(T)$ data. The results are compared with the predictions of Dill et al. [159] (reproduced from [165]). The inset presents $r_u^{QENS}(T)$ as function of $a_u^{QENS}(T)$, both determined from QENS data.

Interestingly, the maximum growth rate of the cell, which increases with temperature, resides just below T_{CD}. Further support of our results comes from reproducing the growth rate graph, $g(T)$, for *E. coli* (Figure 20). The calculation used a model suggested by Dill et al.,[159] where $g(T)$ is modelled by an Arrhenius reaction rate containing the temperature dependent fraction of unfolded by replacing the fraction of folded proteins by our experimental results. The calculations are in excellent agreement with the data, unless when one assumes that the growth rate is completely rate-limited by diffusivity and the dominant activation barrier is negligible, i.e., $\Delta H^{\dagger} = 0$. This illustrates the relation between molecular dynamics of the *E. coli* proteome, the bacterial metabolism as function of temperature and cell death.

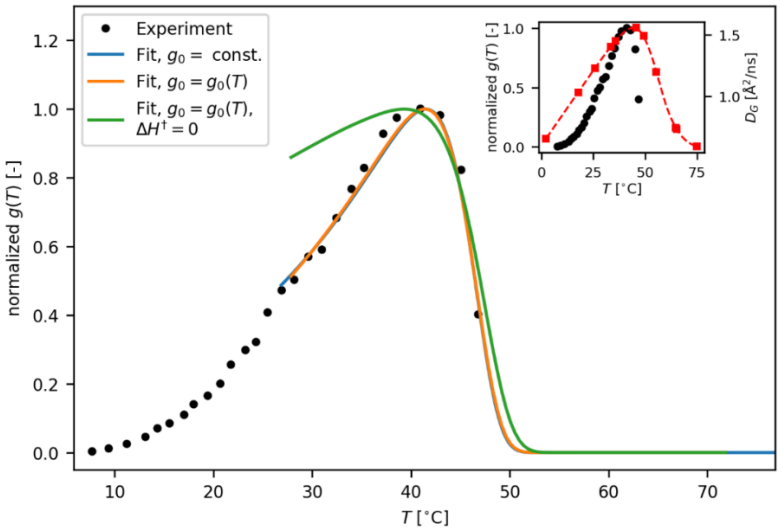

Figure 20. Temperature dependence of the growth rate of *E. coli* cells. Experimental points are from [178] (reproduced with permission). The inset shows the growth rate (black dots) obtained by using experimental results for the fraction of unfolded proteins compared with that of the experimentally measured apparent self-diffusion coefficient, *D* (red squares) (reproduced from [165]).

The unfolding of proteins in the cytoplasm induces a strong local variation in viscosity, which significantly affects the mobility of neighboring molecules. When the proteins unfold, they collapse and can form a kind of gel. Such an increase in viscosity could be sufficient to block vital signaling and metabolic processes controlled by efficient local diffusivity, finally leading to cell death. Matsarskaia et al.[179] have already observed that the increase in viscosity in crowded protein solutions can involve such a significant slowing down of molecular dynamics.

6.3. Relation to External Stress: Pressure

High hydrostatic pressure has the effect of reducing the volume inside a biological system,[24] which involves the increase of crowding and confinement. A recent investigation on the protein lysozyme at two different concentrations of 80 and 160 mg/mL permitted inspection of the impact of both self-crowding and HHP (Figure 21 A) up to 4 kbar.[79] At the lower concentration of 80 mg/mL, HHP had the expected effect of reducing the dynamics by 40% from 1 to 2000 bar. Beyond that pressure, the MSDs stayed essentially constant. NMR studies demonstrated that HHP had the effect of first compressing internal cavities of the proteins, which are not accessible to the solvent.[66] Beyond kbar pressures, cavities open to the solvent and let it intrude into the interior of the protein, initiating unfolding, typically beyond 2-8 kbar, which does not take place below 5 kbar for lysozyme at ambient temperature, however. At the self-crowding condition of 160 mg/mL, the MSD of lysozyme is strongly reduced and the pressure dependence becomes almost negligible, indicating a significant impact of such conditions. Such findings are in line with the reduced impact of the temperature dependence on the global and backbone diffusion under crowding and with a higher stability of the protein (Figure 15). Such crowding effect can be explained by the higher concentration, which generates intermolecular distances between protein molecules reduced to a few (~5) water layers on average, only. When water is compressed within such thin hydration layers, it presents characteristics clearly different from bulk water. Its structural properties are now impacted by the surface of the protein

molecule (e.g., by electrostriction effects of charged and polar surface groups upon hydration). The compressibility of the protein, which is positively charged at neutral pH (z = +8), is probably limited by the strong electrostatic repulsion which might hinder further compression at higher pressures. This observation is in line with the changes of the intermolecular interaction potential, $V(r)$, upon pressure application derived from high-pressure SAXS data using the DLVO (Derjaguin−Landau−Verwey−Overbeek) model in the mean spherical approximation (Figures 21 B and C).[90] At the higher protein concentration, the SAXS intensity shows a strong maximum of the intermolecular correlation peak around a momentum transfer, q, of about 0.7 nm^{-1}, which does not change significantly with pressure, indicating a strong electrostatic repulsion below 0.1 nm. The attractive part, J, of $V(r)$ shows a minimum at around 1.5 kbar, which could be due to a dynamical clustering in concentrated lysozyme solutions.[180] However, water is also subjected to marked changes in the hydrogen-bond network structure beyond 2-3 kbar.[181] These effects most likely contribute to the limited pressure dependence of the MSDs of hydrogen atoms in the protein. In conclusion, such tight crowding conditions, as also prevail in parts of the biological cell, strongly constrain the sub-nanosecond dynamics of protein motions, rendering their pressure dependence almost negligible. These findings may help to shed light on the high stability of the proteome of organisms thriving under hydrostatic pressure conditions.

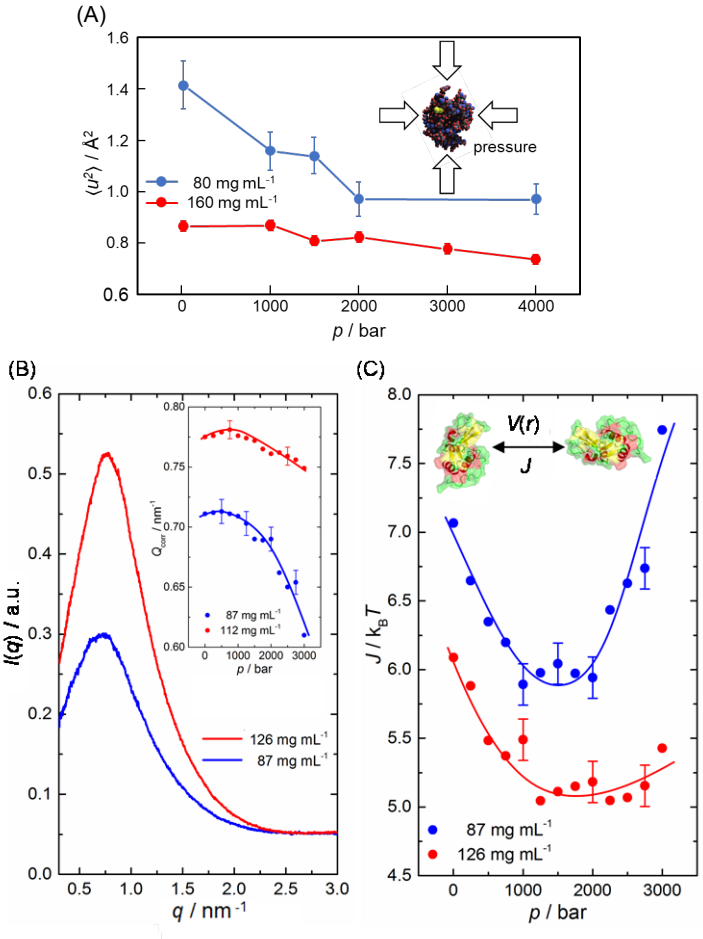

Figure 21. (A) Pressure dependence of MSDs of lysozyme at two different concentrations at T = 20 °C. (B) SAXS intensity $I(q)$ and the depth J of the intermolecular interaction potential $V(r)$ in units of k_BT. Adapted from ref. [79] Copyright 2015 American Chemical Society.

Considering again whole cells as proxy for strong polydisperse crowding in a natural system, we used the same hyperthermophilic archaeal species as before, namely the piezosensitive prokaryote *T.*

kodakarensis and the piezophile *T. barophilus*, exposed to HHP. Crowding is present in both cells, but the piezophile is additionally adapted to a HHP environment. Both systems were at room temperature, but subjected to ambient and 400 bar pressure, the pressure where *T. barophilus* thrives. At this temperature, the cells are in a metabolically inactive state and the cell membrane is largely impermeable permitting the study in D_2O because an H_2O/D_2O exchange is largely suppressed. H_2O was only present in intracellular form and in the volume available between cells. The use of QENS allowed us to access the dynamics of the proteome and, simultaneously, the dynamics of hydration and bulk water under the conditions considered as hydrogen atoms are the most visible by neutrons.[129]

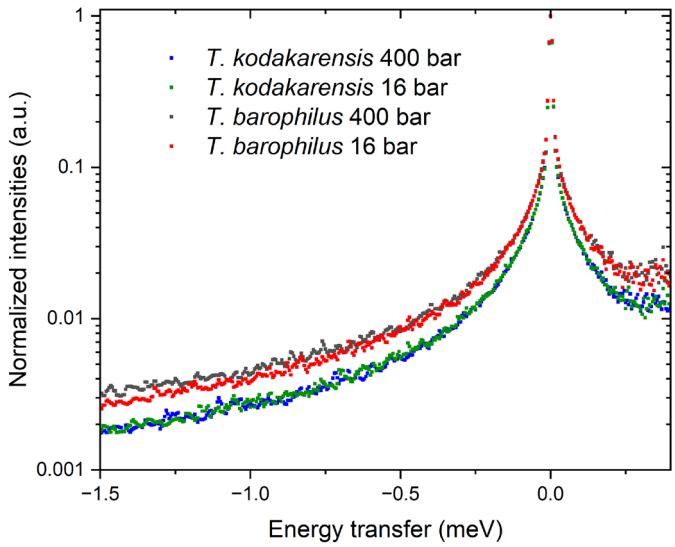

Figure 22. Semi-logarithmic representation of normalized QENS spectra averaged over all available momentum transfer values for *T. barophilus* and *T. kodakarensis* samples at ambient pressure and at 400 bar (adapted from [130]).

Table 2. Summary of the dynamical parameters of *T. barophilus* and *T. kodakarensis* samples at 1 bar and 400 bar as obtained by QENS experiments (reproduced from [130]).

	T. barophilus		***T. kodakarensis***	
	1 bar	**400 bar**	**1 bar**	**400 bar**
p_{el}	0.01 ± 0.01	0.01 ± 0.01	0.03 ± 0.01	0.03 ± 0.01
p_{hyd}	0.10 ± 0.01	0.10 ± 0.01	0.17 ± 0.01	0.18 ± 0.02
p_{bulk}	0.67 ± 0.04	0.66 ± 0.03	0.60 ± 0.03	0.60 ± 0.03
p_{prot}	0.23 ± 0.03	0.23 ± 0.03	0.23 ± 0.03	0.22 ± 0.03
$D_{T,bulk}$ (10^{-5} cm^2s^{-1})	1.98 ± 0.02	1.98 ± 0.02	1.98 ± 0.02	1.98 ± 0.02
τ_{bulk} (ps)	1.05 ± 0.11	1.55 ± 0.16	1.28 ± 0.13	1.15 ± 0.12
$D_{R,bulk}$ (ps^{-1})	0.11 ± 0.01	0.09 ± 0.01	0.11 ± 0.01	0.11 ± 0.01
$D_{T,hyd}$ (10^{-7} cm^2s^{-1})	5.17 ± 0.12	3.34 ± 0.07	4.86 ± 0.10	4.41 ± 0.09
$D_{R,hyd}$ (ps^{-1})	0.06 ± 0.02	0.09 ± 0.03	0.05 ± 0.01	0.05 ± 0.01
Γ_{prot} (meV)	0.431 ± 0.004	0.451 ± 0.003	0.363 ± 0.005	0.347 ± 0.005

We observed small, albeit significate differences in the dynamics at the two HHP values for the different components. Generally speaking, HHP had the effect of reducing the molecular dynamics (Figure 22 and Table 2) as seen by the slight narrowing of the dynamic structure factors, complying with Le Châtelier's principle of decreasing the volume.[24] In total, the variations were somewhat higher for the piezophile. The fractions of atoms contributing to the different motions, p_{el}, p_{bulk}, p_{hyd}, and p_{prot}, have different sensitivities. Although the proportion of hydrogen atoms seen as immobile and of those belonging to the proteome do not change within the experimental accuracy, there seems to be a certain exchange between the populations of bulk and hydration water in the role they play for the two species. *T. kodakarensis* has a higher hydration water population than *T. barophilus* and vice versa for the bulk water proportion. Such findings resemble the results described for other cells in the literature [182], so we could safely attribute them to bulk and hydration water. However, *T. kodakarensis* appears to bind more water at the cell surface.

Water molecules perform simultaneously translational and rotational motions, however, the rotations are generally found to be much smaller and faster. We assume that external conditions have not much impact on these small movements, what is indeed reflected in the almost constant values found for D_R, and can hence be neglected in the following discussion. As water is essentially incompressible, HHP has no impact on the bulk water mobility in this pressure range, what translates into a constant value for its translational diffusion coefficient $D_{T,bulk}$, in close agreement with the literature value of pure bulk water.[183] The residence time, τ, could only be evaluated for bulk water due to the limited q-range accessible for the data analysis. It stands for interactions between molecules and is slightly enhanced for *T. barophilus* at the higher pressure, but remains within the error limits for *T. kodakarensis*. Remarkably, the diffusion coefficient of hydration water $D_{T,hyd}$, which is smaller than that of bulk water by almost two orders of magnitude, is drastically reduced under HHP, in particular for the piezophilic species. Such a change in the hydration water property could be part of the adaptation strategy of the prokaryotes.

The most striking feature was found for Γ_{prot}, the width of the proteomic structure factor, representing its flexibility. While HHP is generally expected to reduce the flexibility of biological systems, a broadening was found for *T. barophilus* under HHP, which is in line with the MSD values being larger for *T. barophilus* (and for the lysed cells of *T. kodakarensis*) than for *T. kodakarensis* (Figure 14). In contrast, the proteome of *T. kodakarensis* behaved as expected. In addition, the proteome of the piezosensitive species exhibits a much smaller conformational flexibility, indicating stronger intramolecular non-covalent and hydrophobic interactions. The peculiar dynamic features of *T. barophilus* suggest that they are part of the adaptation mechanism to HHP, in conjunction with the reduced diffusivity of hydration water at 400 bar (these results are schematically summarized in Figure 23).

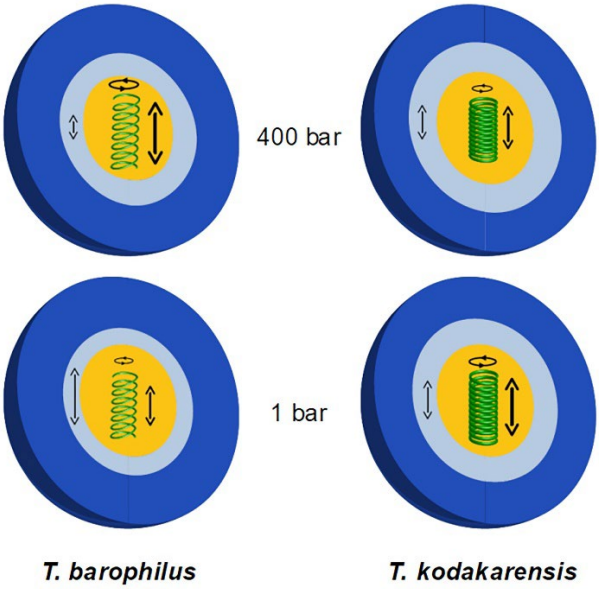

Figure 23. Schematic representation of the HHP effects on the proteome of *T. barophilus* and *T. kodakarensis* cells. Bulk water is shown in dark blue, the light blue surface represents hydration water. The green spring indicates schematically the proteome and its dynamic features (translational and rotational motions). The arrow in the light blue area symbolizes the pressure sensitivity of the hydration water dynamics (reproduced from [130]).

In conclusion, we found opposite effects of the fast proteome dynamics regarding the temperature and pressure dependence on whole cells of *T. barophilus* and *T. kodakarensis* despite the limitations imposed by crowding. Temperature tends to increase the flexibility as more thermal energy is provided to the system, and HHP reduces globally the mobility as the internal cavities of proteins are compressed and the volume available for motions is diminished at HHP. We note, however, that an organism adapted to HHP conditions has the capacity to maintain or even slightly increase the flexibility of its proteome upon a pressure increase, at least until its natural living conditions are reached. At first glance this might appear counterintuitive, but could correspond to a higher resilience with respect to its natural harsh pressure environment. *T. kodakarensis* presents overall a higher stability against pressure application and binds more hydration water on its surface, indicating stronger bonds.

6.4. Relation to External Stress: Salinity

In organisms living at high salinity, but lower than 1.5 M, proteome stability is maintained through the accumulation of organic osmolytes concomitant with the exclusion of the inorganic ions Na^+ and K^+ by the cells to maintain the intracellular concentration of ions in the physiological range. The impact of organic osmolytes as crowders on protein behavior is presented in detail in Section 7.

As described in Section 2.3., species living at salt concentrations higher than 1.5 M adjust their intracellular salinity to match that of the environment (*salt-in* strategy). To maintain functionality, the proteome had to undergo extensive reformatting during evolution.[57] Halophilic proteins exhibit an increased proportion of specific amino acids in their sequence: aspartic and glutamic acids and residues with short polar side chains, while residues with hydrophobic side chains are penalized[62] which is known as the halophilic signature. Amino acid substitutions are found to occur mostly at the surface

of the protein, which is congruent with observations that protein-solvent interactions are altered under high salts.[184, 185] Halophilic proteins contain fewer hydrophobic amino acids and an increase in negatively charged amino acids at the surface. As a consequence of adaptation, obligate halophilic proteins require high salt concentrations to fold properly and remain active and stable.[57, 186] In terms of protein structure and stability, it is very important to understand the adaptation to high salt content and its consequences on protein behavior, since the presence of salts affects the main physical parameters that make a protein stable: hydrogen bonding, disulfide bonding, van der Waals interactions, and the interaction with the aqueous solvent. Several studies showed that protein denaturation by salt is prevented by the increase of interactions between hydrated salt ions and the modified amino acids at the surface of the protein. The main adaptation is the replacement of neutral amino acids at the surface of the protein by acidic residues. This creates a very acidic surface, which under the neutral pH of the intracellular space, is highly negatively charged, giving the proteins a large negative isoelectric potential and the capacity to recruit more solvent in the salt-rich medium. To maintain protein functionality, this excess of acidic residues is absent at specific locations, such as the catalytic site, where specific amino acids may be required. A second adaptation is the presence of ion binding sites. They are often present at subunit interfaces. The presence of salt bridges has been associated with thermal tolerance of proteins, and is supposed to play a similar role in halophilic proteins. The third adaptation mechanism also involves salt bridges. Salt-driven water enrichment at the surface of proteins has the potential to destabilize them. The increased number of salt-bridges, by preventing the local water enrichment, protect halophilic proteins from denaturation.

The molecular dynamic properties of the proteome from the obligate halophile *Halobacterium salinarum* has been measured by neutron scattering.[187] The results of the experiments yield the MSDs, which reflect sample flexibility at a given temperature and an effective force constant, <*k*>, which corresponds to both structural rigidity (the enthalpic term due to internal forces) and conformational sampling (an entropic term). Measurements of macromolecular internal motions in the cell by neutron scattering under the crowding conditions of intact live and active cells revealed significant differences in proteome behavior between the mesophilic bacterium *Escherichia coli* and the obligate halophile *Halobacterium salinarum*. The salt-adapted proteome is stiffer and smaller, indicating less mobile hydration water. Previous data obtained on the enzyme malate dehydrogenase (MalDH) could correlate this modification of molecular dynamics to an increased rigidification of the proteins themselves,[188] which in turn is explained by the structural adaptation of the proteome to high salt. Halophilic proteins are less susceptible to attractive intermolecular interactions than non-halophilic proteins, ultimately leading to aggregation.[185]

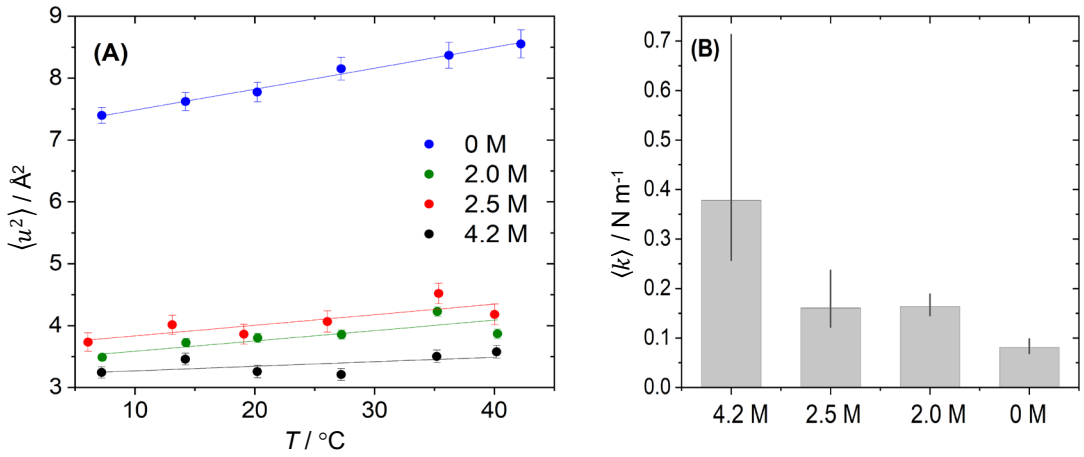

Figure 24. Dynamic response in live *H. salinarum* to hyposaline stress (modified with permission from [187]). (A) Mean-squared displacement, $\langle u^2 \rangle$, plotted against temperature for unstressed and low-salt-stressed cells. (B) The corresponding effective force constants, $\langle k \rangle$.

Interestingly, under low-salt concentrations, the proteome displayed a marked modification of its molecular dynamics (Figure 24 A), demonstrating the salt-dependence of the proteome in this species. The increase in molecular dynamics measured under reduced salt concentration is as important as that measured under thermal stress (Figure 25)[189] congruent with an extensive protein unfolding when cells of the halophile experience low salt concentrations. Furthermore, this suggests that structural adaptation to high salt concentrations to counteract the impact of the charged ions on the proteins occurs at the expense of the stability of the structure under mesophilic conditions.

The adaptation of proteins to the presence of molar salt concentrations, but not in the presence of osmolytes, requires weakening of the hydrophobic interactions at the level of the core and conserved hydrophobic contacts. The weakening of these interactions can offset their strengthening caused by the presence of salts in solution and in turn prevents protein aggregation or loss of function. As a consequence of reduced hydrophobicity, the salt adapted proteins become unstable at low-concentrations of salt. It is interesting to note that in most cases evolution has selected adaptations that follow the "corresponding state principle", put forward by Vihinen[190] and Jaenicke,[191] i.e., the physical parameter values are maintained in the same range of values through structural modifications, regardless of the environmental stressor. In contrast, the halophilic proteome has accumulated mutations to counteract the destabilizing effect of the K^+ and Na^+ ions which have modified its overall rigidity, while maintaining its functionality.

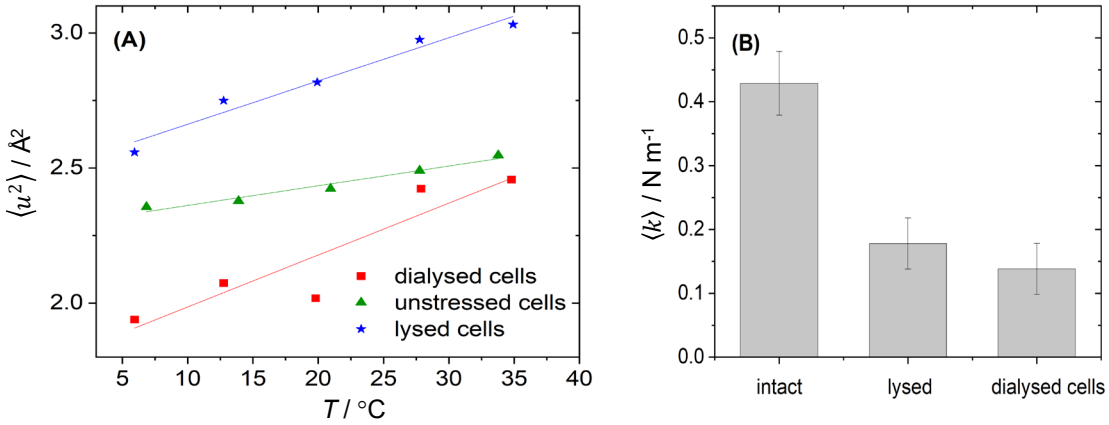

Figure 25. Dynamic response in live or lysed *Halobacterium salinarum* cells to thermal stress. (A) MSDs $\langle u^2 \rangle$ for large amplitude fluctuations plotted for live, intact, unstressed cells (green), lysed cells (blue), and lysed cells dialysed against a 3.4 M NaCl buffer (red). (B) Histograms of the effective mean force constants, $\langle k \rangle$, from the same cell samples. Modified from Marty.[192]

Similar to the high pressure experiments reported above, the molecular dynamics of the *Halobacterium salinarum* proteome was compared with reduced crowding conditions following cell lysis. The MSDs of the cells before and after lysis (Figure 25) were obtained by EINS and represent averaged motions of atomic nuclei around their equilibrium positions. MSD values for the lysed cells show a marked difference from those of intact cells. Dialysis against a 3.4 M NaCl buffer significantly decreases the flexibility of the proteome as evidenced by the decrease of $\langle u^2 \rangle$. It does not significantly alter its rigidity. A similar experiment performed with cells from the mesophilic bacterium *Escherichia coli* did not show a marked difference between the intact and lysed cells,[192] neither in terms of flexibility nor in terms of the rigidity of the proteome. Taken together, these observations suggest that a significant part of halophilic adaptation is due to 'crowding' by the inorganic osmolytes (K^+ and Na^+) and another part is due to the 'normal' intracellular macromolecular crowding effect.

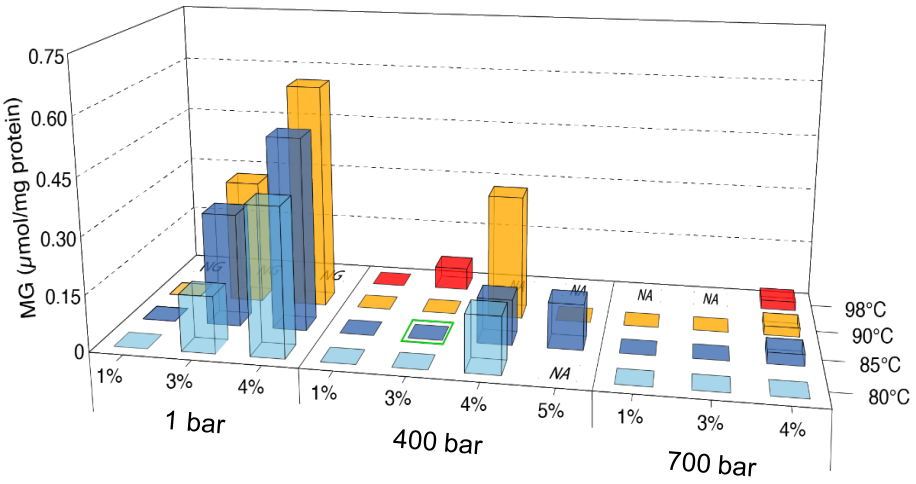

Figure 26. MG accumulation measured in *T. barophilus* as a function of combined stresses in hydrostatic pressure, salinity and temperature. Optimal growth conditions (no stress) is highlighted by

a green rectangle. NG: No growth, i.e. *p*/*T*/salinity combination incompatible with growth of *T. barophilus*, e.g. 98 °C at atmospheric pressure. NA: Not analyzed. Modified from [193].

In obligate halophiles, the adaptation to high salt follows the *salt-in* strategy, which implies extensive modifications of the proteome. As mentioned above, halotolerant and moderate halophiles, whose adaptation relies on the *salt-out* strategy, tend to accumulate organic osmolytes to counteract the effects of salinity. Osmolytes accumulate only under high-salt stress, as the proteome of these species is not destabilized under low salt conditions. Osmolytes generally interact with the water molecules of the hydration shell of the proteins, creating a favorable environment for proteins to fold, and thus maintain their activity. As mentioned above, increased temperature and increased HHP have opposite effects, while decreased salinity has a very similar effect as an increase in temperature. In the natural environment, microorganisms often experience multiple stresses simultaneously (thermal, pH or high pressure stresses), all of which impact cellular macromolecules in specific ways. The cells must then counteract these multiple stressors simultaneously. In a study of the high-pressure adapted archaeon *T. barophilus*, Cario and colleagues monitored the stress response of this species to a combination of three stressors, temperature, salinity, and high hydrostatic pressure (Figure 26).[193] *T. barophilus* is a polyextremophile and an obligate thermophile. Its optimal temperature is 85 °C with a requirement for at least 70 °C for growth. It is also a piezophile with an optimal growth pressure of 400 bar and a halotolerant with an optimal salinity of 3% and a requirement for at least 1% salt. In this species, the proteome is structurally adapted to both high temperature and HHP, although the molecular basis for the latter is not yet fully understood. Under stress, cells accumulate only one type of organic osmolyte, mannosylglycerate (MG), and no inorganic ones. By varying the stressors from the lowest suboptimal values possible to the highest ones, one can observe how this species copes with multiple stressors and how the cell response is modulated by the structural adaptation of the proteome.

Under optimal conditions (85 °C, 400 bar, 3% NaCl), no osmolyte is accumulated, as expected. Under optimal hydrostatic pressure conditions, the osmolyte is accumulated under high salt and high temperature. Strikingly, osmolytes accumulate most at suboptimal hydrostatic pressure. Similar to what has been reported for halophily, the structural adaptation of the proteome to HHP is obtained at the expense of its stability at low pressures. MG accumulation is most important for a combination of all three stresses at low pressure, high salt and high temperature (1 bar, 4% NaCl, 95 °C). In contrast, supra-optimal hydrostatic pressure seems to be able to counteract the impact of thermal and salinity stresses as almost no osmolyte is accumulated at 700 bar. This simple example illustrates the complexity of deciphering the behavior of biomacromolecules in the context of a cell, as many parameters may respond to counteract the effect of a stressor and substantially modify the crowding to which the proteome is exposed.

7. Crowding and Cosolvent effect on Protein Dynamics under Extreme Conditions

Many organisms which are thriving in extreme environmental conditions of temperature, pressure, salinity, pH or others, were found to accumulate inorganic osmolytes (mostly halophiles) or small organic molecules which are soluble in the intracellular cytosol. As they are osmotically active solutes, they are usually called osmolytes.[35] They are organic compounds with small molecular masses, which are also termed compatible solutes as they do not disturb the structural and functional properties of

the cellular constituents.[194] Conversely, next to their function as osmoregulators, they also contribute the stabilization of the native fold of the biomolecules, such as proteins, and, in particular instances, promote the conformational dynamics and function (see Chapter 8) of biomolecular systems within the crowded cellular milieu. Compatible solutes are found to be polyhydric alcohols (polyols) or sugars such as glycerol or sucrose, free amino acids and their derivatives. Glycine, for instance, is the main osmolyte found in invertebrates living in shallow water. One also finds urea and methylamines, particularly TMAO, synthesized by organisms that inhabit the deep sea to counteract the perturbing factors imposed by high pressure stress,[195] betaine or sarcosine.[196] Notably, the osmolyte urea, which has a perturbing effect on proteins, when combined with TMAO (typically at the urea:TMAO ratio 2:1 as found in deep sea invertebrates), loses it deteriorating effect. Some extremophiles produce other organic osmolytes, which appear to be better adapted to the stresses encountered in their habitat. For instance, the small organic osmolyte mannosyl-glycerate is encountered in hyper- and thermophiles, only.[193, 197]

To explore the properties of these organic cosolvents, which may also be viewed as microcrowders, they should also be studied in physiologically relevant scenarios, that is, under macromolecular crowding conditions. To this end, besides natural crowding solutions, model crowding agents such as the synthetic neutral polymers Ficoll, dextran and PEG of variable length and molecular weight (MW) are often employed. The inertness, i.e., the absence of non-specific interactions with biomolecular components has to be checked beforehand, however. Such crowding agents cannot reproduce the polydispersity and heterogeneity of a natural cytosolic environment, however. To avoid such artificial crowding situation, M. Salvador-Castell et al.[37] grew the hyperthermophilic piezophile *T. barophilus* under its native conditions, 85 °C and 400 bar, but also at the same temperature at ambient pressure (1 bar), which is perceived as stress to the cells. This results in the production of the osmolyte mannosyl-glycerate (MG) by the cells, in order to counteract the stress (Figure 27).

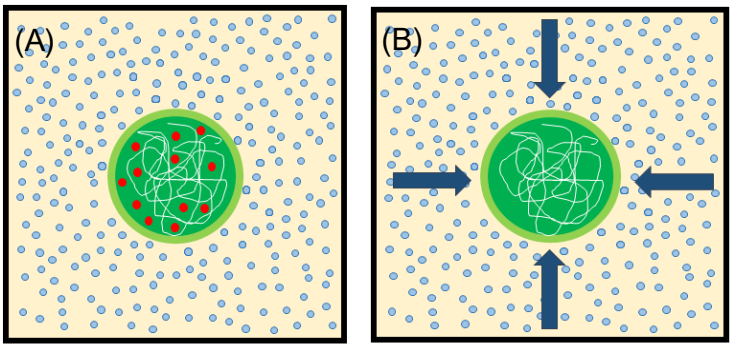

Figure 27. Sketch of the two cells of *T. barophilus*: Tba_MG (left) is grown at optimal temperature, but under atmospheric pressure and has accumulated MG (red circles). Tba_Ø (right) is grown under optimal pressure and temperature conditions.

By proceeding with incoherent neutron scattering experiments, the molecular dynamics arising from the cellular proteome and the surrounding solvent could be determined separately inside the cells,[138] both for the cells grown in optimal conditions, and for those under low pressure stress that accumulated the osmolyte. EINS data were taken and summed intensities were calculated, which are inversely proportional to the MSDs, as a function of temperature and HHP (Figure 28).

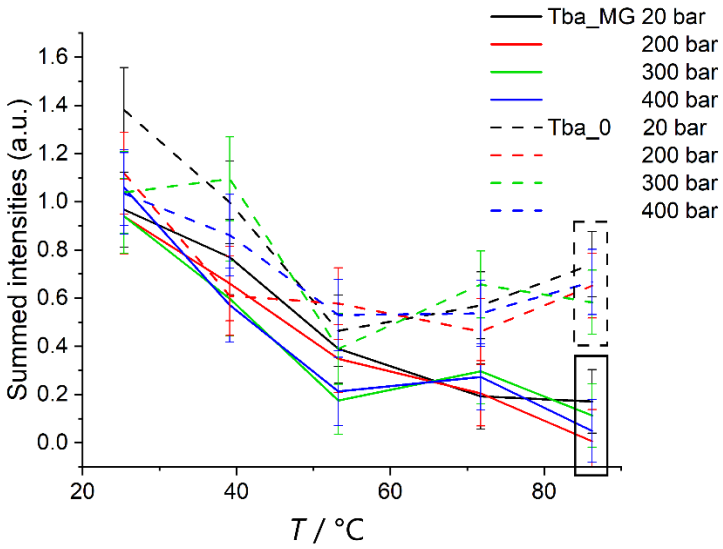

Figure 28. Summed neutron intensities from EINS experiments on Tba_Ø, the piezophile grown under optimal conditions, and Tba_MG grown under stress conditions and accumulating MG, as a function of temperature and for selected pressure values (modified from [37]).

For both samples, the summed intensities show a similar temperature dependence in the range between 20 and 52 °C, displaying enhanced dynamics with increasing temperature, as expected, but no significant changes were observed upon compression. Around 52 °C, the samples begin to show a divergent behavior. Whereas the piezophile grown under optimal conditions, Tba_Ø, shows slightly increasing summed intensities above 52 °C (corresponding to decreasing or almost constant MSDs), reflecting the fact that the molecular dynamics is stabilized close to the optimal growth temperature (85 °C). Although the statistics is not very good here due to the mandatory thickness and high absorption of neutrons by the HHP cell, this could be seen in agreement with the findings for the local diffusion coefficient of *E. coli* (Figure 16 B), which tends to a plateau just below T_{CD}, corresponding to highest growth rates. The sample called Tba_MG, grown under stress conditions and accumulating MG, presents summed intensities which continue to decrease with a smaller slope, i.e., the MSDs continue to increase with temperature. Such behavior is symptomatic for a restructuring of cell proteins. Note that the minimal growth temperature of *T. barophilus* is 48 °C,[198] i.e., the temperature range covered corresponds to a window between the minimal and the optimal growth temperature. Within this temperature range, the cells show stable dynamics, but are destabilized below and above it, which manifests itself in the inability to grow. On the contrary, the osmolyte MG seems to limit the structural rearrangements of the proteome, thereby stabilizing it.

We proceeded with the QENS data analysis with respect to hydration and bulk water and the proteome's motions according to the model described by Eq. (7) (Table 3). It becomes clear that the osmolyte is not able to provide fully equivalent dynamical characteristics to the cell grown under optimal conditions, but supports the functioning of the stressed cell.

Table 3. Fit parameter values for the samples of Tba_MG and Tba_0 at different pressures (1 bar and 400 bar) and temperatures (25 °C and 85 °C). The fields in green show characteristic responses to HHP for piezophiles. Dark green indicates similarities between samples, light green fields point out

parameters differing between samples. The fields in blue correspond to the osmolyte effect on bulk water. The fields in red are indicative of a different response to HT between samples (reproduced from [37]).

	Tba_MG		Tba_Ø	
25 °C	**1 bar**	**400 bar**	**1 bar**	**400 bar**
p_{el}	0.01 ± 0.01	0.01 ± 0.01	0.01 ± 0.01	0.01 ± 0.01
p_{hyd}	0.11 ± 0.02	0.11 ± 0.02	0.10 ± 0.02	0.11 ± 0.02
p_{bulk}	0.65 ± 0.03	0.65 ± 0.03	0.66 ± 0.03	0.65 ± 0.03
p_{prot}	0.25 ± 0.03	0.25 ± 0.03	0.24 ± 0.03	0.25 ± 0.03
$D_{T,bulk}$ (10^{-5} cm^2s^{-1})	1.85 ± 0.05	1.85 ± 0.05	1.85 ± 0.05	1.85 ± 0.05
τ_{bulk} (ps)	0.91 ± 0.10	1.64 ± 0.07	0.96 ± 0.09	1.45 ± 0.11
$D_{T,hyd}$ (10^{-7} cm^2s^{-1})	5.9 ± 0.3	4.5 ± 0.3	5.7 ± 0.3	2.9 ± 0.3
Γ_{prot} (meV)	0.43 ± 0.01	0.43 ± 0.01	0.43 ± 0.01	0.43 ± 0.01
85 °C				
p_{el}	0.01 ± 0.01	0.01 ± 0.01	0.01 ± 0.01	0.01 ± 0.01
p_{hyd}	0.22 ± 0.03	0.21 ± 0.03	0.21 ± 0.03	0.21 ± 0.03
p_{bulk}	0.47 ± 0.05	0.47 ± 0.05	0.47 ± 0.05	0.46 ± 0.05
p_{prot}	0.31 ± 0.03	0.32 ± 0.05	0.32 ± 0.05	0.33 ± 0.05
$D_{T,bulk}$ (10^{-5} cm^2s^{-1})	5.2 ± 0.1	5.1 ± 0.1	6.7 ± 0.1	6.6 ± 0.1
τ_{bulk} (ps)	0.10 ± 0.05	0.11 ± 0.05	0.46 ± 0.09	0.47 ± 0.08
$D_{T,hyd}$ (10^{-7} cm^2s^{-1})	5.6 ± 0.4	4.0 ± 0.4	2.7 ± 0.4	1.8 ± 0.4
Γ_{prot} (meV)	0.61 ± 0.01	0.61 ± 0.01	0.61 ± 0.01	0.61 ± 0.01

¶

The diffusion coefficient of hydration water, $D_{T,hyd}$, was reduced by HHP application, as expected. At room temperature, where the prokaryotes are supposed to be in a metabolically inactive state and *T. barophilus* resides below its minimal growth temperature, the accumulation of the osmolyte MG limits the changes as opposed to the cells lacking it. The latter is reminiscent of the lysed cells of *T. kodakarensis*, in which crowding was abolished, resulting in a more pressure sensitive response. [131] At high temperature close to the optimal growth conditions, the decrease is slightly smaller for Tba_Ø. At 85 °C and 400 bar, close to the native conditions of *T. barophilus*, $D_{T,hyd}$ is found in agreement with results for other cell types, e.g. red blood cells[199], *E. coli*[200] and *H. marismortui*[168], indicating that the cells require a very similar hydration water dynamics, regardless of the exact native conditions of the cell. This is reminiscent of the "corresponding state principle", put forward by Vihinen[190] and Jaenicke[191], to explain the resemblance of dynamical characteristics of extremophiles and non-extremophiles under their respective optimal living conditions. This result, together with the observed slight increase of the residence time of bulk water, τ_{bulk}, under pressure application, which indicates stronger interactions between molecules and the presence of exchange mechanisms between biomolecules and their hydration water[167], can be considered characteristic of the adaptation to HHP in these organisms.

The translational diffusion coefficient $D_{T,bulk}$ does not vary with HHP in this pressure range, as already observed before. However, at high temperature $D_{T,bulk}$ differs for Tba_MG and Tba_Ø, with the latter having a higher value, demonstrating the stabilizing effect the osmolyte has on the proteome and its surrounding. This feature can be attributed to an impact of the presence of MG. The dynamics of the proteome itself, represented by Γ_{prot}, is in agreement with the value found previously for *T. barophilus* and is essentially constant when the crowding or HHP are changing, but it increases with temperature, as expected. All motional fractions, p_{el}, p_{bulk}, p_{hyd}, and p_{prot} do not vary with HHP or crowding, but the bulk water fraction diminishes when temperature is rising at the expense of both the proteome and hydration water fractions. The metabolically active state appears to be able to involve more particles from the proteome to the dynamics and better bind the hydration water at the cell's surface.

Overall, these findings confirm the hypothesis that a compatible osmolyte such as MG has a significant impact on crowding within the cells, leading to stabilization or rigidification of the proteome, although the exact mechanism of action is not yet known.[201] This indicates that the osmolyte is not directly acting on the protein dynamics, but through a crowding-type of excluded volume effect. These results from live cells require, however, further confirmation.

7.1. Effect of Organic Osmolytes, Level of Hydration, and Crowders

To gain more insights into the effects by organic osmolytes, we studied their implications on self-crowded proteins, i.e., highly concentrated lysozyme solutions.[78] The stabilizing effect of TMAO and the denaturing effect of urea were probed directly on the protein dynamics, as well as the compensating effect of the two osmolytes at a 2:1 TMAO:urea ratio.[52, 59] The latter phenomenon can be understood in terms of the different interactions the two osmolytes have with water: while urea preferentially interacts with the protein backbone,[202] TMAO is predominantly excluded from the protein's hydration layer, leading to preferential hydration and strengthening of the hydrogen bond network around the protein (Figure 29).[203]

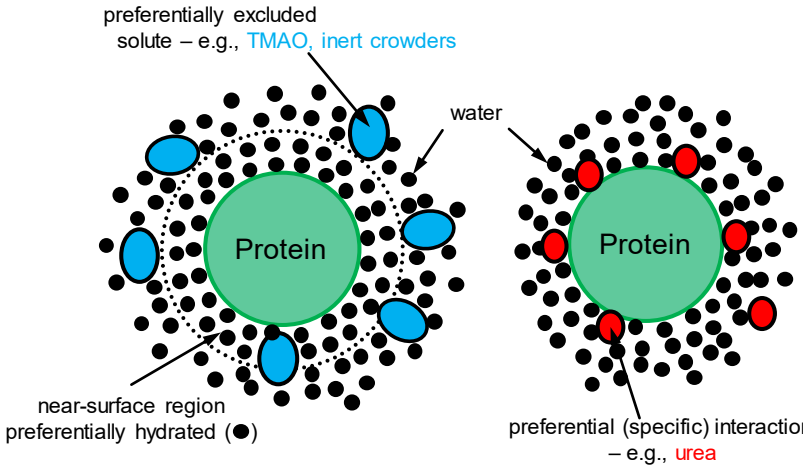

Figure 29. Schematics of the location of different cosolutes around a protein. Compatible cosolutes such as TMAO or inert crowders are preferentially excluded from the protein interface, leading to its preferential hydration, whereas other cosolutes, like urea, penetrate the hydration shell and interact preferentially with surface groups of the protein.

At the lower concentration of 80 mg/mL, the MSDs of the pure protein sample decrease with increasing pressure until 2000 bar from where on it stays essentially constant (Figure 30).[204] Upon addition of the osmolytes the MSDs' pressure dependence remains almost unchanged within the error bars, but all MSDs are decreased by 35% (urea) to 70% (TMAO) compared to the case lacking the cosolvent. This indicates that the osmolytes strongly affect the pressure dependence of the fast protein dynamics. One could speculate that their effect is due to changes in the structure of the protein's hydration water. Decreased protein hydration is expected in presence of urea, due to its preferential interaction with the surface of proteins, replacing hydration water molecules. Drying a protein is known to imply a reduction of the internal motions.[139] TMAO is known to be preferentially excluded from the protein interface, strongly interacting with bulk water molecules, and strengthening the structure of hydration water around the protein. As hydration 'slaves' the conformational fluctuations of the sidechains at the protein's surface, this effect may reduce the conformational flexibility of the protein. Adding urea to a TMAO-lysozyme mixture does not induce major changes in the dynamics, indicating the capacity of the compatible deep-sea osmolyte TMAO to compensate for the effect of urea.

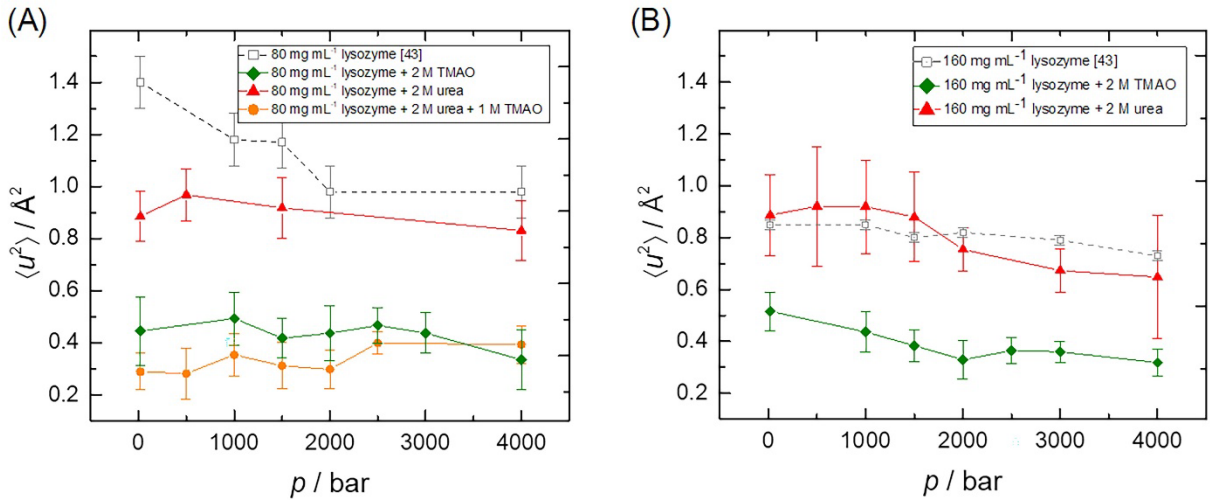

Figure 30. Pressure dependence of the MSDs, $\langle u^2 \rangle$, of 80 mg/mL (A) and 160 mg/mL (B) lysozyme in the presence of TMAO and urea. Data for lysozyme in pure buffer solution, i.e., in the absence of any cosolvents, are shown as reference. Reproduced from ref. [78] Copyright 2017 PCCP Owner Societies.

Self-crowding by lysozyme leads to a lowering of the molecular dynamics and almost insensitivity to HHP application. Still, TMAO does reduce the MSDs markedly, by a factor of about two, even at this high protein concentration. The sole addition of urea does not modify the MSDs at this high protein concentration. The measurements were further complemented by DSC and FT-IR spectroscopy investigations, which probe the stability of the protein and the impact of the osmolytes on its secondary structure,[78] revealing the strong stabilizing effect of TMAO (destabilizing effect of urea), leading to an increase (decrease) of the temperature and pressure of unfolding. Further exploration is needed to elucidate the complex effect that osmolytes have on the internal dynamics of the protein, invoking molecular dynamics simulations and exploring different time scales of the dynamic features of the protein. The impact of such osmolytes on biomolecular function, such as ligand binding and enzymatic activity, will be discussed below.

The effect of TMAO on protein dynamics was also investigated in a more compelling scenario by examining its effects on pressure-adapted proteins. The previously described data on the markedly different dynamical properties of *T. barophilus*' and *T. kodakarensis*' proteomes, and their different responses to high pressure[121, 126] and crowding,[122] inspired the study of single homologous proteins from these two organisms to characterize the adaptation to high-pressure at the molecular level. This strategy allowed the elimination of complicating factors associated with the experiments on whole cells while maintaining the advantage of selecting of two nearly isogenic species that differ only in one characteristic adaptation. The first results of this investigation[18] performed on the *Phosphomannose Isomerases* (PMIs) from the two organisms indicate existence of a specific amino-acidic substitution pattern aimed at eliminating cavities in the hydrophobic core of the proteins by employing bulkier residues and rearranging surface charges in the piezophilic proteins. The first kind of substitutions leads to an increased pressure stability of the *T. barophilus* (Tba) PMI, granting it the ability to retain its dynamical properties up to and beyond the optimum growth pressure of the organism, while the *T. kodakarensis* (Tko) PMI loses flexibility with increasing pressure as a result of water intrusion into its internal cavities. The second kind of substitution results in decoupling of protein-water cooperative relaxations at the surface of the piezophilic protein, effectively preventing the aforementioned water penetration and protecting the protein from the deleterious effects of high pressure.

Nevertheless, evidence of production of MG by *T. barophilus* under stress conditions[187] and findings on its effect on the proteome of the organism[37] indicate that osmolytes are extensively used by piezophiles to modulate the dynamics of their proteome. EINS studies of the dynamics of Tba PMI and Tko PMI with and without added TMAO revealed that it has a structuring effect on the surrounding water molecules,[205] likely leading to the emergence of a potential barrier that impedes free rotation of the molecule and only allows three-site jumps[142] as detected within the sub-ns time scale of the experiment. Global fittings of the two-state model[146] provided information about the temperature dependence of the total MSDs, Δx_{tot}^2, the distance between the wells in the two-state potential, *d*, and the difference in enthalpy, ΔH, and entropy, ΔS, between them.

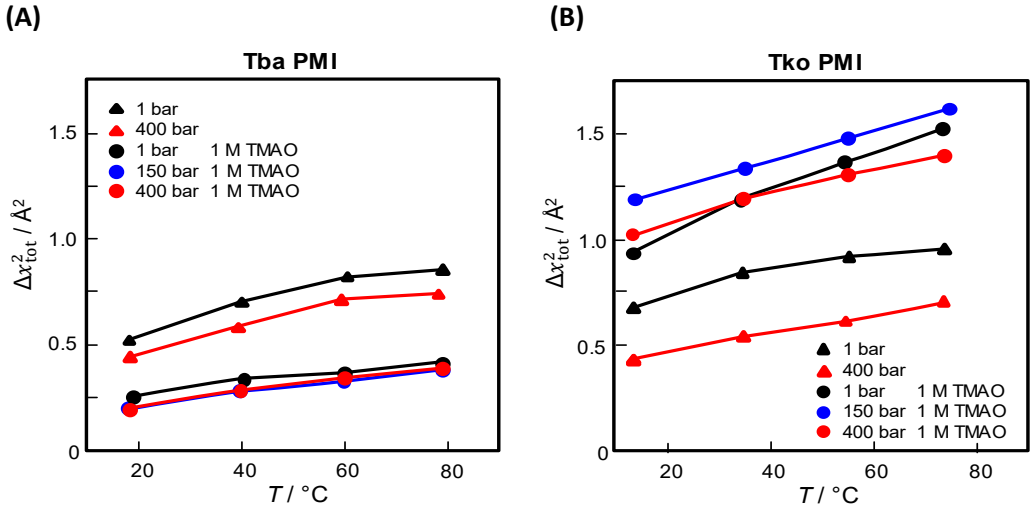

Figure 31. (A) Total MSDs for Tba PMI and (B) Tko PMI as a function of temperature at different pressure points, in the absence (empty circles) and presence (full circles) of TMAO (reproduced from [206]).

Figure 31 exhibits the total MSDs for all the samples. When TMAO is not present, the results are in line with preceding studies,[18] Tba PMI being able to retain most of its dynamics under high-pressure conditions, while Tko PMI becomes significantly stiffer. Upon the addition of 1 M TMAO, the two proteins react in opposite ways. On one hand, the amplitude of the motions of H-atoms in Tba PMI decreases by a factor of two, and it becomes even more pressure-insensitive. On the other hand, Tko PMI becomes more flexible and remains so even at 400 bar.

A similar trend is observed by the other relevant parameters obtained from the model,[146] such as the distance between potential wells, d (Figure 32 A), which reports on the roughness of the protein's energy landscape,[207] the entropy difference ΔS (Figure 32 B), which is connected to the hydration of the proteins,[138] and the free energy difference ΔG (Figure 32 C) between the two states, calculated for T = 27 °C. In our previous study,[18] we showed that the decrease in d and the increase in ΔS for Tko PMI under high pressure corresponds to a general stiffening of the protein and to the loss of structural stability. This can also be observed in the current results for Tko PMI in the absence of TMAO. At the same time, the addition of TMAO seems to help the protein regain its flexibility, consistent with the hypothesis that the osmolyte is able to maintain protein function under pressure. Conversely, Tba PMI becomes stiffer upon addition of TMAO and exhibits an increased roughness of its energy landscape, but its entropy increases with pressure, indicating enhanced hydration.

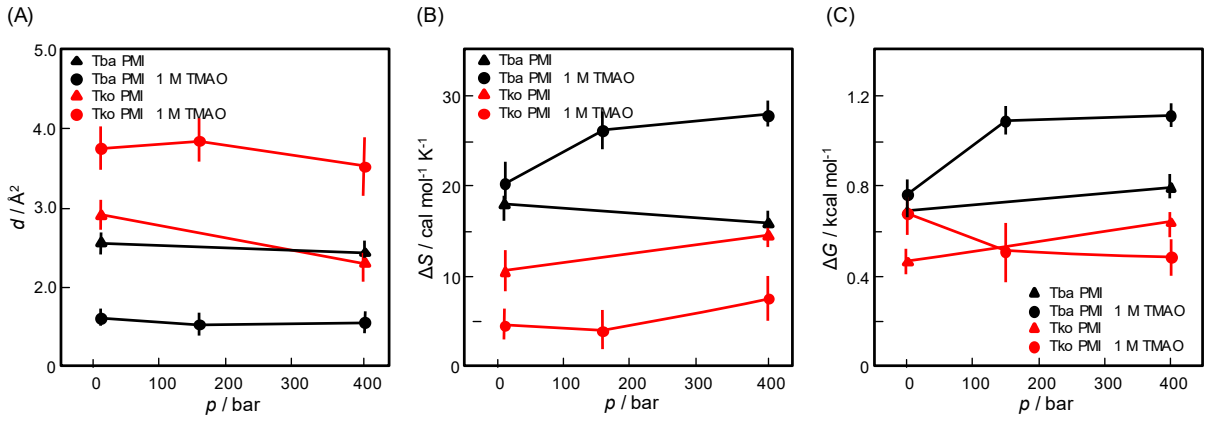

Figure 32. Distance between potential wells, *d*, representing the roughness of the energy landscape (panel A), and the entropy difference (panel B) and free energy difference (panel C) between the two states for Tba PMI (black circles) and Tko PMI (red circles) in the absence (empty circles) and the presence (full circles) of TMAO (reproduced from [206]).

These results may appear counterintuitive, as increased hydration is typically connected to enhanced dynamics and vice versa. However, the presence of TMAO and the strong structuring effect it has on water molecules leads to significant enthalpic effects due to electrostatic interactions. The combination of enthalpic and entropic effects results in ΔG, the free energy difference between the two states (Figure 32 C). It must be emphasized that in the temperature range studied here, the two-state model does not refer to actual states of the protein, but rather reflects an average representation of multiple states of the protein's energy landscape that are populated at that temperature, so that ΔG is an average measure of the potential barriers that the protein has to overcome during its motions. The addition of TMAO to Tba PMI steeply raises the potential barrier height, which explains the severe hindrance of its dynamics. Conversely, when added to Tko PMI, TMAO induces a slight increase of the energy barrier at ambient pressure, but the trend reverses upon pressurization, consistently with the enhanced dynamics observed in the MSDs.

The contrasting response of the two proteins to the addition of the osmolyte can be explained by the different amino-acidic compositions they present on their surfaces. We have shown that Tba PMI tends to avoid direct interactions with water by virtue of specific substitutions at the protein surface, which promote the formation of salt bridges and therefore decrease the availability of some residues to interact with water.[18] This, in turn, decouples protein-water cooperative dynamics, which seems to be advantageous in the framework of pressure adaptation. Therefore, when TMAO is added, its preferential hydration brings about solvent-induced polarization,[208] resulting in pressure-enhanced hydrogen bonding, which most likely causes the observed reduced flexibility of the protein. This picture would explain why *T. barophilus* accumulates osmolytes under stress conditions such as low pressure or temperatures beyond its optimum growth temperature, as its proteome would be too flexible in both these situations, whereas under optimal conditions no osmolytes are produced, as the proteome is already adapted to be sufficiently flexible under high pressure. In the case of Tko PMI, more charges are available on the surface of the protein, allowing it to win the competition with TMAO for water molecules and enhancing its dynamics.

Proteins need a solvent environment to achieve their functionality through protein flexibility, but a rather small amount (around 0.2 g of solvent/g of protein) is sufficient to ensure their operation. Therefore, it is possible to investigate them in hydrated powder form rather than in solution [209, 210], even though one has to treat carefully the data in both contexts.[137] Such powders are consequently highly self-crowded ensembles. They strongly bind water molecules at their surface, which corresponds to hydration water and is different in its characteristics from bulk water. Owing to the lack of freezing of hydration water in such protein samples at subzero ^{o}C temperature, they can be studied at temperatures below the freezing point of water, for example using neutron scattering techniques. Neutron scattering includes always a coherent part, giving access to structural information and collective motions, and an incoherent part, which represents the molecular dynamics.[138] When water is freezing, its coherent signal in terms of Bragg peaks largely dominates the total scattering intensity, so that the incoherent signal is hardly detectable. Conversely, working with hydrated powders permits to explore the dynamic features also at low temperatures. As already mentioned above (section 2), an example of an important finding was the determination of the so-called dynamical transition in the MSDs of a hydrated protein around 200 K,[146] which was interpreted by Frauenfelder et al.[147] as the onset of anharmonic motions that are mandatory for proper protein function. This goes hand in hand with the emergence of non-vanishing global diffusion motions in the sample, once more highlighting the importance of molecular dynamics for biomolecular function.[211]

The protein surroundings may be classified as plasticizers or stabilizers.[211] Water, which is the natural solvent of biosystems, is probably the most efficient plasticizer, because it makes them softer and more flexible, and this even at low moisture contents. Further, it allows proteins to explore transitions between largely isoenergetic states of their conformational landscape, denoted conformational substates. Other media, such as polyols (e.g., trehalose or glycerol), are stabilizers owing to their capacity to prevent degradation of the biomolecules and increasing their shelf-life. This is likely due to extensive suppression of jumps between these conformational substates. In fact, the functionality of proteins is largely affected by its molecular dynamics, which is significantly influenced by these cosolutes as well.

Paciaroni et al. studied the counteracting effects of the stabilizer glycerol and the plasticizer water on lysozyme powders hydrated at different levels between h = 0 and h = 0.83 g D_2O/g protein.[209] They found that the dynamics of the anhydrous protein in neat glycerol was identical to the MSDs of pure glycerol, implying that the protein motions are strongly coupled ('slaved') to their environment. On the other hand, when steadily increasing the amount of water, its specific plasticizing potential becomes dominant. This can be ascribed to preferential hydration as known for glycerol-water solutions,[212] causing glycerol to be mainly excluded from the surface of the protein. When coating a protein with a carbohydrate compound (e.g., trehalose), the stabilizing, and thus cryoprotectant effect is predominant,[213] suggesting possible biotechnological applications, for instance in the field of drug storage. In such a case, the harmonic motions around equilibrium positions are mainly conserved up to room temperature. The same findings hold for dry lysozyme samples, which present a harmonic behavior up to 177 °C.[210] Tsai et al. studied the relation between the dynamical transition temperature, T_d, and the heat denaturation temperature, T_m, where the protein loses its stability and unfolds. The T_d value was lowest for a sample containing 30% D_2O (- 63 °C). However, a T_d value was also observed when the lysozyme was solvated in glycerol instead of water, but was surprisingly higher at 20% than at 50% glycerol content (57 °C versus -3 °C). Obviously, glycerol facilitated motions in lysozyme which were not possible in the water-free sample at temperatures above T_d, rendering it less stable and more heat labile, in apparent contradiction to the stabilizing effect of glycerol. The authors found further that, on the one hand, glycerol favored anharmonic motions, but not to the same extent as water, and that below T_d, the presence of glycerol resulted in smaller MSDs. Otherwise, T_m was highest for the dry protein and lowest for the protein hydrated with water, where large-scale collective motions can develop and finally cause heat denaturation. They concluded that the interdependence between the motions of the protein, the hydration water, and the cosolvent is very complex and cannot be described by global inherent features of the protein, only.

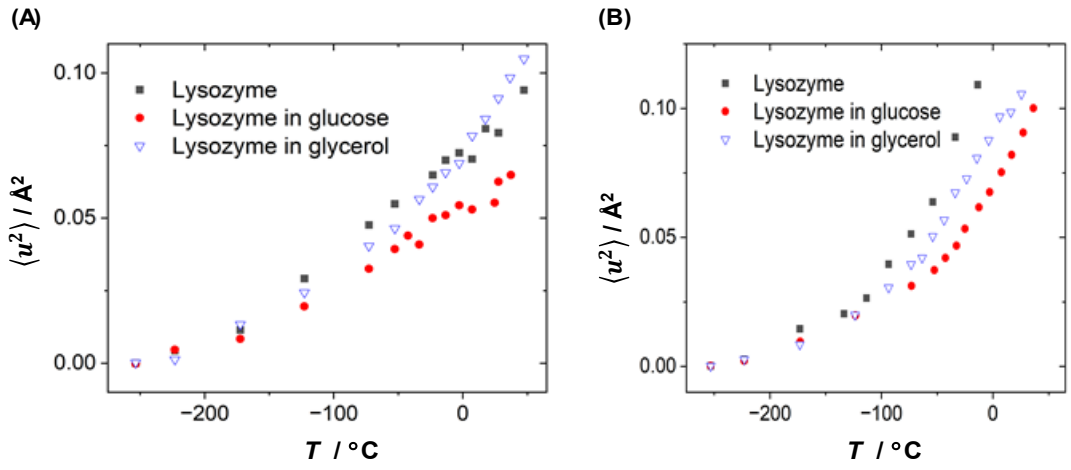

Figure 33. MSD as function of temperature for (A) dry lysozyme, pure, in the presence of glucose or glycerol, and (B) at h = 0.4 for pure lysozyme and in the presence of glucose or glycerol (adapted with permission from ref. [214]).

In a subsequent publication, Paciaroni et al. [214] studied lysozyme in its dry and hydrated form (h = 0 and h = 0.4), in the absence and presence of glycerol and glucose (Figure 33). While the behavior at higher hydration shows a clear dependence on the cosolute's plasticizing ability along with a decrease of the temperature T_d, the situation is more complex for the anhydrous state. Glucose definitely

dampens the amplitudes by forming a molecular network of sugar molecules at the protein surface, in contrast to glycerol, which first suppresses motions below T_d and supports them above. Thus, the interplay between hydration and organic solvents appears to allow some shaping of the protein's fluctuations.

Using inelastic neutron scattering methodology, our laboratory investigated the enzyme mouse acetylcholinesterase (mAChE), hydrated in D_2O, in the absence and presence of sucrose, which affects the water activity (osmotic pressure) and the hydration properties of the enzyme.[215] mAChE, which terminates the signal of neurotransmission in the synapses, presents a deep (20 Å) and narrow (about 5 Å) cleft where the active site is situated, which cannot be functional if the protein is rigid. MD simulations have shown that the protein can undergo so-called breathing modes, opening and narrowing periodically the entrance of the gorge.[216, 217] Substrate hydrolysis takes place inside the gorge, largely isolated from the bulk solvent.[218] Since the sucrose molecule is too voluminous to penetrate through the entrance of the cleft, it functions as a semi-permeable membrane and pumps water molecules out of the interior of the gorge. We studied mAChE samples highly hydrated with D_2O (the samples resembled more a gel than a powder) by adding 0%, 5%, 10% and 15% of deuterated sucrose. We have chosen per-deuterated solvents to highlight the signal from the H-atoms of the enzyme.

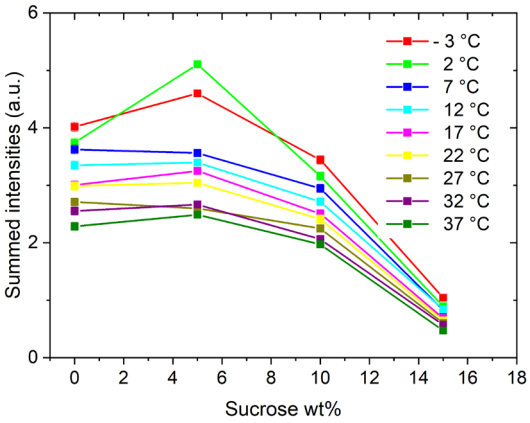

Figure 34. Neutron intensities of mAChE summed over all available scattering angles as function of sucrose concentration in wt%. Error bars are within the symbols (reproduced from [215]).

EINS experiments revealed the incoherent neutron scattering signal at various sucrose concentrations in wt%. Figure 34 presents the scattering intensities integrated over the full angular range of the spectrometer. As temperature increases, more and more hydrogen atoms undergo diffusive motions and are no longer perceived as elastic scatterers, so the intensity drops with temperature, i.e. it is inversely proportional to the MSDs. Unexpectedly, the summed intensities showed a non-linear dependence on sucrose concentration in the sense that they first increase at 5 wt% and decrease beyond about 10 wt% sucrose. Complementary MD simulations operating in the same sub-ns time window as neutron spectroscopy, have shown that, as in the case of glycerol, 5 wt% of sucrose dampens the amplitudes of motions and renders the enzyme less flexible despite the water molecules inside the gorge which become more flexible and depleted from the active site. At 10 wt% and 15 wt% of sucrose, sugar molecules replace some water molecules at the protein's surface through

preferential interaction. These interactions are able to reorganize some intra-protein bonds, thereby increasing the molecular dynamics.

These results can be compared with measurements on lysozyme with or without the disaccharides sucrose and trehalose and at different pressure points. The disaccharides have the same formula but different geometrical structures and are often used to stabilize proteins when they are stored in different conditions, e.g. during cryo-storage and freeze drying, where trehalose, in particular, appears to provide a stable environment for biomolecules that maintains a rigid, vitrified environment. While the pressure resistance of biomolecules in marine organisms is mainly enhanced by the synthesis of methylamines, especially TMAO, yeast and other organisms reveal an increased synthesis of the disaccharide trehalose to deal with pressure stress.[219] HHP applied to the pure protein, solvated in a D_2O-based Tris buffer, had the expected effect of decreasing the MSDs by compressing the protein beyond about 1.5 kbar. Sucrose stabilized the protein so that its molecular dynamics was largely insensitive to HHP application. Surprisingly, in the presence of trehalose, the MSDs were generally much higher on an absolute scale, remained essentially constant up to 2000 bar, then decreased significantly upon compression (Figure 35). The dynamics in the probed time window was largely affected by the contributions of the protein's hydration. Unlike sucrose, which is largely excluded from the protein interface, trehalose exhibited a major effect on the hydration shell's dynamics by replacing a certain amount of water molecules and by forming hydrogen bonds with the protein.[220] Such a water replacement scenario seems to enhance the protein's sub-ns dynamic properties and moreover stabilizes the dynamics up to 2 kbar. Beyond this pressure, the MSDs decrease to the same level as for the sample in the presence of sucrose. However, both cosolutes maintain the MSDs at a higher level than the lysozyme/water-only sample. Sucrose shows no such behavior and does not influence the MSD values significantly.

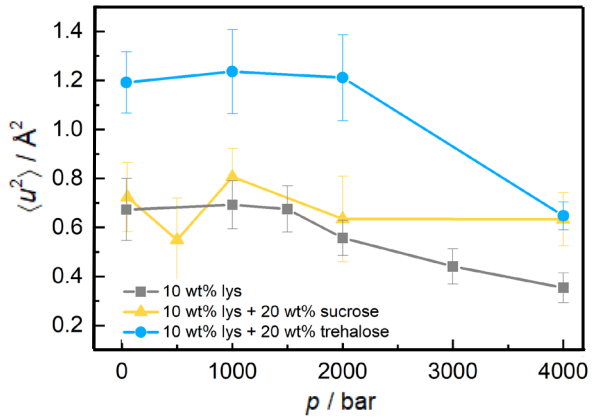

Figure 35. Pressure dependence of the MSDs, $<u^2>$, of 10 wt% lysozyme (lys) in the absence and in the presence of 20 wt% sucrose and 20 wt% trehalose, respectively.[221]

8. Protein Interactions and Reactions at Crowding Conditions

8.1 Ligand Binding

Interactions among macromolecules and small ligands play a key role in the regulation, in time and space, of biochemical processes that are fundamental to all forms of life.[222-224] Phenomena such as DNA transcription, RNA translation, enzymatic reactions, signal transmission across cell membranes

and communication pathways among cells all share such kind of recognition events, i.e., the interactions among two or more binding partners. Thus, understanding the forces involved in the complex formation is of particular interest, not only for increasing our knowledge about biological processes, but also in the development of new pharmaceuticals for medical purposes and for biotechnological applications.[225] Usually, during the complex formation, non-covalent interactions are established between the interacting molecules, and hydrogen bonds, hydrophobic and electrostatic interactions are formed.[226, 227] The binding event can be accompanied by a local or even long-range conformational change of the macromolecule and, possibly, of the ligand, and changes in their hydration spheres.[224] Regardless of the peculiar established interactions and the subsequent changes during complex formation, binding phenomena are generally outlined as reversible processes, quantitatively described by the binding constant, K_b. For a simple 1:1 binding reaction, where one molecule of macromolecule interacts with one molecule of ligand ($M + L \rightleftarrows ML$), K_b is the ratio between the concentration of the complex formed and the product of the concentrations of the free macromolecule and the ligand, thus:

$$K_b = \frac{[ML]}{[M][L]} \tag{9}$$

where [*ML*], [*M*] and [*L*] are the concentrations (in molar unit) of the complex, the free macromolecule (e.g., protein), and the free ligand, respectively. It is important to note that Eq. 9 is expressed in terms of concentrations, and thus, it is not the true thermodynamic binding constant, which should be expressed in terms of activities.[228] The value of K_b is an indication of the strength of the interaction and can assume any value from 0 (no binding) up to 10^{15} M^{-1}, which is the value of the strongest complex known, determined for the interaction of biotin with streptavidin.[224] Often, the binding is also described using the dissociation constant, K_d, that is simply the inverse of K_b, i.e., $K_d = 1/K_b$. By performing a titration experiment, the binding constant can be determined. In this experiment, the concentration of one of the interacting partners (usually the macromolecule, *M*) is kept constant, and the concentration of the other one (usually the ligand, *L* - or the other way around) is varied in an appropriate range, until saturation is reached.[226] A physical observable, here denoted as *Y*, (e.g., fluorescence intensity, absorbance in spectroscopic measurements or heat evolved in isothermal titration calorimetry (ITC)) is recorded during the titration, which is directly related to the extent of binding. Interpolation of experimental data with an appropriate binding model (binding isotherm) is then performed and the value of K_b is obtained.[224, 226, 228] The binding isotherm links the observed physical parameter (or any manipulation of it, for example Y/Y_0, or $\Delta Y = Y_0 - Y$, where Y_0 and Y are the signals of *M* without and with the ligand *L*, respectively) to the binding constant and the concentration of *L*. As the free ligand concentration, [*L*], is generally an unknown quantity,[228] an analytical expression linking [*L*] to the total ligand concentration, $[L]_{total}$, K_b and the total macromolecule concentration, $[M]_{total}$, should be used.[227-230] In other words, the value of [*L*] is a function of K_b and the total concentrations used, i.e., $[L] = f([L]_{\mathrm{total}}, [M]_{\mathrm{total}}, K_b)$. The analytical expression of [*L*] for the appropriate binding model will be used to fit the experimental data (*Y* vs. $[L]_{total}$) to finally yield the value of the binding constant.[227, 228] Complications may come from the choice of the appropriate model,[224] which depends on the mechanism of complex formation and the binding stoichiometry (denoted by *n*), which represents the molecules of *L* bound to one molecule of *M*. Further, the affinities, i.e. K_b values, of the ligand for multiple sites on the macromolecule may be different (e.g., multiple and equivalent binding or non-equivalent and independent binding sites). Finally, cooperativity between binding sites can be present. Positive cooperativity means that binding of the

first ligand will favor the binding of a second ligand, as in the case of oxygen binding to hemoglobin.[223] In complex binding scenarios, iterative algorithms can be used to obtain the free ligand concentration, which in turn can then be used to fit the binding isotherm to determine K_b.

Knowledge of the binding constant allows evaluation of the standard Gibbs energy change of the binding reaction, $\Delta G_b^\circ = -RT\ln K_b$, which is linked to the corresponding enthalpy and entropy changes of the reaction through $\Delta G_b^\circ = \Delta H_b^\circ - T\Delta S_b^\circ$, which can be determined from the temperature dependence of K_b.[231, 232] Generally, the entropy term contains contributions from rotational and translational motion, conformational as well as solvational changes. To yield a full thermodynamic description of the binding process, the standard volume change upon binding, ΔV_b°, can be determined (the sign of the standard state, °, is omitted in the following) from the pressure dependence of K_b (Eq. 4), which yields additional information about packing and hydration changes.[107, 233] Moreover, pressure can alter the conformational landscape of the protein, which may lead to population of a particular conformational substate that it more prone to ligand binding than others.[27, 43] High-pressure binding studies can be performed by employing different techniques such as high-pressure UV/Vis, fluorescence or NMR spectroscopies.[27, 43, 107, 233] The ΔV_b determined from the $K_b(p)$ data signifies the difference between the partial molar volume of the complex ($V_{complex}$) and the sum of the partial molar volumes of the free ligand and free macromolecule ($V_{ligand} + V_{macromol}$), i.e., $\Delta V_b = V_{complex} - (V_{ligand} + V_{macromol})$. $\Delta V_b > 0$ indicates that the partial molar volume of the complex state is larger than those of *M* and *L*. Conversely, if $\Delta V_b < 0$, the volume occupied by the complex is smaller with respect to the volume of the uncomplexed state. $\Delta V_b \approx 0$ indicates an almost perfect packing between the ligand and the macromolecule and the absence of large hydration changes, as, for example, observed for the complexation of the enzyme α-chymotrypsin and the aromatic ligand proflavine.[227] When the dissociation constant, $K_d = 1/K_b$, is used, the sign of the binding volume is reversed. In general, binding sites can be classified in "soft" and "hard", according to their structural rigidity.[227, 234] An increase of the binding constant with pressure can be expected when soft binding sites are involved. In soft binding sites, some conformational freedom is available, rendering the binding site compressible and leading to a reduction of the overall volume of the system upon pressurization. Hard binding sites generally respond to pressure stimulation through a decrease of K_b. However, the influence of pressure on the types of interactions formed in the complex and on the accompanying hydration changes need to be considered as well. For example, the release of hydration water molecules upon binding is usually accompanied by a positive volume change, since bulk water has a larger partial molar volume. Instead, hydration around charged or polar residues leads to a volume decrease due to the electrostriction effect.[231, 234] The formation of void volumes in a macromolecule upon ligand binding (due to, for example, conformational changes or to an unfavorable fit of the ligand in the binding pocket) contributes positively to the binding volume. Conversely, upon binding and formation of a tight complex, the reduction in fluctuations of the macromolecule's structure, both locally in the binding site and eventually further away in other regions, leads to the reduction of the total volume of the system, negatively contributing to the value of ΔV_b.[107] Finally, a negative contribution to the binding volume may arise from the tight association of planar, aromatic ligands with aromatic residues in proteins. Hence, the experimental value of ΔV_b determined and its sign are the result of a delicate balance among all these factors. The presence of cosolutes may add a further contribution.

The effect of crowders, such as the neutral polymers PEG, dextran and Ficoll, is generally thought to increase locally the concentrations of the interacting partners via the excluded volume effect.[232]

When only the excluded volume effect is active (which is the case for inert polymers), an increase of the binding constant in crowded media can be expected, due to the reduction of the free energy barrier for the complex formation.[232] In addition, both the conformation and hydration of the interacting partners can be affected in such crowded media through direct interactions of the crowder with the binding partners.[235, 236] For example, crowding can favor a more compact structure compared to a more open one, i.e. a conformational substate with smaller partial volume which can have a different affinity for a given ligand. Moreover, partial occlusion of the binding site could occur, rendering the crowder a competitor of the ligand, as reported for the binding of maltose to MBP (maltose binding protein) in the presence of Ficoll.[237] In such kind of scenario, a lower value of K_b can be expected compared to that in dilute solutions.

When binding studies of biomolecular systems in the presence of crowding agents are performed at high-pressure conditions (HHP-crowding), further modulation of the molecular determinants underpinning the complex formation between a ligand and a macromolecule can be expected.[44] Up to date, such studies are still very scarce. The complex formation between the aromatic molecule 8-anilinonaphthalene-1-sulfonic acid (ANS) and bovine serum albumin (BSA) performed is a particularly interesting example.[229] In this work, the binding of ANS to BSA (Figure 36 A) was studied in the aqueous two-phase system (ATPS) composed of dextran and PEG, a model LLPS system that simulates the highly crowded environment found in membraneless organelles of cells. At appropriate concentrations, PEG and dextran spontaneously separate,[238] forming droplets enriched in dextran dispersed in a solution of PEG.[44, 239, 240] The protein BSA and ANS preferentially localize in the dextran-enriched droplets, where the polymer concentration is around 30 wt%. HHP fluorescence spectroscopy binding experiments showed that on average three molecules of ANS molecules bind to one BSA macromolecule (Figure 36 B), both at neat buffer conditions and in the ATPS system at ambient pressure. Through docking studies, it was found that one ANS is bound in a binding pocket located in the subdomain IB. The other two are localized in subdomain IIIA. These results were also confirmed by employing the method of continuous variation (also known as Job's plot), a model-free method for the estimation of the binding stoichiometry (inset of Figure 36 B).[228, 241] It was found that in neat buffer, the three ANS molecules are bound to BSA with the same affinity ($K_b = 4.2 \cdot 10^6$ M^{-1}). Conversely, in the ATPS, the equivalency of binding sites is lost: two ANS molecules bind to BSA with the same affinity ($K_{b1} = 4.3 \cdot 10^6$ M^{-1}), and for the other one, the binding constant is about one order of magnitude smaller ($K_{b2} = 0.42 \cdot 10^6$ M^{-1}), showing the strong impact that a crowded medium can have on the complex formation. In fact, the dextran-rich crowded medium imposes a small but significant conformational change of the protein, most likely through direct interactions. This can lead to a partial occlusion of the protein pocket, rendering the K_b for this binding event lower. Corresponding pressure dependent data are depicted in Figure 36 C, showing the binding isotherms for the formation of the complex formed at neat buffer conditions between 1 bar and 2000 bar. The binding volume, determined from the slope of the $\ln K_b$ *vs. p* plot, is shown in Figure 36 D. In all cases, an increase of pressure led to a decrease of K_b, revealing that the volume of the complex is larger with respect to the volume occupied by the uncomplexed state. In neat buffer solution, a ΔV_b value of 14.5 ± 1.5 mL/mol was determined, which can be ascribed to the formation of some void space inside the binding pocket and/or release of some hydration water to the bulk solvent, factors that will both contribute positively to the binding volume. Conversely, in the dextran-enriched droplets, the volume change for the binding of the first two ANS molecules is ΔV_{b1} = 33.2 ± 12.5 mL/mol. For the binding of the other ANS molecules, ΔV_{b2} amounts to 18.9 ± 4.1 mL/mol, indicating that the binding sites strongly differ in packing and hydration properties.

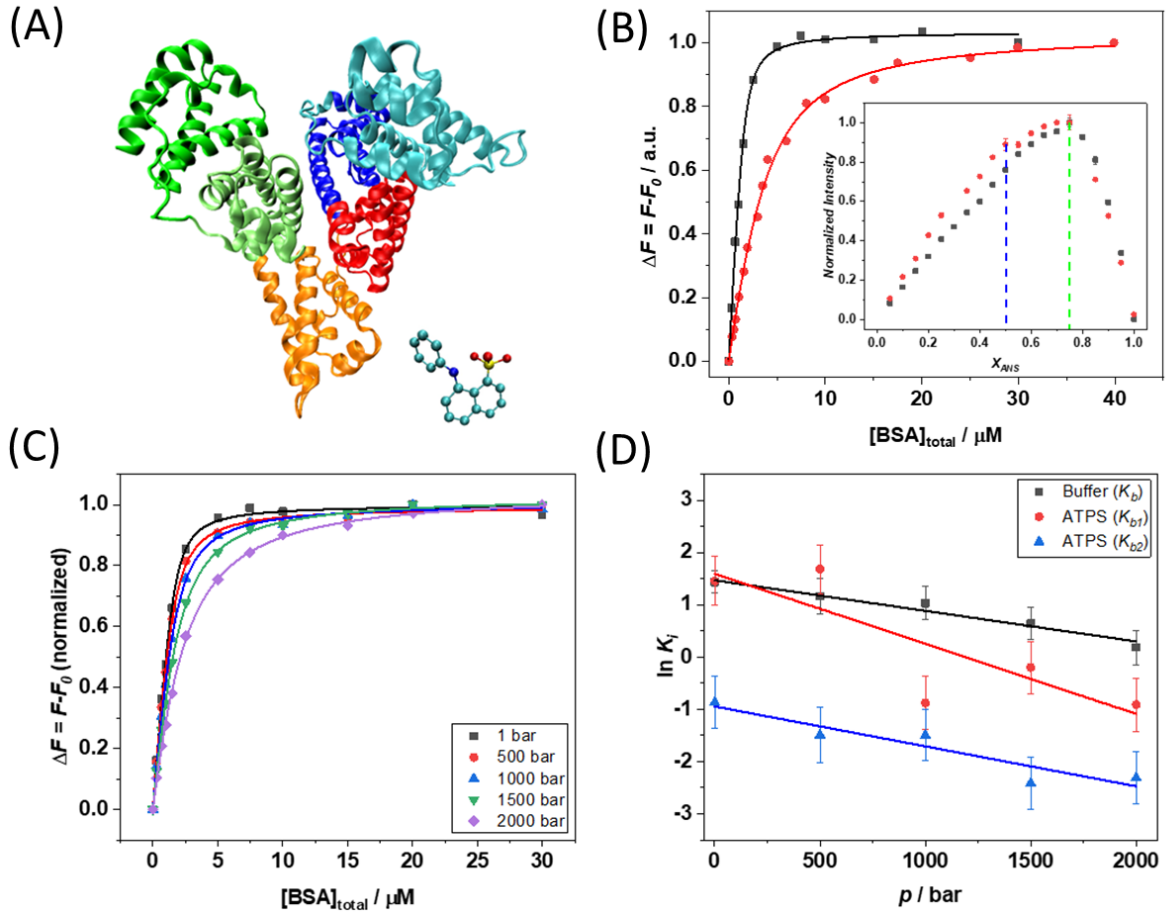

Figure 36. (A) Left: Structure of the protein BSA (PDB code: 3V03) presented as ribbon diagram. The different colors highlight the six subdomains present in the protein structure: IA (cyan), IB (blue), IIA (red), IIB (orange), IIIA (light green), IIIB (dark green). The structure of ANS is represented as balls and sticks on the right-hand side. (B) Plots of binding isotherms obtained from a titration of ANS solution with BSA in neat buffer conditions (black squares) and in the ATPS (red circles) obtained at the temperature of 25 °C and pressure of 1 bar. The binding isotherms were obtained by plotting the difference in the ANS fluorescence emission intensity in the presence (F) of the protein BSA and in its absence (F_0) as a function of the total BSA concentration. The solid lines are the best fit to experimental points according to a multiple and independent binding sites model. In the inset of panel B, the Job's plots obtained for the system in neat buffer (black squares) and in the ATPS (red circles) are shown. The dashed lines highlight the inflection points in the Job's plots, revealing the stoichiometry (n) of the complex. The blue line highlights the presence of the 1:1 (BSA:ANS) complex, and the green line the 1:3 (BSA:ANS) complex, centered at ANS mole fraction (X_{ANS}) of 0.5 and 0.75, respectively. Of note, the inflection point at 0.5 is present for the system in ATPS only, showing that the equivalence among the three binding sites is lost in moving from buffer to ATPS. (C) Binding isotherms (at T = 25 °C) for the complex formation between ANS and BSA obtained in neat buffer solution at pressures of 1, 500, 1000, 1500 and 2000 bar. (D) Plots of the natural logarithm of the binding constant, ln(K_b), *vs.* p obtained at neat buffer conditions (black squares) and in the highly crowded dextran droplets (red circles for the first two binding sites, blue triangles for the last one). According to Eq. 4, the slope corresponds to -$\Delta V_b/RT$. Adapted from ref [229]. Copyright 2020 The Authors, Springer Nature under Creative Commons CCBY license.

The combined effects of HHP and crowding on binding processes was also investigated for the complex formation between non-canonical DNA structures (the human 22AG G-quadruplex) and the

ligand thioflavin-T (ThT).[242] The study was carried out at neat buffer conditions, in the presence of monovalent cation (sodium and potassium) as well as in the presence of the crowder Ficoll (25 wt%). It was demonstrated that both pressure and crowding have a strong impact on the value of the binding constant, the stoichiometry of the complex formed and the conformation adopted by 22AG. At ambient pressure, on average three ThT molecules are bound to one 22AG, with the same affinity (K_b = 8.7·10^4 M^{-1}) in neat buffer. Conversely, under crowding conditions, a marked increase of the binding constant was observed ($K_b \approx 1.4 \cdot 10^5$ M^{-1}). Interestingly, only two ThT molecules were found to be bound, indicating that Ficoll imposes two effects: it increases the affinity of the first two ligands for the quadruplex, but at the same time can completely hamper the binding of the third one. The differences in the stoichiometries were attributed to the conformation adopted by 22AG. In neat buffer, 22AG is largely unfolded, offering an open structure where ThT binding is easily facilitated. Under crowding conditions, a significant fraction of 22AG is adopting a more compact structure (hybrid/antiparallel), reducing the accessibility of ThT to the DNA structure. For this system, in neat buffer, an increase of pressure led to a significant increase of the binding affinity, i.e., the strength of complex formation is larger at higher pressures, highlighting that the volume occupied by the 22AG/ThT complex is lower with respect to the free 22AG and ThT ($\Delta V_b \approx$ -27 mL/mol). Here, the negative ΔV_b value was attributed to the release of void volume upon binding, which leads to a reduction of the whole volume of the system. In the presence of Ficoll, the pressure behavior of K_b is biphasic: a decrease in the pressure range 1 to 1000 bar ($\Delta V_b > 0$) and an increase from 1000 bar to 2000 bar ($\Delta V_b < 0$). This behavior was attributed to the presence of multiple subpopulations in terms of conformations adopted by 22AG (parallel, antiparallel and hybrid) that are induced by the concomitant effect of HHP and crowding. Both examples presented clearly show that ligand-binding reactions can be strongly modulated both by pressure and crowding which alter the binding constant and the stoichiometry of the complex formed, and can notably differ from the observed behavior at neat buffer conditions, even at the level of single binding site events.

8.2 Enzymatic Reactions at High Pressure in Crowded Environments

The thermodynamics and kinetics of enzymatic reactions depend on several variables, not only on temperature and the concentration of the reactants, but also on pressure and the solution conditions, including the presence of cosolutes in the reaction medium.[243-254] An in-depth comprehension of their effects on such reactions is a key step not only towards understanding the mechanisms of adaptation of extremophiles, but also for the development and optimization of industrially relevant enzymatic reactions. The use of HHP in modulating enzymatic activity can have several advantages: (1) Given that the rate of an enzyme-guided reaction is often limited by the thermostability of the enzyme itself, owing to low unfolding temperatures, combining pressure-induced enzyme thermostabilization (e.g., for α-chymotrypsin which exhibits an elliptic-like (*p*-*T*)-phase diagram) with an accelerated substrate conversion at higher temperatures can lead to an improved overall reaction rate; (2) HHP can also directly enhance the catalytic activity if the activation volume, $\Delta V^{\neq}$, associated with the reaction step is negative; (3) HHP can also alter the specificity of the substrate and the stereoselectivity by promoting the conversion of a substrate to a product with a smaller overall volume; (4) generally, HHP may also modulate the conformational dynamics of the enzyme, which is also affected by the surrounding solution embedding cosolutes. Cosolutes, i.e. cosolvents and macromolecular crowding agents, may be added since they are either required as enzyme stabilizers (such as glycerol or PEG), as solubilizers, or to overcome thermodynamic or kinetic limitations. Generally, enzyme catalysis

under crowded conditions is a combined effect of volume exclusion and nonspecific enzyme/substrate-crowder interactions. It also depends on the crowder concentration (for example, if the crowding agent is below or above its overlap concentration, *c**) and on the chemical make-up of the protein/substrate-crowder interface. For example, high crowder concentrations may reduce the Michaelis constant (i.e., increase the enzyme-substrate affinity) through the volume exclusion mechanism, and at the same time elevate the enzymatic efficiency. Strong association of the crowder with the enzyme may result in slower turnover rates, however. Depending on the sign of the activity coefficients of the reactants, low crowding situations with weak affinities to the enzyme may also increase the turnover rate. Owing to this high complexity of the reaction system, a quantitative and predictive description of the process is still largely lacking.

As an example, we show the reaction of the serine protease α-chymotrypsin (α-CT) in the absence and presence of selected cosolutes, the nanocrowder and compatible omolyte TMAO and macromolecular crowders, dextran and PEG, on the pressure-dependent activity of the enzyme, using *N*-succinyl-Ala-Ala-Pro-Phe-*p*-nitroanilide (SAAPP*p*NA) as substrate. The enzyme is capable of hydrolyzing peptide bonds, preferably aromatic amino acids (Trp, Tyr, Phe). In the active site of α-CT, a catalytic triad is present, which is formed by three amino acids (Ser195, His57, Asp102) and connected via hydrogen bonds (Figure 37). Using high-pressure FT-IR spectroscopy, the enzyme has been shown to be stable against pressure-induced denaturation up to about 5 kbar.[249-251]

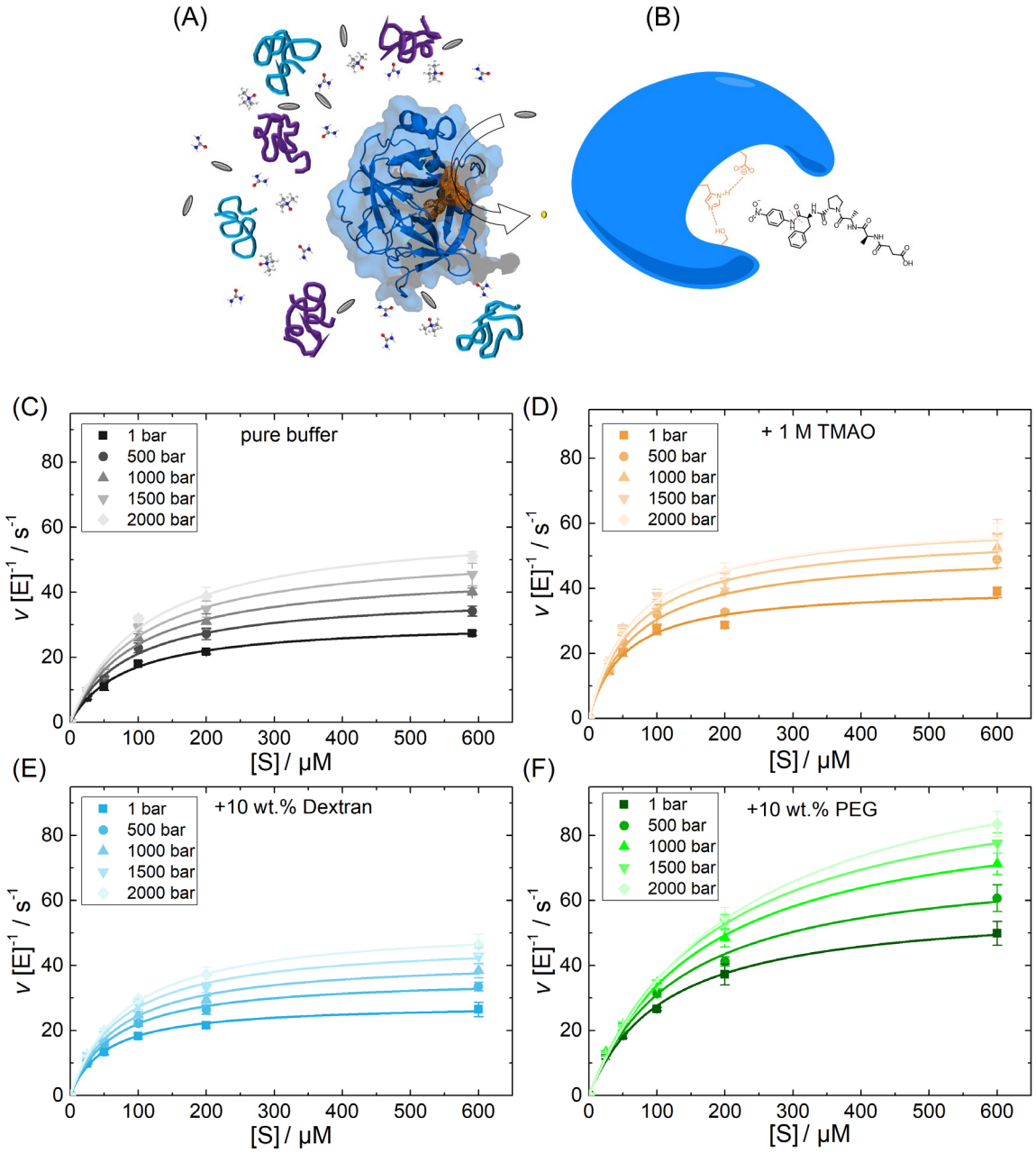

Figure 37. (A) Graphic representation of the reaction catalyzed by α-CT (PDB: 1yph; substrate: dark grey; product: yellow) in the presence of crowders (PEG: turquoise, dextran: purple,) and cosolvent (nanocrowder) TMAO for comparison. (B) The enzyme's catalytic triad in complex with the substrate *N*-succinyl-Ala-Ala-Pro-Phe-*p*-nitroanilide. (C - F) Michaelis–Menten plots for the hydrolysis, catalyzed by α-CT, of the substrate SAAPP*p*NA at different substrate concentrations, [S], and pressures, *p*, at *T* = 25 °C for all explored solution conditions (pure buffer with the addition of 1 M TMAO, 10 wt.% dextran, and 10 wt.% PEG). Reproduced from ref. [249] Copyright 2018 PCCP Owner Societies.

Under the chosen reaction conditions, the enzyme kinetics can be described by the Michaelis-Menten scheme:[249]

$$\mathrm{E} + \mathrm{S} \underset{k_{-1}}{\overset{k_1}{\rightleftharpoons}} \mathrm{ES} \xrightarrow{k_2} \mathrm{E} + \mathrm{P} \qquad (10)$$

where k_1, k_{-1} and k_2 are the rate constants, and E, S, P, and ES denote the enzyme, the substrate, the product, and the enzyme-substrate complex, respectively. The reaction's initial rate, v_0, was determined by calculating $v_0 = \mathrm{d[P]}/\mathrm{d}t$, where [P] is the concentration of the product, from the slope of the linear fit of the time dependent absorbance data of the product *p*-nitroanilide at 410 nm. To determine the turnover number, k_{cat} (here equal to k_2), and the Michaelis constant, $K_M = (k_{-1}+k_2)/k_1$, plots of the initial velocity *vs.* the substrate concentration and fits to the Michaelis-Menten equation were used:

$$v = \frac{v_{\max} \cdot [\mathrm{S}]}{K_\mathrm{M} + [\mathrm{S}]} = \frac{k_2 \cdot [\mathrm{E}]_{\mathrm{tot}} \cdot [\mathrm{S}]}{K_\mathrm{M} + [\mathrm{S}]} \qquad (11)$$

($[\mathrm{E}]_{tot}$ = total enzyme concentration, [S] = initial substrate concentration, $v_{max} = k_2 \cdot [\mathrm{E}]_{\mathrm{tot}} =$ maximal rate of the reaction when the enzyme is saturated with its substrate). The ratio $k_{eff} = k_{cat}/K_M$ denotes the enzymatic efficiency. Pressure dependent measurements were carried out using a HHP stopped-flow system with a deadtime of ~10 ms, capable of reaching pressures up to 2 kbar (for details, see refs.[249-254]).

Figures 37 shows the Michaelis-Menten plots in the pressure range 1-2000 bar for all solution conditions. With increasing substrate concentration, the initial rate of the reaction, v_0, increases, and approaches a plateau value at high substrate concentrations (note that at this concentration, the enzyme is saturated with substrate). As shown in Figure 37, the application of high pressure accelerates the enzymatic activity, as demonstrated by higher reaction rates for almost all solution conditions, indicating that the enzymatic activity is enhanced through a negative activation volume. The comparison of the Michaelis-Menten curves obtained in the neat buffer solution with the one obtained in the presence of 10 wt.% PEG shows an additional positive effect on the rate of the reaction. Differently, when 10 wt.% of dextran is present in solution, no distinct changes in the rate of the enzyme reaction was observed with respect to the pure buffer solution, demonstrating that the two crowder types affect the reaction rate differently.

Figure 38 summarizes the kinetic parameters for all pressures measured. In 1 M TMAO, the affinity of the substrate to the enzyme is largest. The values of K_M increase with increasing pressure for all solution conditions, i.e., the affinity of the substrate to the enzyme is higher upon compression. The 10 wt.% PEG solution shows the largest pressure effect on K_M. The turnover number also increases (about 1.5-2 fold) in all solutions upon pressurization, with largest values observed in the presence of 10 wt.% PEG. The catalytic efficiency, K_{eff}, obtained in 1 M TMAO solution is the largest, also at high pressures, and is similar to that obtained for neat buffer, the 10 wt.% PEG, and the 10 wt% dextran solution. Thus, the addition of the deep-sea osmolyte TMAO shows by far the most positive effect on K_{eff}. Instead, PEG and dextran, being two representative crowding agents of different nature, show nearly similar values for K_{eff} compared to that obtained in the pure buffer. A negative synergistic effect of a crowder and TMAO could only be observed for the Michaelis constant in the 10 wt.% PEG-containing solution, whereas dextran does not show such additional effect.

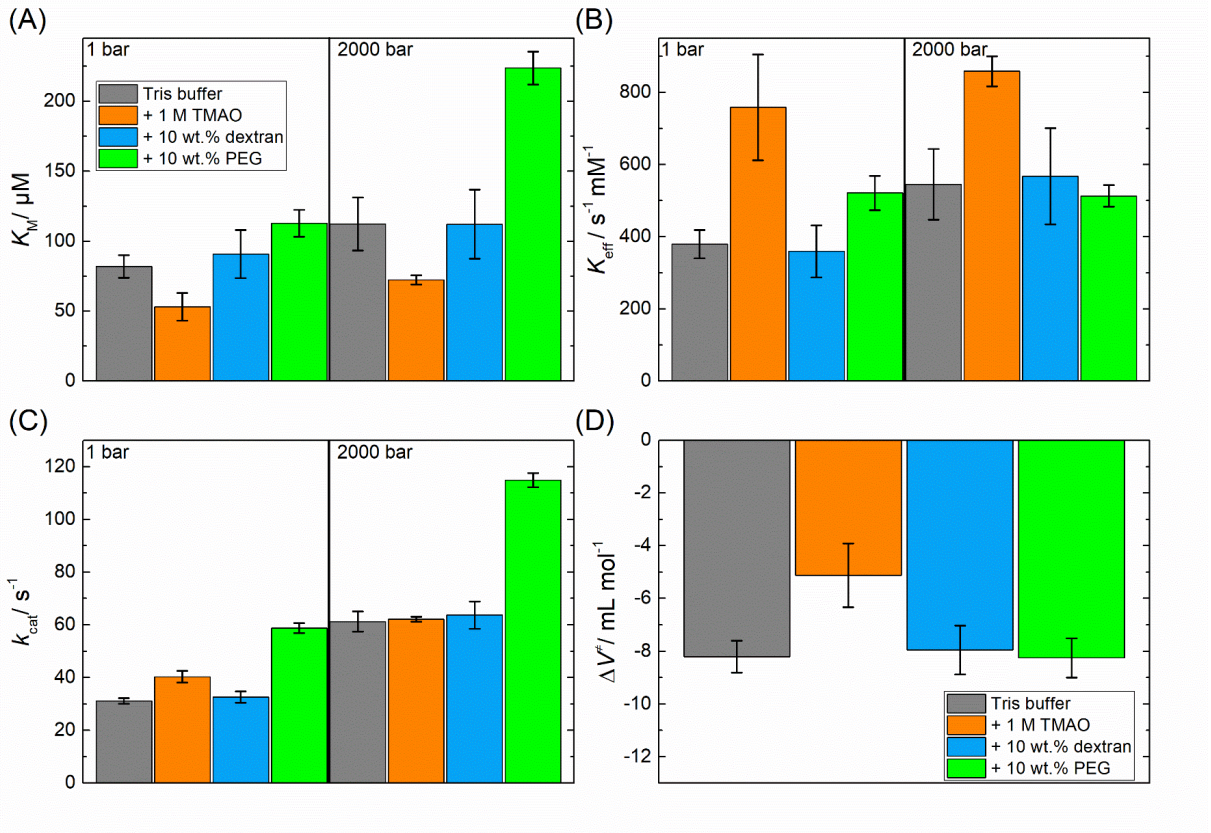

Figure 38. Plots showing the pressure dependence of the kinetic constants for the hydrolysis, catalyzed by α-CT, of SAAPP*p*NA in different solutions (as indicated in the legend): (A) Michaelis constant, (B) catalytic efficiency, (C) turnover number, and (D) activation volume.

The positive pressure effect indicates that the activation volume, $\Delta V^{\neq}$, of α-CT is negative for all solution conditions, meaning that the transition state volume, ES$^{\neq}$, is smaller with respect to that of the ES complex. This effect might be due to the reduction of some void volume in the enzyme, to hydration changes and/or also some minor conformational changes inside the active site of α-CT in the course of the reaction. Please note that the order of magnitude of $\Delta V^{\neq}$, -4 …-8 mL mol^{-1}, is very small, about 10 times smaller than the typical volume change accompanying protein unfolding, and corresponds to less than the molar volume of only one water molecule (18 mL/mol). This also demonstrates how accurately volume changes can be determined by this method. The similar $\Delta V^{\neq}$-values for the various solution conditions suggest minor differences in the transition state complex (ES$^{\neq}$), i.e., the structure of the reaction center itself. The lower affinity (i.e., higher K_M value), in the presence of 10 wt.% PEG for this enzymatic reaction may be due to an increased diffusion resistance within the sample and/or direct interactions of the slightly hydrophobic PEG with some hydrophobic patches of the protein and/or the hydrophobic substrate, which might lead to deviations of the activity coefficients from the ideal behavior. In fact, Oliva et al. reported a weak interaction between the enzyme lysozyme and PEG, with a binding constant of about 10^3 M^{-1}, the process being mainly entropy controlled, i.e., the release of water molecules bound to the protein surface and polymer chains could account for this phenomenon.[236] Surprisingly, also k_{cat} increases upon addition of PEG, which is quite uncommon for this crowder. In this case, changes of the activity coefficients of the released products and a water activity change in the presence of the polymer may be the most likely reasons. Conversely, the more hydrophilic dextran does not show a significant effect on the kinetic parameters. TMAO

reveals the highest K_{eff} compared to all other solutions. TMAO is preferentially excluded from the interface of the protein, which is due to its ability to interact strongly with bulk water, which ultimately leads to an increase in hydrogen bonding and structuring of the solvent.[203]

To reveal the origin of the observed changes of the kinetic parameters and to quantitatively predict the impact of the various parameters in concert, knowledge of the reactants' thermodynamic activities of such multi-component solutions as used here could be useful. To this end, the activity coefficients of all reactant species involved in the enzymatic reaction are required for the various solution conditions, which is a daunting task. As shown for some selected systems already,[250-252] such information can be obtained from experiments and theory via Perturbed-Chain Statistical Associating Fluid Theory (PC-SAFT). Such information would also be fundamental in optimizing enzymatic reactions for biotechnological applications, for the pharmaceutical industry, and for protein engineering. The thermodynamic equilibrium constant, K_{th}, as reported in Equation 12, is the product of the thermodynamic activities, a_i, of all the species *i* involved in the reaction, exponentiated with the respective stoichiometric factor, v_i (positive for products, negative for educts):

$$K_{\mathrm{th}}(T,p) = \prod_i a_i^{v_i} = \prod_i \left(x_i^{v_i} \cdot \gamma_i^{v_i}\right) = K_x K_\gamma \qquad (12)$$

where x_i is the mole fraction and γ_i the activity coefficient of species *i*. Similarly, the activity-based kinetic constant, $K_{\mathrm{M}}^{\mathrm{a}}$, is given by $K_{\mathrm{M}}^{\mathrm{a}}(T,p) = K_{\mathrm{M}}^{\mathrm{m}}\gamma_{\mathrm{S}}$; $K_{\mathrm{M}}^{\mathrm{m}}$ is the apparent Michaelis constant and γ_{S} the activity coefficient of the substrate. Equation 11, which is based on the Michaelis-Menten reaction mechanism with one rate-limiting substrate, assumes that the thermodynamic activities of the enzyme (E) and complex (ES) are equal. The main advantage of using K_{th} and $K_{\mathrm{M}}^{\mathrm{a}}$ is that they are independent of any concentration effects caused by the reacting agents or inert components such as cosolutes. In sharp contrast, the measured apparent quantities K_x and $K_{\mathrm{M}}^{\mathrm{m}}$ are concentration-dependent. With the reaction constants $K_{\mathrm{M}}^{\mathrm{a}}$ and K_{th} in hand, the cosolutes' effects on the experimental quantities K_x and $K_{\mathrm{M}}^{\mathrm{m}}$ can be quantitatively predicted if the activity coefficients in the multi-component solutions are known and accounted for. In several recent works, this approach has been successfully applied.[250-252, 254] In these works, it was also demonstrated that neglecting activity coefficients or employing poor models describing activity coefficients fails to predict the kinetics and equilibrium thermodynamics of enzymatic reactions.

As an example, we show kinetic parameters of the formate dehydrogenase (FDH) reaction. The enzyme FDH catalyzes the oxidation of the formate anion to carbon dioxide, coupled with the concomitant reduction of NAD^+ to NADH (Figure 39), the catalytic step involving hydride ion transfer. To quantitatively describe the observed effects, thermodynamic modeling has been applied, taking into account the chemical potentials (activities) of the individual compounds in this non-ideal solution.[254] PC-SAFT was used for this task, which allows to predict the temperature, pressure, and cosolvent dependent effects on the catalytic parameters of the reaction catalyzed by the enzyme. Under the conditions employed here (high concentration of one substrate at a time, only), the kinetics could be described with the Michaelis-Menten equation for a pseudo-one substrate reaction. The activation volume, $\Delta V^{\neq}$, according to Eyring´s theory, could be determined from the pressure dependence of k_{cat}, $(\mathrm{d}\ln k_{\mathrm{cat}}/\mathrm{d}p)$, and the binding volume, ΔV_{b}, from the pressure dependence of the Michaelis constant $(\mathrm{d}\ln K_{\mathrm{M}}^{-1}/\mathrm{d}p)$ (Eqs. 4). The activation volume is the difference between the partial molar volume of the transition state (TS = $ES^{\neq}$) and the ground state of the enzyme-substrate complex (ES), and the binding volume represents the difference in the volume of the ES-complex and

the unbound reactant state (E+S). After the fast mixing process has taken place (with a dead time of ~10 ms), the absorbance was measured up to 100 s. The kinetics was followed through the release of the product NADH, which was measured by means of UV/Vis absorbance at 340 nm employing Lambert-Beer's law.[254]

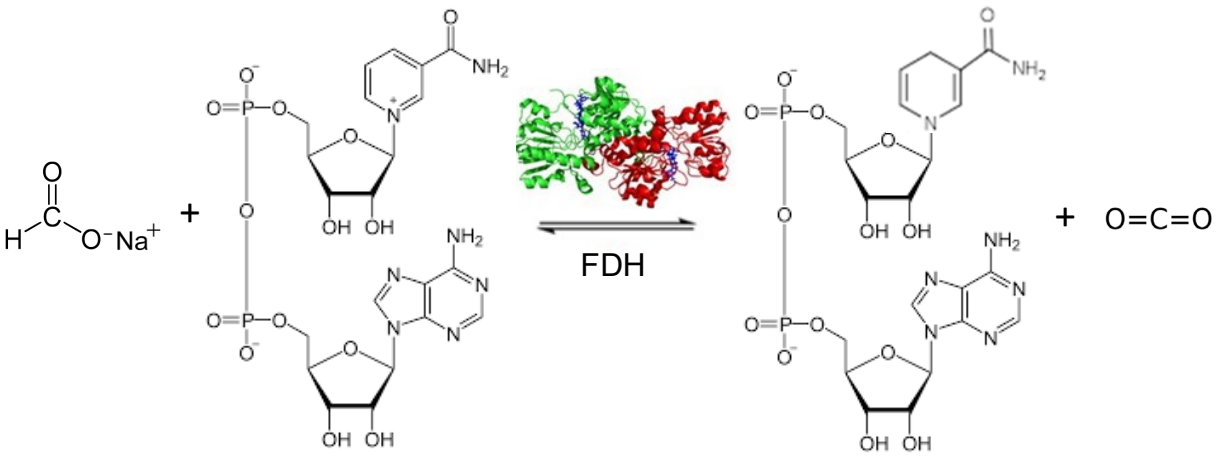

Figure 39. The formate dehydrogenase (FDH, pdb: 5DN9) catalyzes the conversion of NAD^+ and formate to the products NADH and CO_2.

Figure 40 depicts the pressure dependence of the kinetic parameters for the FDH reaction at temperatures of 25, 35 and 45 °C (Figs. 40 A, C, E) and in the presence of different cosolutes (Figs. 40 B, D, F) relating to the substrate formate. The $K_{M,formate}$ value decreases with increasing pressure, even at higher temperatures, clearly showing that the affinity of the substrate for the enzyme increases upon pressurization. However, at higher temperatures, the $K_{M,formate}$-value increases markedly, i.e., the affinity decreases, probably due to an unfavorably increased conformational dynamics of the protein. At higher temperatures, $k_{cat,formate}$ and $K_{eff,formate}$ show a drastic increase. Regarding the catalytic efficiency, pressure lead to higher values due to the decrease of $K_{M,formate}$ upon compression since $k_{cat,formate}$ is not markedly affected by pressure here.

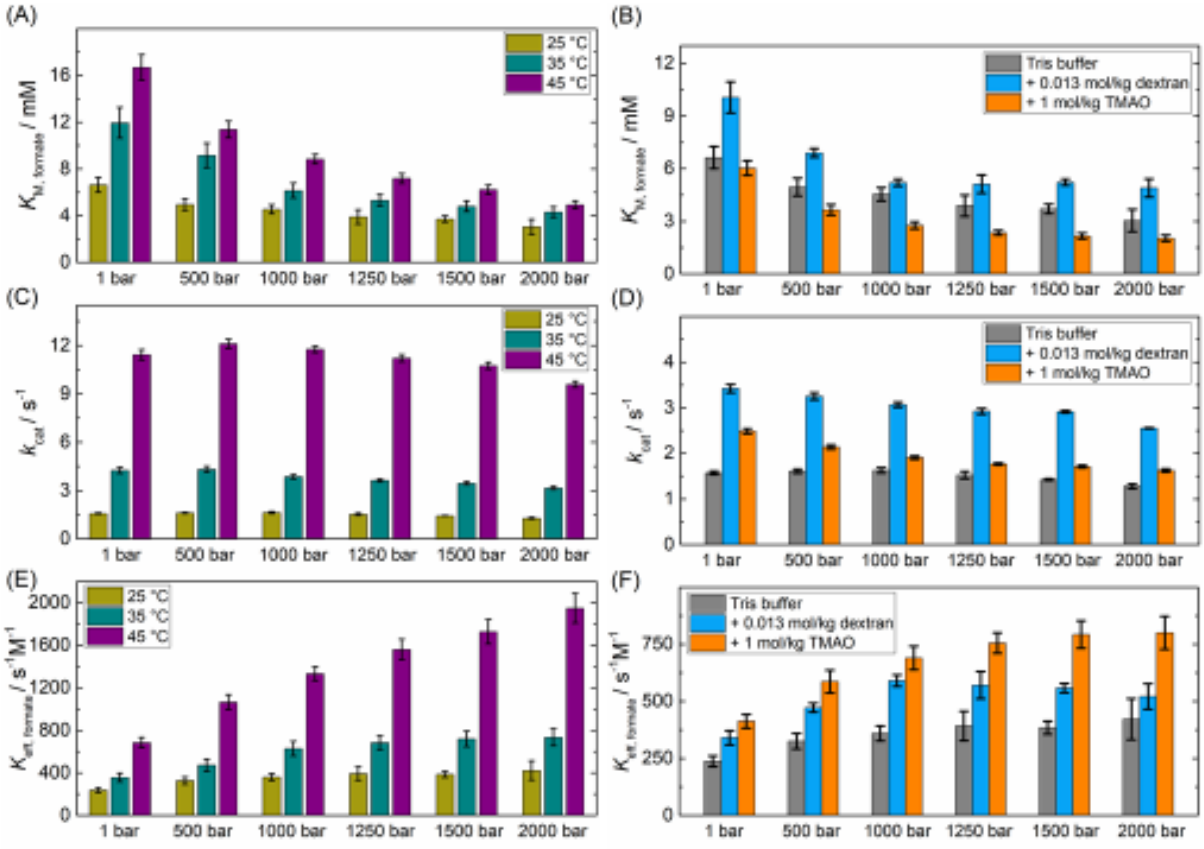

Figure 40. Bar diagrams showing the pressure dependence of the kinetic constants for the FDH-catalyzed redox reaction of NAD^+ and formate at the indicated temperatures and in different solutions by varying the formate concentration: (A, B) Michaelis constant, (C, D) catalytic constant, (E, F) catalytic efficiency. Conditions: pH 7.5; (B, D, F): Measurements at 25 °C. Reproduced with permission from ref. [254] Copyright 2021 Elsevier.

The TMAO solution at 25 °C caused the lowest K_M value and highest enzymatic efficiency. The crowding agent dextran (10 kDa, 0.013 mol kg^{-1}) revealed a slightly negative effect on $K_{M,formate}$, the catalytic efficiency being larger compared to the neat (i.e., cosolvent-free) buffer solution, however. Using the $K_{M,formate}$ values for the pure buffer conditions as input parameters, PC-SAFT was able to successfully predict the kinetic efficiency in the presence of the cosolvents. Figure 41 shows the comparison between experimental values of $K_{M,formate}$ (A, C) and $K_{eff,formate}$ (B, D) with the values predicted by PC-SAFT, revealing reasonable agreement with the experimental data obtained for $K_{M,formate}$, i.e., its increase upon addition of dextran and its decrease in the presence of TMAO. Even in the presence of higher cosolvent concentrations and high pressure, PC-SAFT allowed the prediction of $K_{M,formate}$ values with less than 30% deviation from the experimental data, and the $K_{eff,formate}$ data deviated within ~20% from the experimental values, which is similar to the experimental uncertainty.

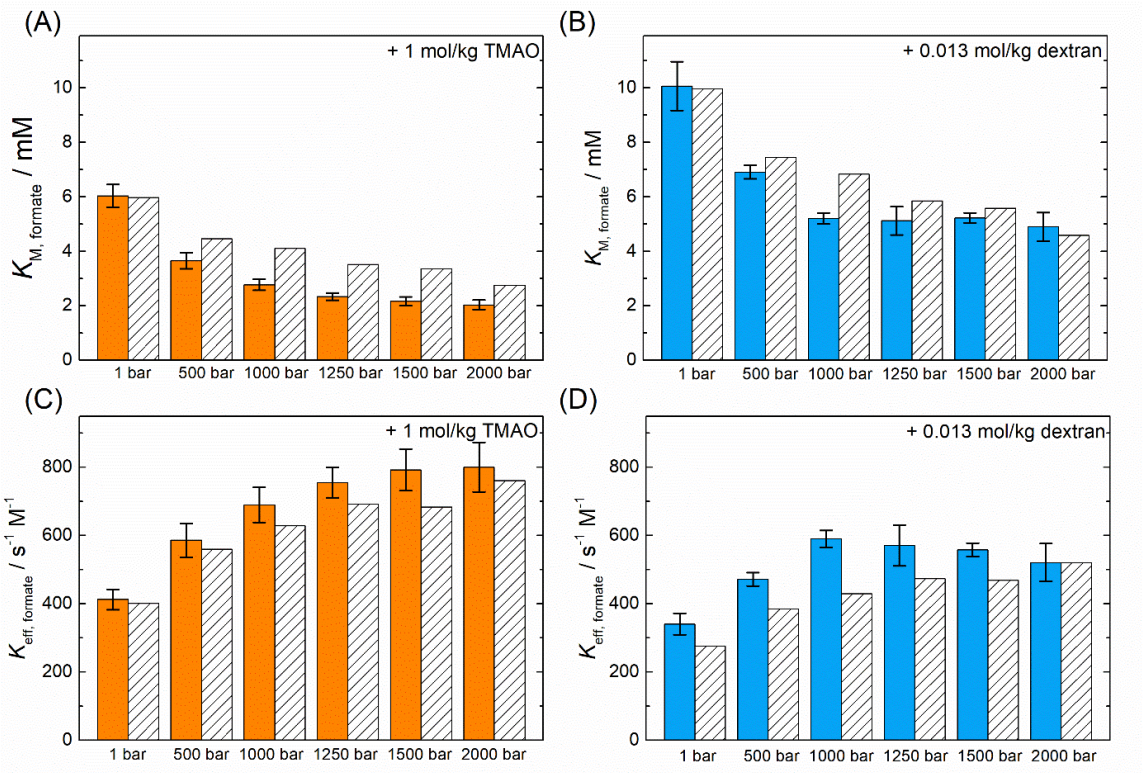

Figure 41. Pressure dependence of the kinetic constants for the redox reaction of NAD^+ and formate catalyzed by FDH at 25 °C, pH 7.5 in neat buffer, at different pressures and co-solvents. A, C: Michaelis constant, B, D: catalytic efficiency. Experimentally determined (solid bars) and PC-SAFT predictions (patterned bars). Reproduced with permission from ref. [254] Copyright 2021 Elsevier.

Recently, our laboratory studied also the combined effects of high pressure and an aqueous two-phase system (ATPS) composed of PEG and dextran, invoking liquid–liquid phase separation, on an enzymatic hydrolysis reaction.[240] It was found that simple steric crowding effects cannot explain the kinetic constants and the observed pressure dependence in the ATPS. Additional contributions have to be taken into account to explain the results obtained, such as changes in the water activity and non-specific weak (quinary) interactions with ATPS components. The findings are relevant for an in-depth understanding of cellular processes taking place in piezophiles and might also have significant bearings on biotechnological applications using liquid–liquid phase separation and pressure in concert for modulating enzymatic reactions.

To conclude this part, chemical as well as pharmaceutical industries strictly depend on measures to protect enzymes against the various stresses that accompany their production, transport, storage and use. In this context, high-pressure treatment has been shown, for example, to be advantageous for the disassembly of protein aggregates, a major drawback in the production of recombinant proteins.[255,256] To this end, the entire parameter space of thermodynamic variables has to be explored, which, in addition to the more common variables temperature, ionic strength and pH, also includes pressure, the presence of cosolvents and crowding agents. In this regard, we can also learn from Nature. The complex cellular milieu of the biological cell is responsible for the so-called quinary structure (and structural dynamics) of proteins (and other biomacromolecules), which represents the fifth level of their organization. The quinary structure is based on all the weak and transient

interactions that take place between the proteins and their surroundings, which are strongly affected by environmental stresses, such as high salt, low/high pH, high/low temperature and high pressure. Using particular cosolutes, extremophiles - such as piezophiles which populate the deep sea at high-pressure conditions - have succeeded in stabilizing their enzymes and modulating their activity, which is not only important for understanding life in extreme ecological settings, but could also be useful for optimizing enzyme-based biotechnological processes. For the development of a predictive theory of protein stability, dynamics, interactions and activity under such challenging solution conditions, further advances in theoretical and computational tools as well as in solvation science of complex mixtures are needed. To enable a better understanding of all the processes associated with the physical limits of deep life, also extensive high-pressure studies on biologically relevant systems at different levels of complexity (genome, proteome, metabolome, lipidome, ...) are still needed, taking into account the particular cellular milieu and geological settings of the extremophiles. The results could not only lead to a deeper understanding of fundamental life phenomena, but also reveal previously unknown adaptation mechanisms.

9. Concluding Remarks

Crowding has multiple effects on the conformation, dynamics, functionality and activity of biosystems, as outlined in this review, and especially so when combined with various extreme environmental conditions under which the systems are thriving. However, due to the high complexity of living systems and their high sensitivity to environmental conditions such as extremes of temperature and pressure, high salt and desiccation, we do not yet know all possible effects in detail. Next to the proteome, studies on other biomolecular entities, such as the lipodome, need to be carried out in response to temperature, pressure, and crowding.[257] It will be beneficial to extent the studies to as many systems as possible in the future and combine them with novel experimental and theoretical approaches. As described in section 6.2, MD simulations, both at the atomic and coarse-grained level, will become more important to study larger biomolecular systems over longer time periods.[258] The correct description of crowding conditions will remain a challenge in this area of research, however.

A second avenue is the exploration of the whole genome phylogeny. Comparison of, for instance, extremophilic proteins could permit to formulate complete genomic models to explain adaptation to particular environmental conditions. When protein sequences are altered, this will indeed not only impact the structure, but also the molecular dynamics. Evolution certainly also plays an important role in explaining adaptation mechanisms in accordance with temporal modifications of living conditions on Earth. This is one of the reasons for the extraordinary interest in the question of the origin of life on Earth.[259]

Finally, further experimental results under realistic crowding conditions are required. The use of synthetic polymeric osmolytes as crowding agents has many advantages, as the experimental conditions can be well controlled, but such an approach comes at the expense of the polydispersity and heterogeneity of natural crowders in the cellular milieu. We have presented here first attempts to circumvent these difficulties and to perform experiments directly on living cells by simulating the crowders by components of lysed cells or, vice versa, by comparing intact and lysed cells in which confinement and thus crowding have been removed. We will need many more such or similar results to improve our understanding of crowding effects in organisms that thrive in inhospitable, harsh

conditions. So far, the effects of crowding on biochemically relevant reactions, protein stability, and protein self-assembly have been extensively studied under non-extreme conditions only, and several excellent reviews on these topics are available.[260-264] The deep sea and outer space are considered one of the final frontiers of human exploration.[265] The unique physicochemical processes that occur under the extreme environmental conditions studied, and the uncovering of biochemical mechanisms evolved by organisms to survive these conditions, can serve as inspiration for scientific and biotechnological advancements. As Deguchi et al.[265] put it, there is plenty of room for chemistry at the bottom of the ocean.

AUTHOR INFORMATION

Corresponding Authors

Judith Peters - Univ. Grenoble Alpes, CNRS, LiPhy, 140 rue de la physique, 38400 St Martin d'Hères, France ; Institut Laue Langevin, 71 avenue des Martyrs, 38000 Grenoble, France; Institut Universitaire de France, Paris, France; E-mail : judith.peters@univ-grenoble-alpes.fr

Roland Winter - Department of Chemistry and Chemical Biology, Biophysical Chemistry, TU Dortmund University, Dortmund, Otto-Hahn-Str. 4a, D-44227 Dortmund, Germany; E-mail: roland.winter@tu-dortmund.de

Authors

Rosario Oliva - Department of Chemical Sciences, University of Naples Federico II, Via Cintia 4, 80126 Naples, Italy; E-mail: rosario.oliva2@unina.it

Antonino Caliò - European Synchrotron Radiation Facility, 71 avenue des Martyrs, 38000 Grenoble, France; E-mail: antonino.calio@esrf.fr

Philippe Oger - Université de Lyon, INSA Lyon, CNRS, MAP UMR 5240, Villeurbanne, France; E-mail: philippe.oger@insa-lyon.fr

Notes

The authors declare no competing financial interests.

Biographies

Judith Peters graduated in Physics at the University Joseph Fourier Grenoble 1 and received her PhD in Theoretical Physics in 1988. She then had a post-doctoral position at the University of Heidelberg working on molecular dynamics simulations. After one year as exchange scientist at the University of St. Petersburg, 7 years as assistant professor at the University of Applied Sciences in Berlin and 10 years as scientist at the Helmholtz Zentrum Berlin, she holds now a professorship of Physics at Université Grenoble Alpes and has been nominated as a senior member of the Institut Universitaire de France in 2021. Her research interests comprise dynamical studies of biosystems including proteins, membranes, whole cells or nucleic acids by neutron scattering techniques, particularly under extreme conditions.

Rosario Oliva obtained his Ph.D. from the University of Naples Federico II (Italy) in 2019. After his Ph.D., he joined the research group of Prof. Roland Winter at TU Dortmund University (Germany) working in the field of high-pressure biophysics, exploring the effect of high pressure, salts and osmolytes on biomolecular systems. In 2022, he was appointed Research Associate at the Department of Chemical Sciences, University of Naples Federico II. His research interest includes also mechanistic studies of the interaction of antimicrobial peptides with model biomembranes, and bioactive peptides induced perturbation of: liquid-liquid phase separation of cancer-relevant proteins and fibrillation of proteins involved in neurodegenerative diseases.

Antonino Caliò studied Physics at the University of Palermo, and obtained his Ph.D. in Biophysics at the University Claude Bernard Lyon 1 in 2022. He then joined the ESRF as a postdoctoral fellow, studying Intrinsically Disordered Proteins and their interactions with DNA. His interests range from the fundamental physics of protein dynamics to the adaptation of proteins to High Hydrostatic Pressure, studied by means of neutron and X-ray scattering techniques.

Philippe Oger received his PhD in Plant Pathology in 1995 from the University of Paris, where he determined the alteration induced by the culture of genetically modified plants on the soil bacteria and their metabolism. From there he moved to the University of Illinois at Ubrana-Champaign to study the evolution of carbon metabolism in Agrobacterium tumefaciens. He joined the CNRS and the Laboratoire de Sciences de la Terre in Lyon in 2000. His current research focuses on the influence of high hydrostatic pressure on microbial metabolism in relation to geological processes. Several analytical techniques have been developed, or adapted, for the study *in situ* under controlled pressures and temperatures of the metabolism of model eukaryotes (yeast and *Emiliana huxleyi*) and several strains of model piezophilic and piezotolerant bacteria and archaea.

Roland Winter studied Chemistry at the Technical University of Karlsruhe. After his doctorate, he joined the Departments of Chemistry at the Philipps-University Marburg and the University of Illinois at Urbana–Champaign, USA, as a postdoctoral fellow. After his habilitation in Physical Chemistry in Marburg, he was appointed Professor of Physical Chemistry at the Ruhr-University in Bochum. Since 1993, he has held the Chair of Physical Chemistry I (Biophysical Chemistry) at TU Dortmund University. His research interests include the study of the structure, dynamics and solvation of biomolecular systems, such as model biomembranes, proteins, and nucleic acids including Q-quadruplexes. A particular focus of his research is on membrane-associated signaling processes, amyloidogenesis, and to pressure effects in molecular biophysics.

Acknowledgements

We are gratefully acknowledging the financing by the French National Research Agency programs: Project No. ANR 2010 BLAN 1725 01, Living deep, and ANR 17-CE11-0012-01, Archeomembranes, to PO and JP. We further acknowledge financing by the Mission pour les Initiatives Transverses et Interdisciplinaires of the CNRS (OriginsUnderPressure and LifeAdapt research projects) as well as by the German-French bilateral research cooperation programme Procope 2018–2019 to J.P. and R.W. A.C. was supported by a PhD grant for international students by the French Ministry of Science and Technology. A.C. was supported by a PhD grant for international students by the French Ministry of Science and Technology and by the European Innovation Council (grant n. 101046920 'iSenseDNA'). J.P. is grateful to the Institut Universitaire de France for providing additional time to be dedicated to

research. R.W. acknowledges funding from the Deutsche Forschungsgemeinschaft (DFG, German Research Foundation) under Germany's Excellence Strategy – EXC 2033 – project number 390677874-RESOLV. R.O. is grateful to the Italian MUR for being granted a research associated position (PON R&I 2014-2020, CUP: E65F21003250003).

References

(1) Milo, R.; Phillips, R. *Cell Biology by the Numbers*; Garland Science, Taylor & Francis group, 2015.
(2) Cheung, M. S.; Klimov, D.; Thirumalai, D. Molecular crowding enhances native state stability and refolding rates of globular proteins. *Proc. Natl. Acad. Sci. USA* **2005**, *102*, 4753 - 4758.
(3) Ellis, R. J. Macromolecular crowding: an important but neglected aspect of the intracellular environment. *Curr. Opin. Struct. Biol.* **2001**, *11*, 114-119.
(4) Fulton, A. B. How crowded is the cytoplasm? *Cell* **1982**, *30*, 345 - 347.
(5) Goodsell, D. S. Inside a living cell. *Trends Biochem. Sci.* **1991**, *16* , 203-206.
(6) Hancock, R. Packing of the polynucleosome chain in interphase chromosomes: evidence for a contribution of crowding and entropic forces. *Semin. Cell. Dev. Biol.* **2007**, *18* , 668-675.
(7) Srere, P. A. The infrastructure of the mitochondrial matrix. *Trends Biochem. Sci.* **1980**, *5*, 120 - 121.
(8) Zimmerman, S. B.; Trach, S. O. Estimation of macromolecule concentrations and excluded volume effects for the cytoplasm of Escherichia coli. *J. Mol. Biol.* **1991**, *222* (3), 599-620.
(9) Sugimoto, N. Noncanonical Structures and Their Thermodynamics of DNA and RNA Under Molecular Crowding: Beyond the Watson–Crick Double Helix. *In. Rev. Cell Mol. Biol.* **2014**, *307*, 205 - 273.
(10) Minton, A. P. Effect of a concentrated "inert" macromolecular cosolute on the stability of a globular protein with respect to denaturation by heat and by chaotropes: a statistical-thermodynamic model. *Biophys. J.* **2000**, *78*, 101-109.
(11) Politou, A.; Temussi, P. A. Revisiting a dogma: the effect of volume exclusion in molecular crowding. *Curr. Opin. Struct. Biol.* **2015**, *30*, 1-6.
(12) Martin, S. R.; Esposito, V.; De Los Rios, P.; Pastore, A.; Temussi, P. A. Cold denaturation of yeast frataxin offers the clue to understand the effect of alcohols on protein stability. *J. Am. Chem. Soc.* **2008**, *130*, 9963-9970.
(13) Taulier, N.; Chalikian, T. V. Compressibility of protein transitions. *Biochim. Biophys. Acta* **2002**, *1595*, 48-70.
(14) Kauzmann, W. Some factors in the interpretation of protein denaturation. *Adv. Protein Chem.* **1959**, *14*, 1 - 63.
(15) Balny, C.; Masson, P.; Heremans, K. High pressure effects on biological macromolecules: from structural changes to alteration of cellular processes. *Biochim. Biophys. Acta* **2002**, *1595*, 3-10.
(16) C.R., W.; O., K.; M.L., W. Towards a natural system of organisms: Proposal for the domains Archaea, Bacteria, and Eucarya. *Proc. Natl. Acad. Sci. USA* **1990**, *87*, 4576 - 4579.
(17) Daniel, I.; Oger, P.; Winter, R. Origins of life and biochemistry under high-pressure conditions. *Chem. Soc. Rev.* **2006**, *35*, 858-875.
(18) Calio, A.; Dubois, C.; Fontanay, S.; Koza, M. M.; Hoh, F.; Roumestand, C.; Oger, P.; Peters, J. Unravelling the Adaptation Mechanisms to High Pressure in Proteins. *Int. J. Mol. Sci.* **2022**, *23*.
(19) Canganella, F.; Wiegel, J. Extremophiles: from abyssal to terrestrial ecosystems and possibly beyond. *Naturwissenschaften* **2011**, *98*, 253-279.
(20) Price, P. B. A habitat for psychrophiles in deep Antarctic ice. *Proc. Natl. Acad. Sci. USA* **2000**, *97*, 1247-1251.
(21) Takai, K.; Nakamura, K.; Toki, T.; Tsunogai, U.; Miyazaki, M.; Miyazaki, J.; Hirayama, H.; Nakagawa, S.; Nunoura, T.; Horikoshi, H. Cell proliferation at 122°C and isotopically heavy CH4 production by a hyperthermophilic methanogen under high-pressure cultivation. *Proc. Natl. Acad. Sci. USA* **2008**, *105*, 10949-10954.

(22) Bartlett, D. H. Microbial Adaptations to the Psychrosphere/Piezosphere. *J. Molec. Microbiol. Biotechnol* **1999**, *1*, 93 - 100.
(23) Marteinsson, V. T.; Birrien, J. L.; Reysenbach, A. L.; Vernet, M.; Marie, D.; Gambacorta, A.; Messner, P.; Sleytr, U. B.; Prieur, D. *Thermococcus barophilus* sp. nov., a new barophilic and hyperthermophilic archaeon isolated under high hydrostatic pressure from a deep-sea hydrothermal vent. *Int. J. Syst. Bacteriol.* **1999**, *2*, 351-359.
(24) Le Châtelier, H. L. Sur un énoncé général des lois d'équilibres chimiques. *C.R. Acad. Sci.* **1884**, *99*, 786 - 789.
(25) Cario, A.; Grossi, V.; Schaeffer, P.; Oger, P. M. Membrane homeoviscous adaptation in the piezo-hyperthermophilic archaeon Thermococcus barophilus. *Front. Microbiol.* **2015**, *6*.
(26) Hawley, S. A. Reversible pressure-temperature denaturation of chymotrypsinogen. *Biochemistry* **1971**, *10*, 2436–2442.
(27) Winter, R.; Lopes, D.; Grudzielanek, S.; Vogtt, K. Towards an understanding of the temperature/pressure configurational and free-energy landscape of biomolecules. *J. Non-Equilib. Thermodyn.* **2007**, *32*, 41-97.
(28) Deole, R.; Challacombe, J.; Raiford, D. W.; Hoff, W. D. An extremely halophilic proteobacterium combines a highly acidic proteome with a low cytoplasmic potassium content. *J. Biol. Chem.* **2013**, *288*, 581-588.
(29) Russell, A. D. Lethal effects of heat on bacterial physiology and structure. *Science progress* **2003**, *86*, 115 - 137.
(30) Tsuchido, T.; Katsui, N.; Takeuchi, A.; Takano, M.; Shibasaki, I. Destruction of the outer membrane permeability barrier of Escherichia coli by heat treatment. *Appl. Env. Microbiology* **1985**, *50*, 298 - 303.
(31) Chang, C. H.; Chiang, M. L.; Chou, C. C. The effect of temperature and length of heat shock treatment on the thermal tolerance and cell leakage of Cronobacter sakazakii BCRC 13988. *Int. J. Food Microbiol.* **2009**, *134*, 184-189.
(32) McGuffee, S. R.; Elcock, A. H. Diffusion, crowding & protein stability in a dynamic molecular model of the bacterial cytoplasm. *PLoS Comput. Biol.* **2010**, *6*, e1000694.
(33) Matsuura, Y.; Takehira, M.; Joti, Y.; Ogasahara, K.; Tanaka, T.; Ono, N.; Kunishima, N.; Yutani, K. Thermodynamics of protein denaturation at temperatures over 100 degrees C: CutA1 mutant proteins substituted with hydrophobic and charged residues. *Sci. Rep.* **2015**, *5*, 15545.
(34) Santoro, M. G. Heat shock factors and the control of the stress response. *Biochem. Pharmacol.* **2000**, *59*, 55-63.
(35) Yancey, P. H.; Clark, M. E.; Hand, S. C.; Bowlus, R. D.; Somero, G. N. Living with water stress: evolution of osmolyte systems. *Science* **1982**, *217*, 1214-1222.
(36) Gao, M.; Held, C.; Patra, S.; Arns, L.; Sadowski, G.; Winter, R. Crowders and Cosolvents-Major Contributors to the Cellular Milieu and Efficient Means to Counteract Environmental Stresses. *ChemPhysChem* **2017**, *18*, 2951-2972.
(37) Salvador-Castell, M.; Golub, M.; Martinez, N.; Ollivier, J.; Peters, J.; Oger, P. The first study on the impact of osmolytes in whole cells of high temperature-adapted microorganisms. *Soft Matter* **2019**, *15*, 8381-8391.
(38) Mackey, B. M.; Miles, C. A.; Parsons, S. E.; Seymour, D. A. Thermal denaturation of whole cells and cell components of Escherichia coli examined by differential scanning calorimetry. *J. Gen. Microbiol.* **1991**, *137*, 2361-2374.
(39) Bridgman, P. W. The coagulation of albumen by pressure. *J. Biol. Chem.* **1914**, *19*, 511 - 512.
(40) Perticaroli, S.; Ehlers, G.; Stanley, C. B.; Mamontov, E.; O'Neill, H.; Zhang, Q.; Cheng, X.; Myles, D. A.; Katsaras, J.; Nickels, J. D. Description of Hydration Water in Protein (Green Fluorescent Protein) Solution. *J. Am. Chem. Soc.* **2017**, *139*, 1098-1105.
(41) Mentre, P.; Hui Bon Hoa, G. Effects of high hydrostatic pressures on living cells: a consequence of the properties of macromolecules and macromolecule-associated water. *Int. Rev. Cytol.* **2001**, *201*, 1-84.
(42) Winter, R. Interrogating the Structural Dynamics and Energetics of Biomolecular Systems with Pressure Modulation. *Annu. Rev. Biophys.* **2019**, *48*, 441-463.

(43) Akasaka, K.; Matsuki, H. *High Pressure Bioscience – Basic Concepts, Applications and Frontiers*; Springer Science, 2015.
(44) Knop, J. M.; Mukherjee, S.; Jaworek, M. W.; Kriegler, S.; Manisegaran, M.; Fetahaj, Z.; Ostermeier, L.; Oliva, R.; Gault, S.; Cockell, C. S.; Winter, R. Life in Multi-Extreme Environments: Brines, Osmotic and Hydrostatic Pressure horizontal line A Physicochemical View. *Chem. Rev.* **2023**, *123*, 73-104.
(45) Silva, J. L.; Oliveira, A. C.; Vieira, T. C.; de Oliveira, G. A.; Suarez, M. C.; Foguel, D. High-pressure chemical biology and biotechnology. *Chem. Rev.* **2014**, *114*, 7239-7267.
(46) Bartlett, D. H. Pressure effects on in vivo microbial processes. *Biochim. Biophys. Acta* **2002**, *1595*, 367-381.
(47) Meersman, F.; Daniel, I.; Bartlett, D. H.; Winter, R.; Hazael, R.; McMillan, P. R. High-Pressure Biochemistry and Biophysics. *Rev. Mineral Geochem.* **2013**, *75*, 607 - 648.
(48) Macdonald, A. *Life at High Pressure: In the Deep Sea and Other Environments*; Springer, 2021.
(49) Yancey, P. H.; Gerringer, M. E.; Drazen, J. C.; Rowden, A. A.; Jamieson, A. Marine fish may be biochemically constrained from inhabiting the deepest ocean depths. *Proc. Natl. Acad. Sci. USA* **2014**, *111*, 4461-4465.
(50) Knorr, D.; Heinz, V.; Buckow, R. High pressure application for food biopolymers. *Biochim. Biophys. Acta* **2006**, *1764*, 619-631.
(51) Ostermeier, L.; de Oliveira, G. A. P.; Dzwolak, W.; Silva, J. L.; Winter, R. Exploring the polymorphism, conformational dynamics and function of amyloidogenic peptides and proteins by temperature and pressure modulation. *Biophys. Chem.* **2021**, *268*, 106506.
(52) Oger, P. M.; Jebbar, M. The many ways of coping with pressure. *Res. Microbiol.* **2010**, *161*, 799-809.
(53) Oren, A. The Order Halobacteriales. In *The Prokaryotes*, Dworkin, M., Falkow, S., Rosenberg, E., Schleifer, KH., Stackebrandt, E. Ed.; 2006; pp 113 - 164.
(54) Mevarech, M.; Eisenberg, H.; Neumann, E. Malate dehydrogenase isolated from extremely halophilic bacteria of the Dead Sea. 1. Purification and molecular characterization. *Biochemistry* **1977**, *16*, 3781-3785.
(55) Pundak, S.; Aloni, H.; Eisenberg, H. Structure and activity of malate dehydrogenase from the extreme halophilic bacteria of the Dead Sea. 2. Inactivation, dissociation and unfolding at NaCl concentrations below 2 M. Salt, salt concentration and temperature dependence of enzyme stability. *Eur. J. Biochem.* **1981**, *118* , 471-477.
(56) Zaccai, G.; Cendrin, F.; Haik, Y.; Borochov, N.; Eisenberg, H. Stabilization of halophilic malate dehydrogenase. *J. Mol. Biol.* **1989**, *208*, 491-500.
(57) Madern, D.; Ebel, C.; Zaccai, G. Halophilic adaptation of enzymes. *Extremophiles* **2000**, *4*, 91-98.
(58) Gunde-Cimerman, N.; Plemenitas, A.; Oren, A. Strategies of adaptation of microorganisms of the three domains of life to high salt concentrations. *FEMS Microbiol. Rev.* **2018**, *42*, 353-375.
(59) Yancey, P. H. Organic osmolytes as compatible, metabolic and counteracting cytoprotectants in high osmolarity and other stresses. *J. Exp. Biol.* **2005**, *208*, 2819-2830.
(60) Andrade, J. M.; Rios, L. R.; Teixeira, L. S.; Vieira, F. S.; Mendes, D. C.; Vieira, M. A.; Silveira, M. F. Influence of socioeconomic factors on the quality of life of elderly hypertensive individuals. *Cien Saude Colet* **2014**, *19* , 3497-3504.
(61) Christian, J. H. B.; Waltho, J. A. Solute concentrations within cells of halophilic bacteria. *Biochim. Biophys. Acta* **1962**, *65*, 508 - 509.
(62) Paul, S.; Bag, S. K.; Das, S.; Harvill, E. T.; Dutta, C. Molecular signature of hypersaline adaptation: insights from genome and proteome composition of halophilic prokaryotes. *Genome Biol.* **2008**, *9* , R70.
(63) Zhou, H. X.; Rivas, G.; Minton, A. P. Macromolecular crowding and confinement: biochemical, biophysical, and potential physiological consequences. *Annu. Rev. Biophys.* **2008**, *37*, 375-397.
(64) Heremans, K.; Smeller, L. Protein structure and dynamics at high pressure. *Biochim. Biophys. Acta* **1998**, *1386*, 353-370.
(65) Roche, J.; Royer, C. A. Lessons from pressure denaturation of proteins. *J. R. Soc. Interface* **2018**, *15* (147).

(66) Roche, J.; Caro, J. A.; Norberto, D. R.; Barthe, P.; Roumestand, C.; Schlessman, J. L.; Garcia, A. E.; Garcia-Moreno, B. E.; Royer, C. A. Cavities determine the pressure unfolding of proteins. *Proc. Natl. Acad. Sci. USA* **2012**, *109*, 6945-6950.
(67) Chen, C. R.; Makhatadze, G. I. Molecular determinant of the effects of hydrostatic pressure on protein folding stability. *Nat. Commun.* **2017**, *8*, 14561.
(68) Somkuti, J.; Torok, Z.; Pfalzgraf, F.; Smeller, L. Low crowding agent concentration destabilizes against pressure unfolding. *Biophys. Chem.* **2017**, *231*, 125-134.
(69) Julius, K.; Al-Ayoubi, S. R.; Paulus, M.; Tolan, M.; Winter, R. The effects of osmolytes and crowding on the pressure-induced dissociation and inactivation of dimeric LADH. *Phys. Chem. Chem. Phys.* **2018**, *20*, 7093-7104.
(70) Grudzielanek, S.; Smirnovas, V.; Winter, R. Solvation-assisted pressure tuning of insulin fibrillation: from novel aggregation pathways to biotechnological applications. *J. Mol. Biol.* **2006**, *356*, 497-509.
(71) Erlkamp, M.; Grobelny, S.; Winter, R. Crowding effects on the temperature and pressure dependent structure, stability and folding kinetics of Staphylococcal Nuclease. *Phys. Chem. Chem. Phys.* **2014**, *16*, 5965-5976.
(72) Zhai, Y.; Winter, R. Effect of molecular crowding on the temperature-pressure stability diagram of ribonuclease A. *ChemPhysChem* **2013**, *14* , 386-393.
(73) Sunde, E. P.; Setlow, P.; Hederstedt, L.; Halle, B. The physical state of water in bacterial spores. *Proc. Natl. Acad. Sci. USA* **2009**, *106*, 19334-19339.
(74) Kahse, M.; Werner, M. D.; Shuang, Z.; Hartmann, M.; Buntkowski, G.; Winter, R. Stability, Hydration, and Thermodynamic Properties of RNase A Confined in Surface-Functionalized SBA-15 Mesoporous Molecular Sieves. *J. Phys. Chem. C* **2014**, *118*, 21523-21531.
(75) Das, N.; Tarif, E.; Dutta, A.; Sen, P. Associated Water Dynamics Might Be a Key Factor Affecting Protein Stability in the Crowded Milieu. *J. Phys. Chem. B* **2023**, *127* , 3151-3163.
(76) Heyden, M.; Brundermann, E.; Heugen, U.; Niehues, G.; Leitner, D. M.; Havenith, M. Long-range influence of carbohydrates on the solvation dynamics of water--answers from terahertz absorption measurements and molecular modeling simulations. *J. Am. Chem. Soc.* **2008**, *130* (17), 5773-5779.
(77) Hishida, M.; Anjum, R.; Anada, T.; Murakami, D.; Tanaka, M. Effect of Osmolytes on Water Mobility Correlates with Their Stabilizing Effect on Proteins. *J. Phys. Chem. B* **2022**, *126* (13), 2466-2475.
(78) Al-Ayoubi, S. R.; Schummel, P. H.; Golub, M.; Peters, J.; Winter, R. Influence of Cosolvents, Self-Crowding, Temperature and Pressure on the Sub-Nanosecond Dynamics and Folding Stability of Lysozyme. *Phys. Chem. Chem. Phys.* **2017**, *19*, 14230 - 14237.
(79) Erlkamp, M.; Marion, J.; Martinez, N.; Czeslik, C.; Peters, J.; Winter, R. Influence of pressure and crowding on the sub-nanosecond dynamics of globular proteins. *J. Phys. Chem. B* **2015**, *119*, 4842-4848.
(80) Gao, M.; Berghaus, M.; Mobitz, S.; Schuabb, V.; Erwin, N.; Herzog, M.; Julius, K.; Sternemann, C.; Winter, R. On the Origin of Microtubules' High-Pressure Sensitivity. *Biophys. J.* **2018**, *114*, 1080-1090.
(81) Gao, M.; Winter, R. Kinetic Insights into the Elongation Reaction of Actin Filaments as a Function of Temperature, Pressure, and Macromolecular Crowding. *ChemPhysChem* **2015**, *16*, 3681-3686.
(82) Schummel, P. H.; Gao, M.; Winter, R. Modulation of the Polymerization Kinetics of alpha/beta-Tubulin by Osmolytes and Macromolecular Crowding. *ChemPhysChem* **2017**, *18*, 189-197.
(83) Rosin, C.; Estel, K.; Halker, J.; Winter, R. Combined effects of temperature, pressure, and co-solvents on the polymerization kinetics of actin. *ChemPhysChem* **2015**, *16* , 1379-1385.
(84) Schummel, P. H.; Haag, A.; Kremer, W.; Kalbitzer, H. R.; Winter, R. Cosolvent and Crowding Effects on the Temperature and Pressure Dependent Conformational Dynamics and Stability of Globular Actin. *J. Phys. Chem. B* **2016**, *120*, 6575-6586.
(85) Woenckhaus, J.; Kohling, R.; Thiyagarajan, P.; Littrell, K. C.; Seifert, S.; Royer, C. A.; Winter, R. Pressure-jump small-angle x-ray scattering detected kinetics of staphylococcal nuclease folding. *Biophys. J.* **2001**, *80* , 1518-1523.
(86) Panick, G.; Malessa, R.; Winter, R.; Rapp, G.; Frye, K. J.; Royer, C. A. Structural characterization of the pressure-denatured state and unfolding/refolding kinetics of staphylococcal nuclease by

synchrotron small-angle X-ray scattering and Fourier-transform infrared spectroscopy. *J. Mol. Biol.* **1998**, *275*, 389-402.
(87) Prigozhin, M. B.; Liu, Y.; Wirth, A. J.; Kapoor, S.; Winter, R.; Schulten, K.; Gruebele, M. Misplaced helix slows down ultrafast pressure-jump protein folding. *Proc. Natl. Acad. Sci. USA* **2013**, *110*, 8087-8092.
(88) Mishra, R.; Winter, R. Cold- and pressure-induced dissociation of protein aggregates and amyloid fibrils. *Angew. Chem. Int. Ed.* **2008**, *47* , 6518-6521.
(89) Gruzielanek, S.; Zhai, Y.; Winter, R. Unraveling the pressure effect on nucleation processes of amyloidogenic proteins. *ChemPhysChem* **2010**, *11*, 2016-2020.
(90) Schroer, M. A.; Markgraf, J.; Wieland, D. C.; Sahle, C. J.; Moller, J.; Paulus, M.; Tolan, M.; Winter, R. Nonlinear pressure dependence of the interaction potential of dense protein solutions. *Phys. Rev. Lett.* **2011**, *106* , 178102.
(91) Schroer, M. A.; Zhai, Y.; Wieland, D. C.; Sahle, C. J.; Nase, J.; Paulus, M.; Tolan, M.; Winter, R. Exploring the piezophilic behavior of natural cosolvent mixtures. *Angew. Chem. Int. Ed.* **2011**, *50*, 11413-11416.
(92) Julius, K.; Weine, J.; Berghaus, M.; Konig, N.; Gao, M.; Latarius, J.; Paulus, M.; Schroer, M. A.; Tolan, M.; Winter, R. Water-Mediated Protein-Protein Interactions at High Pressures are Controlled by a Deep-Sea Osmolyte. *Phys. Rev. Lett.* **2018**, *121* , 038101.
(93) Julius, K.; Weine, J.; Gao, M.; Latarius, J.; Elbers, M.; Paulus, M.; Tolan, M.; Winter, R. Impact of Macromolecular Crowding and Compression on Protein–Protein Interactions and Liquid–Liquid Phase Separation Phenomena. *Macromolecules* **2019**, *52*, 1772–1784.
(94) Julius, K. Impact of Organic Osmolytes and Crowding on the Protein-protein Interaction at High Pressures: A Small-angle X-ray Scattering Study. TU Dortmund, 2019.
(95) Brangwynne, C. P.; Tompa, P.; Pappu, R. V. Polymer physics of intracellular phase transitions. *Nat. Phys.* **2015**, *11*, 899 - 904.
(96) Cinar, H.; Cinar, S.; Chan, H. S.; Winter, R. Pressure-Induced Dissolution and Reentrant Formation of Condensed, Liquid-Liquid Phase-Separated Elastomeric alpha-Elastin. *Chem. Eur. J.* **2018**, *24*, 8286-8291.
(97) Cinar, S.; Cinar, H.; Chan, H. S.; Winter, R. Pressure-Sensitive and Osmolyte-Modulated Liquid-Liquid Phase Separation of Eye-Lens gamma-Crystallins. *J. Am. Chem. Soc.* **2019**, *141* (18), 7347-7354.
(98) Cinar, H.; Fetahaj, Z.; Cinar, S.; Vernon, R. M.; Chan, H. S.; Winter, R. H. A. Temperature, Hydrostatic Pressure, and Osmolyte Effects on Liquid-Liquid Phase Separation in Protein Condensates: Physical Chemistry and Biological Implications. *Chemistry* **2019**, *25*, 13049-13069.
(99) Fetahaj, Z.; Ostermeier, L.; Cinar, H.; Oliva, R.; Winter, R. Biomolecular Condensates under Extreme Martian Salt Conditions. *J. Am. Chem. Soc.* **2021**, *143*, 5247-5259.
(100) Cinar, H.; Oliva, R.; Wu, H.; Zhang, M.; Chan, H. S.; Winter, R. Effects of Cosolvents and Crowding Agents on the Stability and Phase Transition Kinetics of the SynGAP/PSD-95 Condensate Model of Postsynaptic Densities. *J. Phys. Chem. B* **2022**, *126*, 1734-1741.
(101) Li, S.; Yoshizawa, T.; Yamazaki, R.; Fujiwara, A.; Kameda, T.; Kitahara, R. Pressure and Temperature Phase Diagram for Liquid-Liquid Phase Separation of the RNA-Binding Protein Fused in Sarcoma. *J. Phys. Chem. B* **2021**, *125* , 6821-6829.
(102) Moller, J.; Grobelny, S.; Schulze, J.; Bieder, S.; Steffen, A.; Erlkamp, M.; Paulus, M.; Tolan, M.; Winter, R. Reentrant liquid-liquid phase separation in protein solutions at elevated hydrostatic pressures. *Phys. Rev. Lett.* **2014**, *112*, 028101.
(103) Bai, Q.; Chen, X.; Chen, J.; Liu, Z.; Lin, Y. N.; Yang, S.; Liang, D. Morphology and Dynamics of Coexisting Phases in Coacervate Solely Controlled by Crowded Environment. *ACS Macro Lett.* **2022**, *11*, 1107-1111.
(104) Moron, M.; Al-Masoodi, A.; Lovato, C.; Reiser, M.; Randolph, L.; Surmeier, G.; Bolle, J.; Westermeier, F.; Sprung, M.; Winter, R.; et al. Gelation Dynamics upon Pressure-Induced Liquid-Liquid Phase Separation in a Water-Lysozyme Solution. *J. Phys. Chem. B* **2022**, *126*, 4160-4167.
(105) Moron, M. Proteindynamik unter hohem hydrostatischen Druck. TU Dortmund, 2023.

(106) Dubins, D. N.; Lee, A.; Macgregor, R. B., Jr.; Chalikian, T. V. On the stability of double stranded nucleic acids. *J. Am. Chem. Soc.* **2001**, *123* , 9254-9259.
(107) Son, I.; Shek, Y. L.; Dubins, D. N.; Chalikian, T. V. Hydration changes accompanying helix-to-coil DNA transitions. *J. Am. Chem. Soc.* **2014**, *136* , 4040-4047.
(108) Takahashi, S.; Sugimoto, N. Effect of pressure on the stability of G-quadruplex DNA: thermodynamics under crowding conditions. *Angew. Chem. Int. Ed.* **013**, *52*, 13774-13778.
(109) Takahashi, S.; Sugimoto, N. Pressure-dependent formation of i-motif and G-quadruplex DNA structures. *Phys. Chem. Chem. Phys.* **2015**, *17*, 31004-31010.
(110) Patra, S.; Anders, C.; Erwin, N.; Winter, R. Osmolyte Effects on the Conformational Dynamics of a DNA Hairpin at Ambient and Extreme Environmental Conditions. *Angew. Chem. Int. Ed.* **2017**, *129*, 5127 - 5131.
(111) Patra, S.; Anders, C.; Schummel, P. H.; Winter, R. Antagonistic effects of natural osmolyte mixtures and hydrostatic pressure on the conformational dynamics of a DNA hairpin probed at the single-molecule level. *Phys. Chem. Chem. Phys.* **2018**, *20*, 13159-13170.
(112) Patra, S.; Schuabb, V.; Kiesel, I.; Knop, J. M.; Oliva, R.; Winter, R. Exploring the effects of cosolutes and crowding on the volumetric and kinetic profile of the conformational dynamics of a poly dA loop DNA hairpin: a single-molecule FRET study. *Nucleic Acids Res.* **2019**, *47*, 981-996.
(113) Czeslik, C.; Reis, O.; Winter, R.; Rapp, G. Effect of high pressure on the structure of dipalmitoylphosphatidylcholine bilayer membranes: a synchrotron-X-ray diffraction and FT-IR spectroscopy study using the diamond anvil technique. *Chem. Phys. Lip.* **1998**, *91*, 135-144.
(114) Winter, R.; Czeslik, C. Pressure Effects on the Structure of Lyotropic Lipid Mesophases and Model Biomembrane Systems. *Z. Krist.* **2000**, *215*, 454-474.
(115) Winter, R.; Czeslik, C. Pressure effects on the structure of lyotropic lipid mesophases and model biomembrane systems. *Z. Krist.* **2000**, *215*, 454-474.
(116) Trapp, M.; Marion, J.; Tehei, M.; Deme, B.; Gutberlet, T.; Peters, J. High hydrostatic pressure effects investigated by neutron scattering on lipid multilamellar vesicles. *Phys. Chem. Chem. Phys.* **2013**, *15* , 20951-20956.
(117) McCarthy, N. L.; Ces, O.; Law, R. V.; Seddon, J. M.; Brooks, N. J. Separation of liquid domains in model membranes induced with high hydrostatic pressure. *Chem. Commun.* **2015**, *51*, 8675-8678.
(118) Seeliger, J.; Erwin, N.; Rosin, C.; Kahse, M.; Weise, K.; Winter, R. Exploring the structure and phase behavior of plasma membrane vesicles under extreme environmental conditions. *Phys. Chem. Chem. Phys.* **2015**, *17*, 7507-7513.
(119) Guigas, G.; Weiss, M. Effects of protein crowding on membrane systems. *Biochim. Biophys. Acta* **2016**, *1858*, 2441-2450.
(120) Lowe, M.; Kalacheva, M.; Boersma, A. J.; Kedrov, A. The more the merrier: effects of macromolecular crowding on the structure and dynamics of biological membranes. *FEBS J.* **2020**, *287*, 5039-5067.
(121) Al-Ayoubi, S. R.; Schinkel, P. K. F.; Berghaus, M.; Herzog, M.; Winter, R. Combined effects of osmotic and hydrostatic pressure on multilamellar lipid membranes in the presence of PEG and trehalose. *Soft Matter* **2018**, *14* , 8792-8802.
(122) Minton, A. P. Influence of macromolecular crowding upon the stability and state of association of proteins: predictions and observations. *J. Pharm. Sci.* **2005**, *94*, 1668-1675.
(123) Grobelny, S.; Erlkamp, M.; Moller, J.; Tolan, M.; Winter, R. Intermolecular interactions in highly concentrated protein solutions upon compression and the role of the solvent. *J. Chem. Phys.* **2014**, *141* (22), 22D506.
(124) Iborra, F. J. Can visco-elastic phase separation, macromolecular crowding and colloidal physics explain nuclear organisation? *Theor. Biol. Med. Model.* **2007**, *4*, 15.
(125) Grimaldo, M.; Lopez, H.; Beck, C.; Roosen-Runge, F.; Moulin, M.; Devos, J. M.; Laux, V.; Hartlein, M.; Da Vela, S.; Schweins, R.; et al. Protein Short-Time Diffusion in a Naturally Crowded Environment. *J. Phys. Chem. Lett.* **2019**, *10* , 1709-1715.

(126) Roosen-Runge, F.; Hennig, M.; Zhang, F.; Jacobs, R. M.; Sztucki, M.; Schober, H.; Seydel, T.; Schreiber, F. Protein self-diffusion in crowded solutions. *Proc. Natl. Acad. Sci. USA* **2011**, *108* (, 11815-11820.
(127) Phillips, R. J.; Brady, J. F. Hydrodynamic transport properties of hard-sphere dispersions. I. Suspensions of freely mobile particles. *Phys. Fluids* **1988**, *31*, 3462 - 3472.
(128) Atomi, H.; Fukui, T.; Kanai, T.; Morikawa, M.; Imanaka, T. Description of *Thermococcus kodakaraensis* sp. nov., a well studied hyperthermophilic archaeon previously reported as *Pyrococcus* sp. KOD1. *Archaea* **2004**, *1*, 263 - 267.
(129) Sears, V. F. Neutron scattering lengths and cross sections. *Neutron News* **1992**, *3*, 26-37.
(130) Martinez, N.; Michoud, G.; Cario, A.; Ollivier, J.; Franzetti, B.; Jebbar, M.; Oger, P.; Peters, J. High protein flexibility and reduced hydration water dynamics are key pressure adaptive strategies in prokaryotes. *Sci. Rep.* **2016**, *6*, 32816.
(131) Golub, M.; Martinez, N.; Michoud, G.; Ollivier, J.; Jebbar, M.; Oger, P.; Peters, J. The Effect of Crowding on Protein Stability, Rigidity, and High Pressure Sensitivity in Whole Cells. *Langmuir* **2018**, *34* , 10419-10425.
(132) Rahman, A.; Singwi, K. S.; Sjolander, A. Theory of Slow Neutron Scattering by Liquids *Phys. Rev.* **1962**, *126*, 986-996.
(133) Zeller, D.; Telling, M. T. F.; Zamponi, M.; Garcia Sakai, V.; Peters, J. Analysis of elastic incoherent neutron scattering data beyond the Gaussian approximation. *J. Chem. Phys.* **2018**, *149*, 234908.
(134) Zaccai, G. How Soft Is a Protein? A Protein Dynamics Force Constant Measured by Neutron Scattering. *Science* **2000**, *288*, 1604-1607.
(135) Peters, J.; Martinez, N.; Michoud, G.; Cario, A.; Franzetti, B.; Oger, P.; Jebbar, M. Deep sea microbes probed by incoherent neutron scattering under high hydrostatic pressure. *Z. Phys. Chem.* **2014**, *228*, 1121 - 1133.
(136) Al-Ayoubi, S. R.; Schummel, P. H.; Cisse, A.; Seydel, T.; Peters, J.; Winter, R. Osmolytes modify protein dynamics and function of tetrameric lactate dehydrogenase upon pressurization. *Phys. Chem. Chem. Phys.* **2019**, *21*, 12806-12817. DOI:
(137) Perez, J.; Zanotti, J. M.; Durand, D. Evolution of the internal dynamics of two globular proteins from dry powder to solution. *Biophys. J.* **1999**, *77*, 454-469.
(138) Bée, M. *Quasielastic Neutron Scattering:Principles and Applications in Solid State Chemistry, Biology and Materials Science*; Adam Hilger, Philadelphia, 1988.
(139) Gabel, F.; Bicout, B. J.; Lehnert, U.; Tehei, M.; Weik, M.; Zaccai, G. Proteins dynamics studied by neutron scattering. *Q. Rev. Biophys.* **2002**, *35*, 327 - 367.
(140) Bratbak, G. Bacterial Biovolume and Biomass Estimations. *Appl. Environ. Microbiol.* **1985**, *49*, 1488–1493.
(141) Natali, F.; Dolce, C.; Peters, J.; Stelletta, C.; Deme, B.; Ollivier, J.; Leduc, G.; Cupane, A.; Barbier, E. L. Brain lateralization probed by water diffusion at the atomic to micrometric scale. *Sci. Rep.* **2019**, *9*, 14694.
(142) Volino, F.; Dianoux, A. J. Neutron Incoherent-Scattering Law for Diffusion in a Potential of Spherical-Symmetry - General Formalism and Application to Diffusion inside a Sphere. *Mol. Phys.* **1980**, *41*, 271-279.
(143) Jasnin, M.; van Eijck, L.; Koza, M. M.; Peters, J.; Laguri, C.; Lortat-Jacob, H.; Zaccai, G. Dynamics of heparan sulfate explored by neutron scattering. *Phys. Chem. Chem. Phys.* **2010**, *12*, 3360-3362.
(144) Teixeira, J.; Bellissent-Funel, M.; Chen, S. H.; Dianoux, A. J. Experimental determination of the nature of diffusive motions of water molecules at low temperatures. *Phys. Rev. A Gen. Phys.* **1985**, *31*, 1913-1917.
(145) Le Bon, C.; Nicolai, T.; Durand, D. Kinetics of Aggregation and Gelation of Globular Proteins after Heat-Induced Denaturation. *Macromolecules* **1999**, *32*, 6120 - 6127.
(146) Doster, W.; Cusack, S.; Petry, W. Dynamical transition of myoglobin revealed by inelastic neutron scattering. *Nature* **1989**, *337* (6209), 754-756.
(147) Frauenfelder, H.; Parak, F.; Young, R. D. Conformational substates in proteins. *Annu. Rev. Biophys. Biophys. Chem.* **1988**, *17*, 569 - 572.

(148) Ferrand, M.; Dianoux, A. J.; Petry, W.; Zaccai, G. Thermal motions and function of bacteriorhodopsin in purple membranes: Effects of temperature and hydration studied by neutron scattering. *Proc. Natl. Acad. Sci. USA* **1993**, *90*, 9668 - 9672.
(149) Henzler-Wildman, K.; Kern, D. Dynamic personalities of proteins. *Nature* **2007**, *450*, 964 - 972.
(150) Bée, M. Localized and long-range diffusion in condensed matter: state of the art of QENS studies and future prospects. *Chem. Phys.* **2003**, *292* (, 121-141.
(151) Grimaldo, M.; Roosen-Runge, F.; Zhang, F.; Schreiber, F.; Seydel, T. Dynamics of proteins in solution. *Q. Rev. Biophys.* **2019**, *52*, e7.
(152) Corsaro, C.; Mallamace, D. A Nuclear Magnetic Resonance study of the reversible denaturation of hydrated lysozyme. *Physica A* **2011**, *390*, 2904 - 2908.
(153) Murayama, K.; Tomida, M. Heat-induced secondary structure and conformation change of bovine serum albumin investigated by Fourier transform infrared spectroscopy. *Biochemistry* **2004**, *4*, 11526-11532.
(154) Gabel, F.; Masson, P.; Froment, M. T.; Doctor, B. P.; Saxena, A.; Silman, I.; Zaccai, G.; Weik, M. Direct Correlation between Molecular Dynamics and Enzymatic Stability: A Comparative Neutron Scattering Study of Native Human Butyrylcholinesterase and its "Aged" Soman Conjugate. *Biophys. J.* **2009**, *96*, 1489-1494.
(155) Hennig, M.; Roosen-Runge, F.; Zhang, F.; Zorn, S.; Skoda, M. W. A.; Jacobs, R. M. J.; Seydel, T.; Schreiber, F. Dynamics of highly concentrated protein solutions around the denaturing transition. *Soft Matter* **2012**, *8*, 1628 - 1633.
(156) Russo, D.; Pérez, J.; Zanotti, J. M.; Desmadril, M.; Durand, D. Dynamic Transition Associated with the Thermal Denaturation of a Small Beta Protein. *Biophys. J.* **2002**, *83*, 2792 – 2800.
(157) Grimaldo, M.; Roosen-Runge, F.; Hennig, M.; Zanini, F.; Zhang, F.; Jalarvo, N.; Zamponi, M.; Schreiber, F.; Seydel, T. Hierarchical molecular dynamics of bovine serum albumin in concentrated aqueous solution below and above thermal denaturation. *Phys. Chem. Chem. Phys.* **2015**, *17*, 4645-4655.
(158) Grimaldo, M.; Roosen-Runge, F.; Zhang, F.; Seydel, T.; Schreiber, F. Diffusion and dynamics of gamma-globulin in crowded aqueous solutions. *J. Phys. Chem. B* **2014**, *118* (25), 7203-7209.
(159) Dill, K. A.; Ghosh, K.; Schmit, J. D. Physical limits of cells and proteomes. *Proc. Natl. Acad. Sci. USA* **2011**, *108*, 17876-17882.
(160) Dill, K. A.; Ozkan, S. B.; Shell, M. S.; Weikl, T. R. The protein folding problem. *Annu. Rev. Biophys.* **2008**, *37*, 289-316.
(161) Kozak, J. J.; Benham, C. J. Denaturation: an example of a catastrophe. *Proc. Natl. Acad. Sci. USA* **1974**, *71*, 1977-1981.
(162) Leuenberger, P.; Ganscha, S.; Kahraman, A.; Cappelletti, V.; Boersema, P. J.; von Mering, C.; Claassen, M.; Picotti, P. Cell-wide analysis of protein thermal unfolding reveals determinants of thermostability. *Science* **2017**, *355*.
(163) Jasnin, M. Atomic-scale dynamics inside living cells explored by neutron scattering. *J. R. Soc. Interface* **2009**, *6 Suppl 5*, S611-617.
(164) Tehei, M.; Franzetti, B.; Madern, D.; Ginzburg, M.; Ginzburg, B. Z.; Giudici-Orticoni, M. T.; Bruschi, M.; Zaccai, G. Adaptation to extreme environments: macromolecular dynamics in bacteria compared *in vivo* by neutron scattering. *EMBO Rep.* **2004**, *5*, 66-70..
(165) Di Bari, D.; Timr, S.; Guiral, M.; Giudici-Orticoni, M. T.; Seydel, T.; Beck, C.; Petrillo, C.; Derreumaux, P.; Melchionna, S.; Sterpone, F.; et al. Diffusive Dynamics of Bacterial Proteome as a Proxy of Cell Death. *ACS Cent. Sci.* **2023**, *9* , 93-102.
(166) Singwi, K. S.; Sjölander, A. Diffusive Motions in Water and Cold Neutron Scattering. *Phys. Rev.* **1960**, *119*, 863-871.
(167) Jasnin, M.; Stadler, A. M.; Tehei, M.; Zaccai, G. Specific cellular water dynamics observed in vivo by neutron scattering and NMR. *Phys. Chem. Chem. Phys.* **2010**, *12*, 10154–10160.
(168) Tehei, M.; Franzetti, B.; Wood, K.; Gabel, F.; Fabiani, E.; Jasnin, M.; Zamponi, M.; Oesterhelt, D.; Zaccai, G.; Ginzburg, M.; Ginzburg, B. Z. Neutron scattering reveals extremely slow cell water in a Dead Sea organism. *Proc. Natl. Acad. Sci. USA* **2007**, *104*, 766-771.

(169) Link, A. J.; Robison, K.; Church, G. M. Comparing the predicted and observed properties of proteins encoded in the genome of Escherichia coli K-12. *Electrophoresis* **1997**, *18*, 1259 - 1313.
(170) Ahlrichs, P.; Dünweg, B. Simulation of a single polymer chain in solution by combining lattice Boltzmann and molecular dynamics. *J. Chem. Phys.* **1999**, *111*, 8225 - 8239.
(171) Sterpone, F.; Derreumaux, P.; Melchionna, S. Protein Simulations in Fluids: Coupling the OPEP Coarse-Grained Force Field with Hydrodynamics. *J. Chem. Theory Comput.* **2015**, *11*, 1843 - 1853.
(172) Bernaschi, M.; Melchionna, S.; Succhi, S.; Fyta, M.; Kaxiras, E.; Sircar, J. K. MUPHY: A parallel MUlti PHYsics/scale code for high performance bio-fluidic simulations. *Comput. Phys. Commun.* **2009**, *180*, 1495 - 1502.
(173) Sterpone, F.; Melchionna, S.; Tuffery, P.; Pasquali, S.; Mousseau, N.; Cragnolini, T.; Chebaro, Y.; St-Pierre, J. F.; Kalimeri, M.; Barducci, A.; et al. The OPEP protein model: from single molecules, amyloid formation, crowding and hydrodynamics to DNA/RNA systems. *Chem. Soc. Rev.* **2014**, *43*, 4871-4893.
(174) Timr, S.; Melchionna, S.; Derreumaux, P.; Sterpone, F. Optimized OPEP Force Field for Simulation of Crowded Protein Solutions. *J. Phys. Chem. B* **2023**, 127, 3616 - 3623.
(175) Yu, I.; Mori, T.; Ando, T.; Harada, R.; Jung, J.; Sugita, Y.; Feig, M. Biomolecular interactions modulate macromolecular structure and dynamics in atomistic model of a bacterial cytoplasm. *Elife* **2016**, *5*.
(176) Chiricotto, M.; Sterpone, F.; Derreumaux, P.; Melchionna, S. Multiscale simulation of molecular processes in cellular environments. *Philos. Trans. A Math. Phys. Eng. Sci.* **2016**, *374*
(177) Nawrocki, G.; Wang, P. H.; Yu, I.; Sugita, Y.; Feig, M. Slow-Down in Diffusion in Crowded Protein Solutions Correlates with Transient Cluster Formation. *J. Phys. Chem. B* **2017**, *121*, 11072-11084.
(178) Salter, M. A.; Ross, T.; McMeekin, T. A. Applicability of a model for non-pathogenic Escherichia coli for predicting the growth of pathogenic Escherichia coli. *J. Appl. Microbiol.* **1998**, *85*, 357-364.
(179) Matsarskaia, O.; Buhl, L.; Beck, C.; Grimaldo, M.; Schweins, R.; Zhang, F.; Seydel, T.; Schreiber, F.; Roosen-Runge, F. Evolution of the structure and dynamics of bovine serum albumin induced by thermal denaturation. *Phys. Chem. Chem. Phys.* **2020**, *22* , 18507-18517.
(180) Cardinaux, F.; Zaccarelli, E.; Stradner, A.; Bucciarelli, S.; Farago, B.; Egelhaaf, S. U.; Sciortino, F.; Schurtenberger, P. Cluster-driven dynamical arrest in concentrated lysozyme solutions. *J. Phys. Chem. B* **2011**, *115*, 7227-7237.
(181) Mallamace, F.; Corsaro, C.; Mallamace, D.; Vasi, C.; Stanley, H. E. The thermodynamical response functions and the origin of the anomalous behavior of liquid water. *Faraday Discuss.* **2013**, *167*, 95 - 108.
(182) Stadler, A. M.; Embs, J. P.; Digel, I.; Artmann, G. M.; Unruh, T.; Buldt, G.; Zaccai, G. Cytoplasmic water and hydration layer dynamics in human red blood cells. *J. Am. Chem. Soc.* **2008**, *130*, 16852-16853.
(183) Teixeira, J.; Bellissent Funel, M. C.; Chen, S. H.; Dianoux, A. J. Experimental-Determination of the Nature of Diffusive Motions of Water-Molecules at Low-Temperatures. *Phys. Rev. A* **1985**, *31* , 1913-1917.
(184) Fukuchi, S.; Yoshimune, K.; Wakayama, M.; Moriguchi, M.; Nishikawa, K. Unique amino acid composition of proteins in halophilic bacteria. *J. Mol. Biol.* **2003**, *327*, 347-357.
(185) Coquelle, N.; Talon, R.; Juers, D. H.; Girard, E.; Kahn, R.; Madern, D. Gradual adaptive changes of a protein facing high salt concentrations. *J. Mol. Biol.* **2010**, *404*, 493-505.
(186) Lanyi, J. K. Salt-Dependent Properties of Proteins from Extremely Halophilic Bacteria. *Bacteriol. Rev.* **1974**, *38*, 272 - 290.
(187) Vauclare, P.; Marty, V.; Fabiani, E.; Martinez, N.; Jasnin, M.; Gabel, F.; Peters, J.; Zaccai, G.; Franzetti, B. Molecular adaptation and salt stress response of *Halobacterium salinarum* cells revealed by neutron spectroscopy. *Extremophiles* **2015**, *19*, 1099-1107.
(188) Tehei, M.; Zaccai, G. Adaptation to extreme environments: macromolecular dynamics in complex systems. *Biochim. Biophys. Acta* **2005**, *1724*, 404-410.
(189) Marty, V.; Jasnin, M.; Fabiani, E.; Vauclare, P.; Gabel, F.; Trapp, M.; Peters, J.; Zaccai, G.; Franzetti, B. Neutron scattering: a tool to detect in vivo thermal stress effects at the molecular dynamics level in micro-organisms. *J. R. Soc. Interface* **2013**, *10*, 20130003.

(190) Vihinen, M. Relationship of protein flexibility to thermostability. *Protein Eng.* **1987**, *1*, 477 - 480.
(191) Jaenicke, R. Stability and stabilization of globular proteins in solution. *J. Biotechnol.* **2000**, *79*, 193 - 203.
(192) Marty, V. Adaptation de l'Archaea halophile Halobacterium salinarum aux stress environnementaux: mécanismes de survie et rôle de la protéolyse intracellulaire. UJF, Grenoble, 2011.
(193) Cario, A.; Jebbar, M.; Thiel, A.; Kervarec, N.; Oger, P. M. Molecular chaperone accumulation as a function of stress evidences adaptation to high hydrostatic pressure in the piezophilic archaeon Thermococcus barophilus. *Sci. Rep.* **2016**, *6*, 29483.
(194) Galinski, E. A. Osmoadaptation in bacteria. *Adv. Microb. Physiol.* **1995**, *37*, 272 - 328.
(195) Yancey, P. H.; Blake, W. R.; Conley, J. Unusual organic osmolytes in deep-sea animals: adaptations to hydrostatic pressure and other perturbants. *Comp. Biochem. Physiol. A Mol. Integr. Physiol.* **2002**, *133*, 667-676.
(196) Wood, J. M.; Bremer, E.; Csonka, L. N.; Kraemer, R.; Poolman, B.; van der Heide, T.; Smith, L. T. Osmosensing and osmoregulatory compatible solute accumulation by bacteria. *Comp. Biochem. Physiol. A Mol. Integr. Physiol.* **2001**, *130* , 437-460.
(197) Empadinhas, N.; Milton, S. d. C. Diversity and biosynthesis of compatible solutes in hyper/thermophiles. *Int. Microbiology* **2006**, *9*, 199 - 206.
(198) Arns, L.; Schuabb, V.; Meichsner, S.; Berghaus, M.; Winter, R. The Effect of Natural Osmolyte Mixtures on the Temperature-Pressure Stability of the Protein RNase A. *Z. Phys. Chem.* **2017**, *232*, 615 - 634.
(199) Doster, W.; Longeville, S. Microscopic diffusion and hydrodynamic interactions of hemoglobin in red blood cells. *Biophys. J.* **2007**, *93* (4), 1360-1368.
(200) Jasnin, M.; Moulin, M.; Haertlein, M.; Zaccai, G.; Tehei, M. In vivo measurement of internal and global macromolecular motions in Escherichia coli. *Biophys. J.* **2008**, *95*, 857-864.
(201) Faria, T. Q.; Knapp, S.; Ladenstein, R.; Macanita, A. L.; Santos, H. Protein stabilisation by compatible solutes: effect of mannosylglycerate on unfolding thermodynamics and activity of ribonuclease A. *ChemBioChem* **2003**, *4*, 734-741.
(202) Auton, M.; Bolen, D. W. Predicting the energetics of osmolyte-induced protein folding/unfolding. *Proc. Natl. Acad. Sci. USA* **2005**, *102*, 15065-15068.
(203) Canchi, D. R.; Garcia, A. E. Cosolvent effects on protein stability. *Annu. Rev. Phys. Chem.* **2013**, *64*, 273-293.
(204) Marion, J.; Trovaslet, M.; Martinez, N.; Masson, P.; Schweins, R.; Nachon, F.; Trapp, M.; Peters, J. Pressure-induced molten globule state of human acetylcholinesterase: structural and dynamical changes monitored by neutron scattering. *Phys. Chem. Chem. Phys.* **2015**, *17*, 3157-3163.
(205) Zou, Q.; Bennion, B. J.; Daggett, V.; Murphy, K. P. The molecular mechanism of stabilization of proteins by TMAO and its ability to counteract the effects of urea. *J. Am. Chem. Soc.* **2002**, *124*, 1192-1202..
(206) Calio, A.; De Francesco, A.; Oger, P.; Peters, J. Molecular bases of proteome adaptation to high pressure in extremophilic archaea. *ILL report CRG 2876* **2021**.
(207) Librizzi, F.; Carrotta, R.; Peters, J.; Cupane, A. The effects of pressure on the energy landscape of proteins. *Sci. Rep.* **2018**, *8*.
(208) Imoto, S.; Kibies, P.; Rosin, C.; Winter, R.; Kast, S. M.; Marx, D. Toward Extreme Biophysics: Deciphering the Infrared Response of Biomolecular Solutions at High Pressures. *Angew. Chem. Int. Ed.* **2016**, *55*, 9534-9538.
(209) Paciaroni, A.; Cinelli, S.; Onori, G. Effect of the Environment on the Protein Dynamical Transition: A Neutron Scattering Study. *Biophys. J.* **2002**, *83*, 1157 - 1164.
(210) Tsai, A. M.; Neumann, D. A.; Bell, L. N. Molecular Dynamics of Solid-State Lysozyme as Affected by Glycerol and Water: A Neutron Scattering Study. *Biophys. J.* **2000**, *79*, 2728 - 2732.
(211) Gregory, R. B. *Protein-solvent interactions*; Marcel Dekker, Inc., 1995.
(212) Gekko, K.; Timasheff, S. N. Mechanism of Protein Stabilization by Glycerol: Preferential Hydration in Glycerol-Water Mixtures. *Biochemistry* **1981**, *20*, 4667 - 4676.

(213) Cordone, L.; Ferrand, M.; Vitrano, E.; Zaccai, G. Harmonic behavior of trehalose-coated carbon-monoxy-myoglobin at high temperature. *Biophys. J.* **1999**, *76*, 1043-1047.
(214) Paciaroni, A.; Cornicchi, E.; De Francesco, A.; Marconi, M.; Onori, G. Conditioning action of the environment on the protein dynamics studied through elastic neutron scattering. *Eur. Biophys. J. Biophys. Lett.* **2006**, *35* , 591-599.
(215) Lushchekina, S. V.; Inidjel, G.; Martinez, N.; Masson, P.; Trovaslet-Leroy, M.; Nachon, F.; Koza, M. M.; Seydel, T.; Peters, J. Impact of Sucrose as Osmolyte on Molecular Dynamics of Mouse Acetylcholinesterase. *Biomol.* **2020**, *10*.
(216) Tai, K.; Shen, T.; Borjesson, U.; Philippopoulos, M.; McCammon, J. A. Analysis of a 10-ns molecular dynamics simulation of mouse acetylcholinesterase. *Biophys. J.* **2001**, *81*, 715-724.
(217) Shen, T.; Tai, K.; Henchman, R. H.; McCammon, J. A. Molecular dynamics of acetylcholinesterase. *Acc. Chem. Res.* **2002**, *35*, 332-340.
(218) Timasheff, S. N. Protein-solvent preferential interactions, protein hydration, and the modulation of biochemical reactions by solvent components. *Proc. Natl. Acad. Sci. USA* **2002**, *99* (15), 9721-9726.
(219) Dong, Y.; Yang, Q.; Jia, S.; Qiao, C. Effects of high pressure on the accumulation of trehalose and glutathione in the Saccharomyces cerevisiae cells. *Biochem. Eng. J.* **2007**, *37*, 226 - 230.
(220) Fedorov, M. V.; Goodman, J. M.; Nerukh, D.; Schumm, S. Self-assembly of trehalose molecules on a lysozyme surface: the broken glass hypothesis. *Phys. Chem. Chem. Phys.* **2011**, *13* , 2294-2299.
(221) Schummel, P. H.; Al-Ayoubi, S.; Peters, J.; Winter, R. *Influence of Pressure on the Sub-Nanosecond Dynamics of Fibrillar and Cytoskeletal Proteins*; ILL-report 8-04-795; Institut Laue Langevin, 2017.
(222) Mannhold, R.; Kubinyi, H.; Folkers, G. *Protein-ligand interactions*; Wiley-VCH, 2012.
(223) Wyman, J.; S.J., G. *Binding and Linkage: Functional Chemistry of Biological Macromolecules*; University Science Book, 1990.
(224) Woodbury, C. P. *Introduction to macromolecular binding equilibria*; CRC Press, 2007.
(225) Dearmond, P. D.; Xu, Y.; Strickland, E. C.; Daniels, K. G.; Fitzgerald, M. C. Thermodynamic analysis of protein-ligand interactions in complex biological mixtures using a shotgun proteomics approach. *J. Proteome Res.* **2011**, *10*, 4948-4958.
(226) van Holde, K. E.; Johnson, W. C.; Ho, P. S. *Principles of Physical Biochemistry*; Pearson Education, 2006.
(227) Oliva, R.; Jahmidi-Azizi, N.; Mukherjee, S.; Winter, R. Harnessing Pressure Modulation for Exploring Ligand Binding Reactions in Cosolvent Solutions. *J. Phys. Chem. B* **2021**, *125* (2), 539-546.
(228) Connors, K. A. *Binding constants — the measurement of molecular complex stability*; John Wiley & Sons, 1987.
(229) Oliva, R.; Banerjee, S.; Cinar, H.; Ehrt, C.; Winter, R. Alteration of Protein Binding Affinities by Aqueous Two-Phase Systems Revealed by Pressure Perturbation. *Sci. Rep.* **2020**, *10* , 8074.
(230) Kamali, A.; Jahmidi-Azizi, N.; Oliva, R.; Winter, R. Deep sea osmolytes in action: their effect on protein-ligand binding under high pressure stress. *Phys. Chem. Chem. Phys.* **2022**, *24*, 17966-17978.
(231) Marchal, S.; Lange, R.; Tortora, P.; Balny, C. High pressure as a tool for investigating protein–ligand interactions. *J. Phys. Cond. Matt.* **2004**, *16*, S1271 - S1275.
(232) Majumdar, B. B.; Mondal, J. Impact of Inert Crowders on Host-Guest Recognition Process. *J. Phys. Chem. B* **2022**, *126*, 4200 - 4215.
(233) Taulier, N.; Chalikian, T. V. Hydrophobic hydration in cyclodextrin complexation. *J. Phys. Chem. B* **2006**, *110* , 12222-12224.
(234) Heremans, K. High pressure effects on proteins and other biomolecules. *Annu. Rev. Biophys. Bioeng.* **1982**, *11*, 1-21.
(235) Kohn, B.; Schwarz, P.; Wittung-Stafshede, P.; Kovermann, M. Impact of crowded environments on binding between protein and single-stranded DNA. *Sci. Rep.* **2021**, *11*, 17682.
(236) Oliva, R.; Niccoli, M.; Castronuovo, G. Binding and stability properties of PEG2000 to globular proteins: The case of lysozyme. *J. Mol. Liquids* **2022**, *360*, 119514.
(237) Ghosh, A.; Smith, P. E. S.; Qin, S.; Yi, M.; Zhou, H. X. Both Ligands and Macromolecular Crowders Preferentially Bind to Closed Conformations of Maltose Binding Protein. *Biochemistry* **2019**, *58*, 2208-2217.

(238) Atefi, E.; Fyffe, D.; Kaylan, K. B.; Tavana, H. Characterization of Aqueous Two-Phase Systems from Volume and Density Measurements. *J. Chem. Eng. Data* **2016**, *61*, 1531–1539.
(239) Oliva, R.; Winter, R. Harnessing Pressure-Axis Experiments to Explore Volume Fluctuations, Conformational Substates, and Solvation of Biomolecular Systems. *J. Phys. Chem. Lett.* **2022**, *13*, 12099-12115.
(240) Oliva, R.; Banerjee, S.; Cinar, H.; Winter, R. Modulation of enzymatic activity by aqueous two-phase systems and pressure - rivalry between kinetic constants. *Chem. Commun.* **2020**, *56*, 395-398.
(241) Oliva, R.; Mukherjee, S.; Manisegaran, M.; Campanile, M.; Del Vecchio, P.; Petraccone, L.; Winter, R. Binding Properties of RNA Quadruplex of SARS-CoV-2 to Berberine Compared to Telomeric DNA Quadruplex. *Int. J. Mol. Sci.* **2022**, *23*.
(242) Oliva, R.; Mukherjee, S.; Winter, R. Unraveling the binding characteristics of small ligands to telomeric DNA by pressure modulation. *Sci. Rep.* **2021**, *11*, 9714.
(243) Eisenmenger, M. J.; Reyes-De-Corcuera, J. I. High pressure enhancement of enzymes: A review. *Enzyme Microb. Technol.* **2009**, *45*, 331 - 347.
(244) Morild, E. The theory of pressure effects on enzymes. *Adv. Protein Chem.* **1981**, *34*, 93-166.
(245) Mozhaev, V. V.; Lange, R.; Kudryashova, E. V.; Balny, C. Application of high hydrostatic pressure for increasing activity and stability of enzymes. *Biotechnol. Bioeng.* **1996**, *52*, 320 - 331.
(246) Luong, T. Q.; Erwin, N.; Neumann, M.; Schmidt, A.; Loos, C.; Schmidt, V.; Fandrich, M.; Winter, R. Hydrostatic Pressure Increases the Catalytic Activity of Amyloid Fibril Enzymes. *Angew. Chem. Int. Ed.* **2016**, *55*, 12412-12416.
(247) Luong, T. Q.; Winter, R. Combined pressure and cosolvent effects on enzyme activity - a high-pressure stopped-flow kinetic study on alpha-chymotrypsin. *Phys. Chem. Chem. Phys.* **2015**, *17* , 23273-23278.
(248) Ganguly, A.; Luong, T. Q.; Brylski, O.; Dirkmann, M.; Moller, D.; Ebbinghaus, S.; Schulz, F.; Winter, R.; Sanchez-Garcia, E.; Thiel, W. Elucidation of the Catalytic Mechanism of a Miniature Zinc Finger Hydrolase. *J. Phys. Chem. B* **2017**, *121*, 6390-6398.
(249) Jaworek, M. W.; Schuabb, V.; Winter, R. The effects of glycine, TMAO and osmolyte mixtures on the pressure dependent enzymatic activity of alpha-chymotrypsin. *Phys. Chem. Chem. Phys.* **2018**, *20* , 1347-1354.
(250) Wangler, A.; Canales, R.; Held, C.; Luong, T. Q.; Winter, R.; Zaitsau, D. H.; Verevkin, S. P.; Sadowski, G. Co-solvent effects on reaction rate and reaction equilibrium of an enzymatic peptide hydrolysis. *Phys. Chem. Chem. Phys.* **2018**, *20*, 11317-11326.
(251) Knierbein, M.; Wangler, A.; Luong, T. Q.; Winter, R.; Held, C.; Sadowski, G. Combined co-solvent and pressure effect on kinetics of a peptide hydrolysis: an activity-based approach. *Phys. Chem. Chem. Phys.* **2019**, *21*, 22224-22229.
(252) Held, C.; Stolzke, T.; Knierbein, M.; Jaworek, M. W.; Luong, T. Q.; Winter, R.; Sadowski, G. Cosolvent and pressure effects on enzyme-catalysed hydrolysis reactions. *Biophys. Chem.* **2019**, *252*, 106209.
(253) Gault, S.; Jaworek, M. W.; Winter, R.; Cockell, C. S. Perchlorate salts confer psychrophilic characteristics in alpha-chymotrypsin. *Sci. Rep.* **2021**, *11*, 16523.
(254) Jaworek, M. W.; Gajardo-Parra, N. F.; Sadowski, G.; Winter, R.; Held, C. Boosting the kinetic efficiency of formate dehydrogenase by combining the effects of temperature, high pressure and co-solvent mixtures. *Colloids Surf. B* **2021**, *208*, 112127.
(255) Foguel, D.; Robinson, C. R., de Sousa, P. C. Jr., Silva, J. L., Robinson, A. S. Hydrostatic pressure rescues native protein from aggregares. *Biotechol. Bioeng.* **1999**, *63*, 552-558.
(256) St John, R. J.; Carpenter, J. F.; Balny, C.; Randolph, T. W. High pressure refolding of recombinant human growth hormone from insoluble aggregates. Structural transformations, kinetic barriers, and energetics. *J. Biol. Chem.* **2001**, *276*, 46856-46863.
(257) Smith, J. C.; Tan, P.; Petridis, L.; Hong, L. Dynamic neutron scattering by biological systems. *Ann. Rev. Biophys*. **2018**, *47*, 335 - 354.
(258) Winnikoff, J. R.; Haddock, S. H. D.; Budin, I. Depth- and temperature-specific fatty acid adaptations in ctenophores from extreme habitats. *J. Exp. Biol.* **2021**, *224*, jeb242800.

(259) Damer, B.; Deamer, D. The Hot Spring Hypothesis for an Origin of Life. *AsBio.* **2020**, *20*, 429-452.
(260) Speer, S. L.; Stewart, C. J.; Sapir, L.; Harries, D.; Pielak, G. J. Macromolecular crowding is more than hard-core reuplsions. *Annu. Rev. Biophys.* **2022**, *51*, 267-300.
(261) Rivas, G.; Minton, A. P. Macromolecular crowding in vitro, in vivo, and in between. *Trends Biochem. Sci.* **2016**, *41*, 970-981.
(262) Rivas, G.; Minton, A. P. Influence of nonspecific interactions on protein associations: implications for biochemistry in vivo. *Annu. Rev. Biochem.* **2022**, *91*, 321-351.
(263) Rivas, G.; Minton, A. P. Toward an understanding of biochemical equilibria within living cells. *Biophys. Rev*. **2018**, *10*, 241-253.
(264) Youxing, Q.; Bolen, D. W. Efficacy of macromolecular crowding in forcing proteins to fold. *Biophys. Chem*. **2002**, *101*, 155-165.
(265) Deguchi, S.; Degaki, H.; Taniguchi, I.; Koga, T. Deep-Sea-Inspired Chemistry: A Hitchhiker's Guide to the Bottom of the Ocean for Chemists. *Langmuir* **2023**, *39*, 7987-7994.